Impedance modulation: a means to cope with neuromuscular noise

Selen, L.P.J.

2007

document version
Publisher's PDF, also known as Version of record

Impedance modulation:
a means to cope with neuromuscular noise

Luc Paul Jeanne Selen

The work presented in this thesis is part of the research program of the Institute for Fundamental and Clinical Human Movement Sciences (IFKB), and was carried out at the Faculty of Human Movement Sciences, Vrije Universiteit, Amsterdam, The Netherlands.

ISBN: 90 8659 066 7

Cover design: Wendy de Graaf & Luc Selen
Printer: Cambridge Printing, Cambridge (UK)

VRIJE UNIVERSITEIT

Impedance modulation: a means to cope with neuromuscular noise

ACADEMISCH PROEFSCHRIFT

ter verkrijging van de graad Doctor aan
de Vrije Universiteit Amsterdam,
op gezag van de rector magnificus
prof.dr. L. M. Bouter,
in het openbaar te verdedigen
ten overstaan van de promotiecommissie
van de faculteit der Bewegingswetenschappen
op vrijdag 16 februari 2007 om 10.45 uur
in de aula van de universiteit,
De Boelelaan 1105

door

Luc Paul Jeanne Selen

geboren te Tegelen

promotoren: prof.dr. J.H. van Dieën
prof.dr. P.J. Beek

Contents

1 **General introduction** **7**

2 **Can co-activation reduce kinematic variability? A simulation study** **15**

3 **Impedance is modulated to meet accuracy demands during goal-directed arm movements** **35**

4 **Impedance modulation and feedback corrections in tracking targets of variable size and frequency** **59**

5 **Fatigue induced changes of impedance and performance in target tracking** **85**

6 **Epilogue** **107**

References **119**

Summary **129**

Samenvatting **133**

Dankwoord **137**

Publications **140**

1

General introduction

Introduction

'To move things is all that mankind can do whether it be the whisper of a syllable or the felling of a forest.'

(Sherrington, 1906)

These words of Lord Sherrington underscore the importance of movement to human beings as well as the diversity of movements that the human neuro-musculoskeletal system can generate. Not only are we able to make widely diverse movements, also the details of any given movement are different at each repetition (e.g. Bernstein, 1967; Scholz et al., 2000; Tseng et al., 2003). Part of these differences may be accounted for by the inherent noisiness of the neuromuscular system resulting in kinematic variability.

In order to deal with accuracy constraints imposed by the task at hand, we have to control this kinematic variability. Anyone who has ever threaded a needle will have experienced how difficult it is to match the relative position of one's hands. From experience one will recall the high levels of muscular co-activation that are typically associated with executing this task. This thesis focuses on the functional role of muscular co-activation, i.e. modulation of joint impedance, to control kinematic variability.

In this general introduction, I will first discuss the inherent noisiness of the neuromuscular system and how this noise results in the characteristic signal dependency of isometric force variability[1]. Next, motor control theories that take force variability as a starting point will be presented and discussed. This discussion culminates in the presentation of the Neuromotor Noise Theory (NNT, Van Galen and De Jong, 1995) and the discussion of its paradoxical claim that impedance modulation is a relevant degree of freedom[2] in filtering the effects of signal dependent force fluctuations on kinematics. Finally, the aims and outline of this thesis will be presented.

[1] In this thesis the terms signal dependent noise (SDN), force variability and neuromuscular noise all refer to the observation that the standard deviation of force fluctuations increases monotonically with the mean force.

[2] The terminology is adopted from Van Galen. A 'degree of freedom' is generally associated with mechanical degrees of freedom. However, in the present context 'degree of freedom' should be interpreted as a control setting.

Neuromuscular noise

The direct cause of kinematic variability is obviously the variability of the forces generated by the muscles, supplemented by environmental disturbances. I will refer to the variability of muscular origin as *neuromuscular noise*. Although strictly speaking the term *noise* is reserved for random processes, I believe, in line with others, that it well suits the definition of fluctuations in motor output that do not enhance, or even deteriorate, motor performance. Note, however, that part of the fluctuations may help in exploring possible or alternative motor strategies (Sporns and Edelman, 1993; Berthier et al., 2005).

Neuromuscular noise, i.e. force variability, is the result of two peripheral processes, acting in parallel. The first process, called the large motor unit mechanism, has to do with the organisation of the motor unit pool (see Jones et al., 2002; Christakos et al., 2006). Because of the size principle, the last recruited motor unit(s) contributes most to the overall force and force variability. Although the firing rate of the first recruited units is more variable because they fire at a higher rate (Matthews, 1996), their contribution to the force variability is negligible because of their small contribution to the total force in combination with their fused contraction. The last recruited units have a low firing frequency, resulting in non-fused contractions. This not only results in large force variability within this motor unit, but because of its size it also contributes substantially to overall force variability of the muscle. The second process is rhythmical motor unit firing synchrony, which is most likely caused by Ia spindle feedback oscillations (Christakos et al., 2006).

Neuromuscular noise exhibits a characteristic signal dependency. Although the exact form of signal dependent neuromuscular noise (SDN) is still under debate (see Christou et al., 2002, for an overview), all pertinent studies report a monotonically increasing force variability with force magnitude. Jones et al. (2002) have convincingly shown, both experimentally and numerically, that the characteristic signal dependency is caused by the architecture of the motor unit pool. The range of motor unit recruitment thresholds and motor unit twitch forces direct muscular forces to exhibit monotonically increasing SDN.

The organisation of the motor unit pool is responsible for the signal dependency of neuromuscular noise. However, the physical and psychological state of the neuromuscular system affects the magnitude of neuromuscular noise. For example, muscular fatigue results in increased neuromuscular noise (Lorist et al., 2002; Lippold, 1981;

Huang et al., 2006; Hunter and Enoka, 2003), most likely due to increased discharge variability (Hunter and Enoka, 2003). Also cognitive factors, like stress, increase neuromuscular noise (Noteboom et al., 2001; Christou et al., 2004), most likely due to augmented low frequency oscillations from the spinal cord (Christou et al., 2004). As regards the increase of neuromuscular noise with age, results are mixed. Although increased neuromuscular noise with age has been shown (Vaillancourt et al., 2003; Tracy et al., 2005), most of this increase is attributable to decreased force generating capacity (Sosnoff and Newell, 2006; Hamilton et al., 2004). Still, the motor control system will have to account for increased neuromuscular noise regardless of its origin.

Stochastic optimal control theories

Given the presence of signal dependent neuromuscular noise, motor control theories have to account for the resulting kinematic variability. The seminal work of Woodworth (1899) and Fitts (1954) revealed a trade-off between speed and accuracy. Especially Fitts related this trade-off to noise in the motor system. He assumed that noise limits the information capacity of the motor system and he derived his famous logarithmic equation for the speed-accuracy trade-off from information theory as conceptualised by Shannon and Weaver (1949).

In later years, models were presented replicating Fitts' law. The *stochastic optimised submovement model* of Meyer et al. (1988) and the submovement model of Burdet and Milner (1998) take proportional neuromotor noise[3] as a starting point for their models of aiming movements. The simulated movements are composed of a sequence of submovements whose amplitudes are a Gaussian-distributed random variable with a constant coefficient of variation (CV). The models assume that the amplitude and the number of submovements are optimised to the time and position constraints imposed by the task.

More recently, theories have been presented that depart from the variability of the muscular forces and torques (Harris and Wolpert, 1998; Todorov and Jordan, 2002). Not only are these models able to replicate Fitts' law, but also obstacle avoidance (Hamilton and Wolpert, 2002), step tracking wrist movements (Haruno and Wolpert, 2005) and saccades (Harris and Wolpert, 1998) result naturally from minimising endpoint variability under SDN. With noisy feedback added, Todorov and Jordan (2002)

[3]Proportional neuromotor noise refers to both submovement timing and amplitude variability in this case.

showed that task-constrained variability and motor synergies emerge naturally within this framework.

Neuromotor Noise Theory

All previously discussed models have in common that they ignore the dynamics of the muscular system. In essence, they all generate signal dependent torques or submovements so as to optimise, i.e. minimise, endpoint variability, thus resulting in the lowest activations possible to get to the target in time (which is essentially Fitts' law). However, experimental studies show that humans are able to modulate the accuracy of their movements without changing the kinematics of the task (Gribble et al., 2003; Osu et al., 2004). Apparently, the neuromuscular system has additional strategies at its disposal.

A strategy proposed to control the accuracy of movement, leaving the kinematics unaffected, is joint impedance modulation. This notion figures prominently in the Neuromotor Noise Theory (NNT) proposed by Van Galen and colleagues (1992, 1995, 2000, 2002). The basic assumptions underlying this theory are: (1) Motor behaviour is an inherently stochastic and therefore noisy process, not only because of recruitment processes in the muscle, but also because of reflex induced oscillations, feedback and feed forward control mechanisms and oscillations caused by musculoskeletal dynamics. (2) Biophysical, biomechanical and psychological factors all contribute to the instantaneous level of neuromuscular noise in a movement signal. One can think of fatigue as a biophysical factor, limb orientation as a biomechanical factor and stress as a psychological factor. (3) Movement endpoint variability is related to the signal-to-noise ratio of the forces that drive the limb. (4) Optimal signal-to-noise ratios can be achieved by adjusting limb stiffness.

The SDN impedance paradox

Joint impedance helps in limiting the excursions due to environmental perturbations (e.g. Burdet et al., 2001; Franklin et al., 2003), because joint impedance can be controlled independently of the external forces acting on the skeletal system. However, both neuromuscular noise and joint impedance act through the muscles. This creates the paradoxical situation that, on the one hand, the muscles are responsible for force variability while on the other hand they are supposed to help suppress its effects by

modifying joint impedance. Proponents of SDN theories have been surprised by this SDN impedance paradox (Schaal and Schweighofer, 2005; Osu et al., 2004; Guigon et al., 2006; Van Beers et al., 2004), indicating that there is still disagreement about the functional role of impedance in controlling movement accuracy.

Aims and outline of this thesis

The starting point of this thesis was the Neuromotor Noise Theory as presented by Van Galen (e.g. 1992, 1995, 2000, 2002). NNT states that the modulation of joint stiffness is a relevant degree of freedom in controlling movement variability by filtering out neuromuscular noise. Although the theory is appealing, it has at least two lacunae. First, only few studies (Laursen et al., 1998; Van Galen and Van Huygevoort, 2000) were conducted on the modulation of stiffness in response to changes in accuracy constraints before this project. The focus was mainly on the effects of cognitive stressors, which are believed to influence neuromuscular noise, on stiffness modulation (Van Gemmert and Van Galen, 1997, 1998; Van Galen et al., 2002; Van den Heuvel et al., 1998). Second, although NNT makes statements about the mechanical stiffness, only indirect measures such as EMG (electromyogram) and pen pressure have so far been presented.

The aims of this thesis were to verify that joint impedance, in particular around the elbow, is increased in response to increased accuracy demands and/or increased neuromuscular noise. Numerical and experimental studies have been conducted to investigate the tenability of the claim that: '*muscle co-contraction (i.e. joint stiffness) is a relevant in the control of spatial accuracy*' (Van Galen and De Jong, 1995).

First, a theoretical study was conducted on the paradox that muscles on the one hand cause signal dependent force variability while on the other hand providing a means to suppress its effects on the kinematics. In chapter 2, neuro-musculo-skeletal models with different levels of complexity are compared in order to identify the necessary components to consider in the muscle dynamics and to realistically simulate force variability, eventually solving the paradox.

Second, the modulation of elbow impedance in response to changing accuracy constraints was investigated experimentally. In chapter 3 a method is presented to quantify stiffness and damping as measures of joint impedance during movement. This method was applied to investigate impedance changes during goal-directed time constrained elbow extension movements toward differently sized targets. In chapter 4,

the same method was applied to investigate the effects of movement speed and target size on joint impedance during cyclic tracking movements of the elbow. In addition, the presence and organisation of corrective (sub-) movements was investigated in that study.

Third, as a corollary of the Neuromotor Noise Theory, it was hypothesised that an increase of neuromuscular noise, due to fatigue, will also result in increased joint impedance to maintain a certain accuracy level (Van Dieën et al., 2003). Chapter 5 presents a test of this hypothesis in a cyclic elbow tracking experiment.

Finally, in chapter 6, the main findings and conclusions of this thesis are summarised and discussed with respect to motor control theories on movement variability. This chapter provides an outlook of future research directions as well as an evaluation of the use of impedance modulation as a generic strategy for accuracy control.

2

Can co-activation reduce kinematic variability? A simulation study

Selen L.P.J., Van Dieën J.H. & Beek P.J. (2005). Can co-activation reduce kinematic variability? A simulation study. *Biological Cybernetics*, 93(5), 373–381.

The original paper can be found on:
http://www.springerlink.com/content/f156770787q355g4

Abstract

Impedance modulation has been suggested as a means to suppress the effects of internal 'noise' on movement kinematics. We investigated this hypothesis in a neuro-musculo-skeletal model. A prerequisite is that the muscle model produces realistic force variability. We found that standard Hill-type models do not predict realistic force variability in response to variability in stimulation. In contrast, a combined motor-unit pool model and a pool of parallel Hill-type motor units did produce realistic force variability as a function of target force, largely independent of how the force was transduced to the tendon. To test the main hypothesis, two versions of the latter model were simulated as an antagonistic muscle pair, controlling the position of a frictionless hinge joint, with a distal segment having realistic inertia relative to the muscle strength. Increasing the impedance through co-activation resulted in less kinematic variability, except for the lowest levels of co-activation. Model behaviour in this region was affected by the noise amplitude and the inertial properties of the model. Our simulations support the idea that muscular co-activation is in principle an effective strategy to meet accuracy demands.

Introduction

Human motor behaviour is variable yet efficient. The variability is an inevitable consequence of the stochastic nature of neuromuscular processes. On the output side this is manifest in the variability of motor unit spiking behaviour (e.g. Matthews, 1996), isometric force (e.g. Jones et al., 2002), and movement kinematics (e.g. Scholz et al., 2000; Tseng et al., 2003).

Optimal control models have been used to study the relation between variability and task performance. Models of the noisy neuromotor system accurately replicate experimental data of saccades and arm movements when endpoint variance is minimised (Harris and Wolpert, 1998; Hamilton and Wolpert, 2002). When feedback is added, phenomena like task-constrained variability, goal-directed corrections and motor synergies emerge naturally from stochastic optimal control models (Todorov and Jordan, 2002). A shortcoming of these models is that they are driven by pure force and moment actuators and thus ignore the impedance characteristics of the muscles (Osu et al., 2004).

Impedance modulation has been proposed as a means to reduce the contribution of force fluctuations to kinematic variability (Van Galen and De Jong, 1995). This extra degree of freedom, which, in theory, can be controlled by co-activation of muscles (Osu and Gomi, 1999), is supposed to act as a low-pass filter between the force fluctuations and movement kinematics. Burdet et al. (2001) measured hand path error and impedance of point-to-point movements before, during and after the exposure to a negative elastic force field perpendicular to the movement direction. To overcome the trajectory instability due to the force field, subjects increased the mechanical impedance of the arm. Interestingly, after removal of the force field the hand path error was smaller than in the trials prior to the exposure to the force field. Also the variability of jaw movements seems to be influenced by impedance modulation (Shiller et al., 2002). Studies on muscular co-activation have provided more direct evidence for impedance modulation in response to increased accuracy demands. Both in single-joint (Osu et al., 2004) and multi-joint (Laursen et al., 1998; Gribble et al., 2003; Visser et al., 2004) movements co-activation increases with accuracy demands.

The role of joint impedance to resist unpredictable external force perturbations has been investigated in both static (e.g. Perreault et al., 1999) and dynamic (e.g. Burdet et al., 2001; Franklin et al., 2003) tasks. On mechanical grounds it is obvious that excursions from the planned trajectory will decrease with increased impedance

(Wagner and Blickhan, 2003). For internal force fluctuations the role of impedance modulation is less straightforward because both muscular force fluctuations (Jones et al., 2002; Christou et al., 2002) and joint impedance (Osu and Gomi, 1999) increase linearly with muscular contraction levels. This creates the paradoxical situation that, on the one hand, the muscles are the source of the force fluctuations while on the other hand they could help suppress their effects by modifying joint impedance.

The goal of this paper is to elucidate the relations among force variability, impedance modulation and kinematic variability by examining how these relations might be implemented in a neuro-musculo-skeletal model. To anticipate, we show that standard Hill-type muscle models are inappropriate to simulate realistic force variability and that a more detailed description of muscular behaviour and control is needed. In section 2 this results in a model with multiple motor units, whose contraction dynamics are described by Hill-type muscle equations, and a motor unit pool as the control mechanism. Finally, we show that co-activation of muscles of the latter type does not necessarily result in larger kinematic variation in spite of increases in the force variability of the individual muscles.

1. Force variability in a standard Hill-type muscle model

Model and simulation

Our first goal was to obtain a formulation of a dynamic neuromuscular model that produces realistic isometric force variability. In most large scale musculo-skeletal models, muscle behaviour is described by length-force and velocity-force equations (e.g. Pandy et al., 1990; Van Soest and Bobbert, 1993). The characteristics of the individual fibres and motor units are lumped together in a single contractile element (CE) connected to a series elastic element (SE). These lumped models have proved suitable for deterministic simulations of maximal jumping (e.g. Pandy et al., 1990; Van Soest and Bobbert, 1993) and ballistic arm movements (e.g. Welter and Bobbert, 2002). In addition, they have been instrumental in showing that intrinsic muscle properties may compensate for errors in motor planning and small variations in initial conditions (Van Soest and Bobbert, 1993; Wagner and Blickhan, 2003; Van der Burg et al., 2005).

The question is whether these lumped models are also suitable to simulate realistic force variability. To answer this question, we examined the behaviour of a model with excitation-activation-contraction dynamics as described in Van Soest and Bobbert

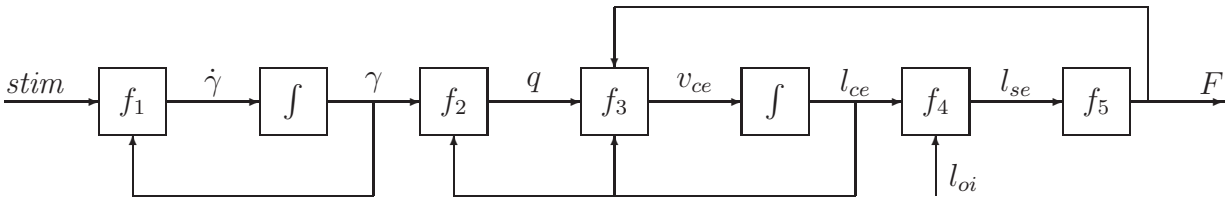

Figure 2.1: *Block diagram showing the flow of calculations in the lumped muscle models. The functions f_1 through f_5 are explained in the text. The integral signs indicate integration with respect to time. External inputs are the stimulation ($stim$) and the origin-insertion length (l_{oi}). $\dot{\gamma}$: calcium concentration change; γ: calcium concentration; q: active state; v_{ce}: contractile element velocity; l_{ce}: contractile element length; l_{se}: tendon length; F: muscle force. Two regimes of stimulus variability were simulated: continuous (CLM) and discrete (DLM).*

(1993) and Ridderikhoff et al. (2004). We compared this with the experimental finding that isometric force variability, as indexed by its standard deviation (SD), increases monotonically with the mean (Christou et al., 2002; Jones et al., 2002; Taylor et al., 2003).

The flow of calculations is depicted in figure 2.1. Input to the model is the stimulation of the muscle ($stim$), a number between 0 and 1 representing both recruitment and rate coding. The calcium concentration (γ) is related to $stim$ by first order dynamics (f_1) with a time constant τ of 89ms. The active state q was calculated from γ through a nonlinear equation (f_2), which also depends on CE length. Function f_3 represents the force-velocity and force-length relations. Contractile element velocity (v_{ce}) was calculated from CE length (l_{ce}), force and active state. Integration of v_{ce} resulted in the new l_{ce}, from which, in combination with the origin-insertion length (l_{oi}), the series elastic element length (l_{se}) was calculated (f_4). Finally, the muscle force was calculated from current SE length (f_5), modelled as a quadratic spring; see table 2.1 and Ridderikhoff et al. (2004) for parameter values.

In order to create force variability, Gaussian distributed noise was introduced at the input stage of the model. The SD of this noise increased linearly with the mean value of $stim$, with a gain of 0.1. In other words, the noise had a constant coefficient of variation (CV) of 0.1. Two regimes were simulated: in the first regime, a new value for $stim$ was drawn from the Gaussian distribution every millisecond. An Euler-Maruyama integration scheme, suitable for studying stochastic differential equations, with a step size of 1ms was used in the simulations. We refer to this model as the Continuous Lumped Model (CLM). In the second regime, the $stim$ value was kept

Table 2.1: *Muscle parameters. All other parameters are either mentioned in the text or are the same as in Ridderikhoff et al. (2004).*

Parameter	Description	Value
F_{max}	Maximum total isometric force [N]	2000
$l_{ce,opt}$	Optimum fibre length [m]	0.136
$l_{se,slack}$	Series elastic slack length [m]	0.170
a	Muscle moment arm [m]	0.03
I	Segment inertia [Nms^2/rad]	0.1

constant over an interval based on the instantaneous firing rate. In this case the forward simulations were performed with a *normal* Euler integration scheme, again with a step size of 1ms. This model will be referred to as the Discrete Lumped Model (DLM). We studied the output variables γ, q and F and their variability for different values of $stim$. Time series of 15s were simulated to quantify (force) variability.

Simulation results and discussion

Figure 2.2 shows how noise on $stim$ propagates through the muscle model with increasing mean levels of $stim$ for both the continuous (left) and the discrete (right) case. Every dot represents the mean and standard deviation of a 15s simulation. The amplitude of the noise on $stim$ was the same in both models, whereas the DLM also contained noise in the timing. In the CLM every mean and SD is based on 15.000 drawings from a Gaussian distribution, whereas the number of drawings in the discrete model is approximately 30 times lower. This accounts for the larger variance in the simulation results of the DLM. The next row of figure 2.2 shows the variability in the calcium concentration. The curve for the continuous model is again linear, whereas that of the discrete model clearly is not. This difference is due to the frequency content of the time series. In the continuous case the frequency content is independent of $stim$, whereas in the discrete case the frequency content increases with higher $stim$. The first order dynamics between $stim$ and γ acts as a low pass filter and as a result the graph of σ_γ against μ_γ is less than linear. In the conversion from γ to q the monotonic relation of mean and standard deviation disappears and changes into a parabolic one. This parabolic relation persists in the force. In contrast, the stan-

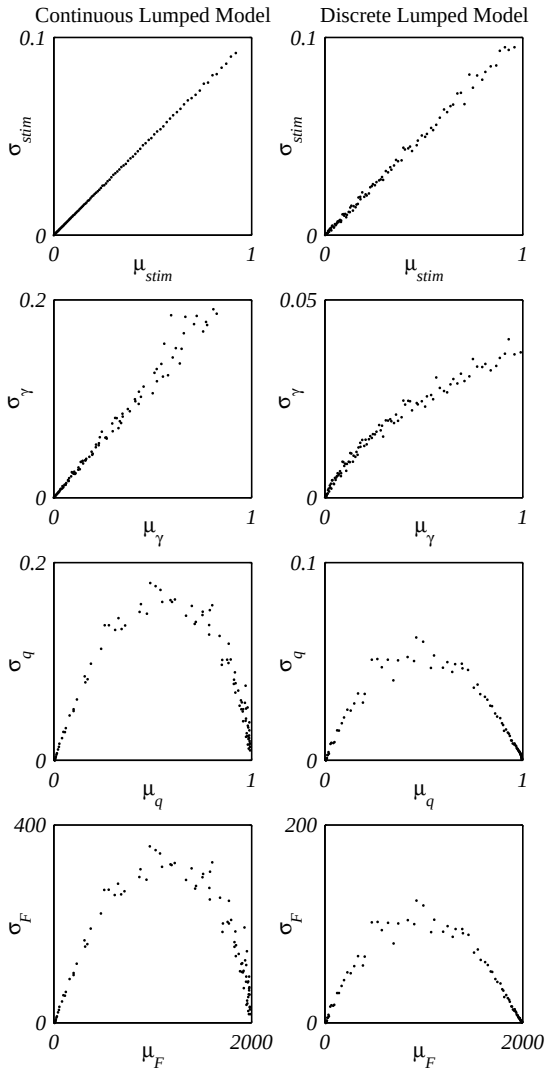

Figure 2.2: *The propagation of noise for increasing average levels of $stim$ in the Continuous Lumped Model (left column) and the Discrete Lumped Model (right column). Note the scale differences in γ, q and F. See text for model descriptions.*

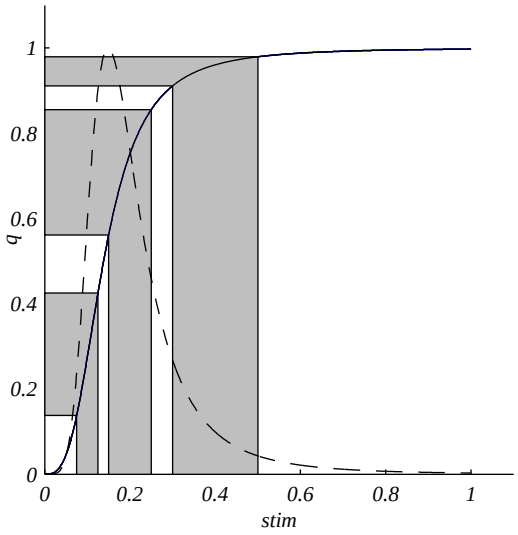

Figure 2.3: *Schematic representation of the noise suppression properties of the CLM. The solid curve represents the steady state relation between $stim$ and active state (q). The bands show the transfer of constant CV stimulus variability to active state variability. The dashed line represents $q \cdot \mathrm{d}q/\mathrm{d}stim$, which is the susceptibility of q to constant CV input noise.*

dard deviation of the force has been shown experimentally to increase monotonically with mean force (Jones et al., 2002; Christou et al., 2002).

Although we can already conclude that the model is inadequate to answer our main question, it is informative to examine which properties of the model render it inadequate for this purpose. The force variability is mainly modulated by the filtering properties of the excitation ($stim$) to activation (q) coupling. Figure 2.3 shows the sigmoid relation between $stim$ and q (solid line) and explains how constant CV variation on $stim$ is heavily attenuated through this relation.

The present results suggest that the filtering properties of the lumped Hill model do not allow modelling of realistic variability in muscular force output. The formulation is a description of average behaviour of all motor units, leaving the processes underlying force variability unaddressed. Whereas the merits of this modelling approach in deterministic simulations are undisputed, it falls short as a basis for studying motor variability.

2. Force variability in a motor-unit pool model

Model and simulation

The organisation of the motor-unit (MU) pool has been mentioned as the main source of isometric force variability (Jones et al., 2002). In the preceding model, the properties of the MU pool were lumped together in $stim$. Since this did not lead to a satisfactory result, the organisation of the MU pool was modelled explicitly.

Figure 2.4 depicts the flow of calculations of the MU pool model. The motor-neuron pool, controlling the motor units, was inspired by the model presented by Fuglevand et al. (1993). Muscular force is modulated by two processes: the number of active motor units (recruitment) and the firing rate of these units (rate coding). In the original formulation, the outputs of the motor neuron pool were the time instances of the discharges. Upon discharge a MU twitch occurred. In our formulation, the motor neuron pool codes the value of $stim_{mu}$ and the time that this value remains constant. A MU is recruited when the excitatory drive (E_{pool}) exceeds the recruitment threshold (*RTE*). The *RTE*s of the different units are expressed as an exponential

$$RTE_{mu} = e^{mu(\ln RR)/n} \tag{2.1}$$

where mu is the index of the motor neuron, RR the recruitment range and n the number of motor units. In our simulations $RR = 30$ and $n = 60$ were used. Upon recruitment the motor neuron starts firing at its minimum firing rate (*MFR*) of 5pps. The firing rate increases linearly with the excitatory drive. The gain (g) of this relation

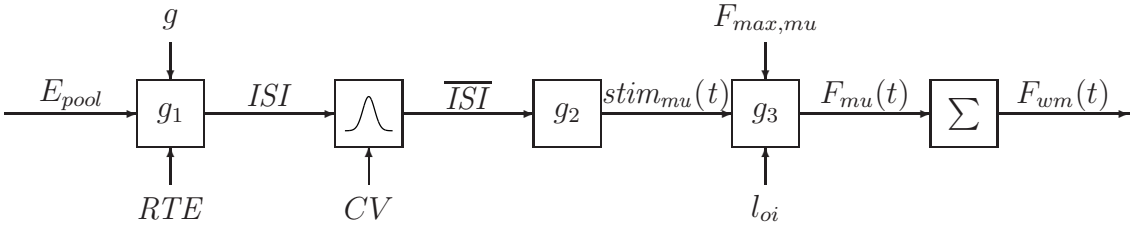

Figure 2.4: *Block diagram showing the flow of calculations in the multiple fibre muscle models. The functions g_1 through g_3 are explained in the text; g_3 comprises the flow diagram of figure 2.1. Two regimes were simulated: with independent tendons (ITM) and with dependent tendons (DTM) of the motor units. E: excitatory drive; ISI: interspike interval of MU; $\overline{ISI}$: Gaussian distributed interspike intervals; $stim_{mu}(t)$: stimulus of MU; $F_{mu}(t)$: MU forces; $F_{wm}(t)$: total force*

is 1.5. The firing rate increases until it saturates at 100pps. Thus, the firing rate (FR_{MU}) response of a motor neuron to a constant excitatory drive is

$$FR_{mu} = g \cdot [E_{pool} - RTE_{mu}] + MFR \qquad E_{pool} \geq RTE_{mu} \tag{2.2}$$

The inverse of the firing rate is the inter spike interval ($ISI_{mu} = 1/FR_{mu}$). These calculations take place in box g_1 in figure 2.4. Fluctuations in the *ISI* due to membrane noise have a Gaussian distribution with a nearly constant CV (Matthews, 1996). For our simulations we chose a CV of 0.2 (Adam et al., 1998). The *ISI* distributions were concatenated to time series of the spiking events of the different MUs. From the ISI we also calculated the normalised firing frequency, which was kept constant within the corresponding inter spike interval ($g_2; stim_{mu}(t)$). The stimulation of a single MU ($stim_{mu}$) is now a representation of its firing rate only.

The maximal isometric force of each MU increased exponentially with the MU number (mu):

$$F_{max,mu} = c \cdot e^{mu \cdot \ln(RF)/n} \tag{2.3}$$

where RF is the range of forces in the pool. In our model the last recruited MU had a maximal force of 30 times the maximal force of the first recruited unit. The parameter c was chosen such that the maximal isometric force of the whole muscle was 2000N.

Two models of the contraction dynamics were formulated (g_3). In the first model every MU, i.e. a lumped cluster of fibres, is described by the equations of the model in section 1. The motor units act independently of one another except for their l_{oi}, resulting in a distribution of l_{ce} and l_{se}. We refer to this model as the Independent Tendon Model (ITM). The second model represents the other extreme of interdependency. All contractile elements attach to the same tendon and all have the same l_{ce} and v_{ce}. We refer to this model as the Dependent Tendon Model (DTM). For this model there is no analytic solution for v_{ce} as a function of F_{ce} and q. In the ITM, F_{ce} equals F_{se}. In the DTM, we only know that the sum of all F_{ce} equals F_{se}. An iterative minimisation of $(\sum_1^{nMU} F_{ce}(v_{ce}) - F_{se})^2$ in every time step of the simulation was used to find the solution; see table 2.1 for the contraction model parameters.

Output variables we looked at were: $stim$, γ, q and F of the individual motor units and their variability for different values of E_{pool}. The main output parameter was the

total force of the muscle (F_{wm}). All calculations were based on 15s time series, which were obtained by Euler integration of the model equations with a time step of 1ms.

Simulation results and discussion

Figure 2.5 shows how SD of total muscle force increases with increasing average simulated whole muscle force, for $l_{oi} = 0.75 \cdot l_{oi,opt}$. The results for $l_{oi} = 0.95 \cdot l_{oi,opt}$ were similar. The force variability increases with the average force. The variability was between 1% and 10% of the average force. This is in accordance with the experimental values of 2% to 10% (Adam et al., 1998; Laidlaw et al., 2000; Jones et al., 2002; Taylor et al., 2003). In the literature there is no consensus about the shape of force variability curves. All studies report a monotonically increasing SD with mean force, but the exact relation is either sigmoid (Slifkin and Newell, 1999; Christou et al., 2002), linear (Jones et al., 2002) or less than linear (decreasing CV, (Laidlaw et al., 2000)).

Figure 2.6 shows how increasing E_{pool} affects the behaviour of the individual motor units. Essentially, the behaviour of the individual units is the same as the behaviour of

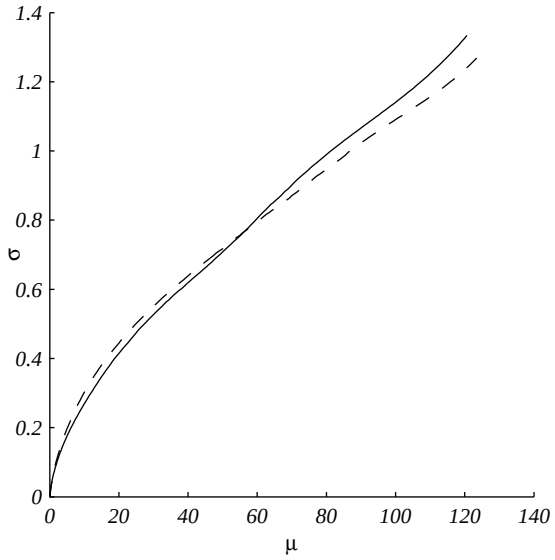

Figure 2.5: *Force variability, expressed as SD (σ), as a function of the average force (μ). Continuous line for the ITM and dashed line for the DTM. The origin-insertion length (l_{oi}) was* $0.75 \cdot l_{oi,opt}$.

the DLM. For clarity only motor units 1, 20, 35 and 50 are shown, at an l_{oi} of $0.75 \cdot l_{oi,opt}$. For $stim$, γ and q the ITM and DTM do not differ markedly and we will discuss them together. In the μ_{stim} curves we recognise equation 2.2 with different RTE for the units and a gain of 1.5. Although the model was constructed to saturate at 1, the stochastic model saturates at a lower value. One can understand this from cutting off the Gauss distribution when approaching the saturation value of 1. This also accounts for the drop and saturation in the σ_{stim} curves. The second row presents the calcium concentration γ. First order dynamics link γ and $stim$. Therefore μ_γ reacts exactly the same to E_{pool} as μ_{stim}. Increasing E_{pool} results in a shift of the main frequency of $stim$. The low-pass filtering properties of the excitation dynamics now suppress the variability of γ (See also section 1). The third row presents the active state q. The relation between E_{pool} and q is sigmoid and therefore σ_q drops after μ_q exceeds 0.5.

From the forces, depicted in the fourth row, we observe that the largest contribution to the force comes from the last recruited units. More importantly, also the force variability is mainly determined by the last recruited MUs. The relative contribution of every MU to the total force and the total force variability is determined by the number of MUs (nmu), the range of MU forces (RF) and the recruitment range (RR) in equations 2.1 to 2.3. The values used in this study are within the physiologic range and changes only mildly alter model behaviour.

Furthermore, several differences between the ITM and DTM come to the fore. In the ITM, μ_F of the individual units saturates, whereas in the DTM the force reaches a peak and then slightly decreases. In the ITM, the l_{ce} of the MUs is fixed after having reached maximum activation. In the DTM, the l_{ce} is not only determined by the activation of the unit itself, but also by the activation of the surrounding units. This is reflected as a higher variability of the DTM in the low force range and a lower variability in the high force range compared to the ITM (figure 2.5).

In conclusion, both the ITM and the DTM exhibit realistic force variability. The models are on the extremes of motor unit interdependency and will be used in addressing the issue of kinematic stability.

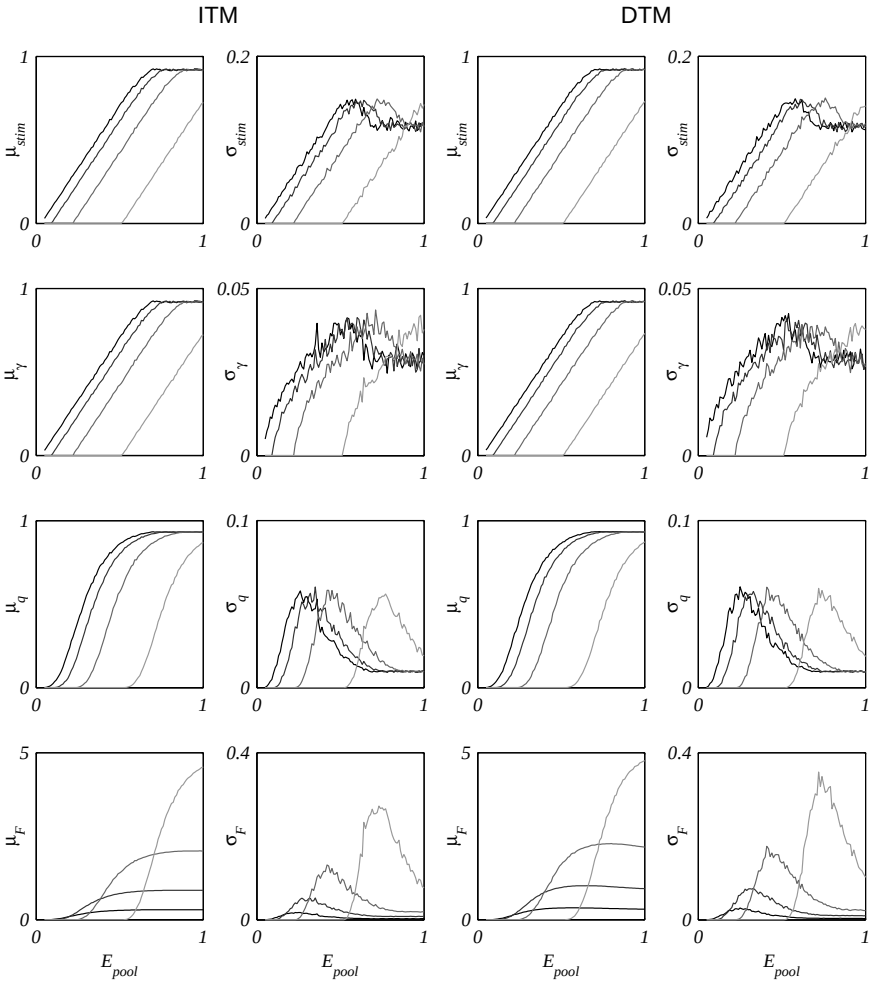

Figure 2.6: *The influence of ISI variability of motor units 1, 20, 35 and 50 on individual motor-unit behaviour in the Independent Tendon Model (ITM, columns 1 and 2) and the Dependent Tendon Model (DTM, columns 3 and 4).* l_{oi} *was* $0.75 \cdot l_{oi,opt}$*. Average behaviour (columns 1 and 3) and variability (columns 2 and 4) of the individual motor units is presented as a function of* E_{pool} *for the excitation (*$stim$*), the calcium concentration (*γ*), the active state (*q*) and the force (*F*). See main text for model descriptions and discussion.*

3. Kinematic stability of the motor-unit pool model

Model and simulation

In order to investigate the relation between force variability, co-activation, impedance and kinematic variability, two neuro-musculo-*skeletal* models were constructed with respectively the ITM and DTM as actuators (see figure 2.7). The planar skeletal model comprised an inertia, connected to the stationary world by means of a frictionless hinge joint. Two antagonistic muscles modelled as in section 2 were connected to the inertia. In addition to the forces, the neuromuscular models also provide the model with stiffness and damping resulting from their length-force and velocity-force relations. No passive stiffness and damping were included. The only objective was to show that co-activation can in principle be an effective strategy to reduce kinematic variability. With no particular joint in mind, the model was symmetric and the moment arms of the muscles were constant; see table 2.1 for the values used. The parameters of the muscles and the inertia are in the range of those known for the lower arm.

The model was simulated at an equilibrium angle of 0 (symmetric case) and 10

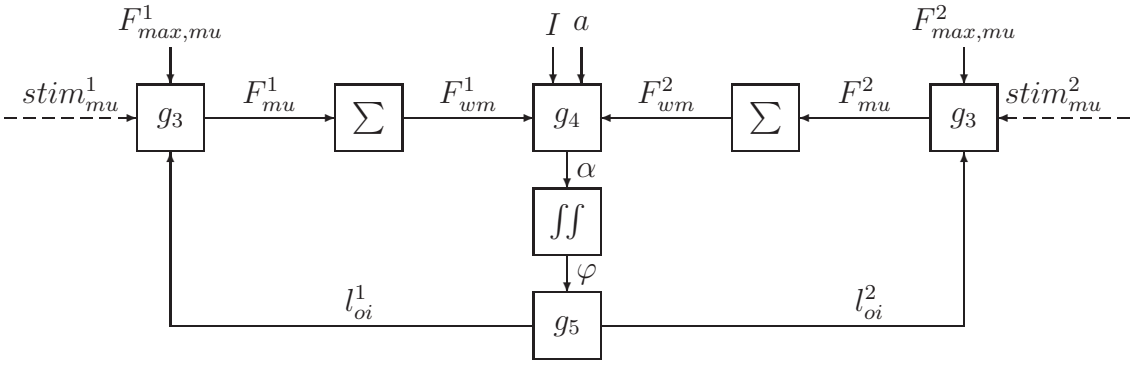

Figure 2.7: *Block diagram showing the flow of calculations for the kinematic stability simulations. The $stim_{mu}$ come from the alpha motor neuron pools of the individual muscles as described in the previous section. The function g_3 comprises the block diagram of figure 2.1 and calculates the individual MU forces (F_{mu}), given the origin-insertion length (l_{oi}). Summation results in the whole muscle forces (F_{wm}), the net moment of which results in an angular acceleration of the inertia (g_4, inputs I (inertia) and a (moment arms)), leading to an angular displacement (φ). This angular displacement creates a negative feedback loop via the l_{oi} of the individual muscles.*

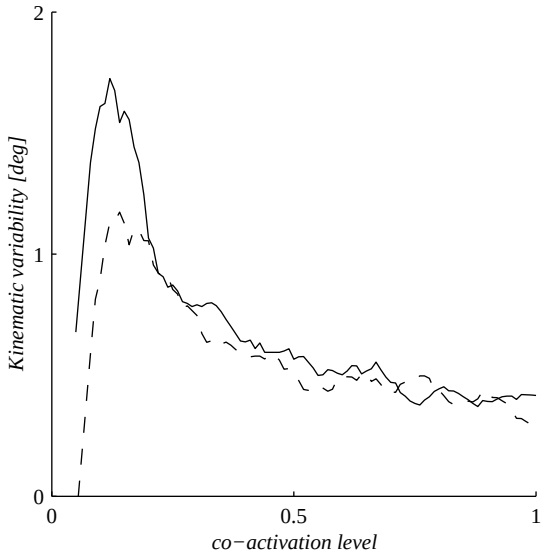

Figure 2.8: *Kinematic variability as a function of co-activation level for the symmetric model. Continuous lines for the ITM and dashed lines for the DTM. The kinematic variability is expressed as SD of the joint angle.*

(asymmetric case) degrees. The latter value was chosen to investigate the effects of asymmetric muscle length and activation. Again time series of 15s were simulated with an Euler integration scheme. Output parameters were the joint angle and the forces of the individual muscles. Co-activation level was expressed as the E_{pool} value of the most active muscle.

Additional simulations were performed to reveal the impedance characteristics of the models. The model was perturbed by a simulated external torque pulse of 1Nm. The impedance was estimated by calculating $\mathrm{d}M/\mathrm{d}\varphi$ over the first 10ms after perturbation onset.

Simulation results and discussion

Figure 2.8 shows the kinematic variability, expressed as SD of the joint angle, as a function of the co-activation level, in the symmetric case for both the ITM and DTM. Both models show a peak in the kinematic variability, irrespective of model asymmetry (not shown in the figure). These peaks are a consequence of two competing factors: force variability and impedance. Figure 2.9 illustrates the results of simulations of

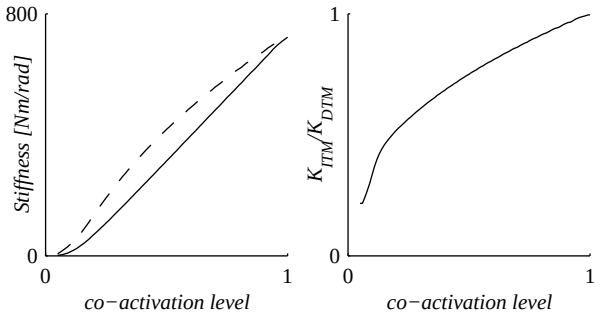

Figure 2.9: *Left: Stiffness estimate of the symmetric ITM (continuous) and DTM (dashed) obtained from simulations of an external perturbations of the inertia. Right: Relative stiffness (K_{ITM}/K_{DTM}).*

an external perturbation. The left panel shows how the impedance changes with the co-activation level. The force variability increase with co-activation is similar to that in the isometric contractions (figure 2.5). Without impedance, the increasing force variability would bring about ever larger kinematic fluctuations, as is visible at low co-activation levels in figure 2.8. The increasing impedance due to co-activation attenuates this effect and eventually decreases the kinematic variability although the force variability still increases.

The above explanation implies that increasing the inertia of the system would shift the peak kinematic variability to higher co-activation values. Furthermore, introducing more force variability, for instance by introducing noise in E_{pool}, would shift the peak kinematic variability to lower values of co-activation and eventually lead to a monotonically decreasing kinematic variability as a function of co-activation. The ITM was put to the test for both manipulations of the model (see figure 2.10) and our expectations were indeed confirmed. The effect of a 10-fold inertia increase was only diminutive, suggesting that the model is rather insensitive to inertia changes. On the other hand, the addition of noise in E_{pool} changes the overall properties of the model and results in a monotonic decrease of kinematic variability with co-activation level.

Based on isometric force variability, we were unable to distinguish between the ITM and the DTM. As regards the kinematic variability there is a marked difference between both models. Especially in the low co-activation range, the DTM shows less

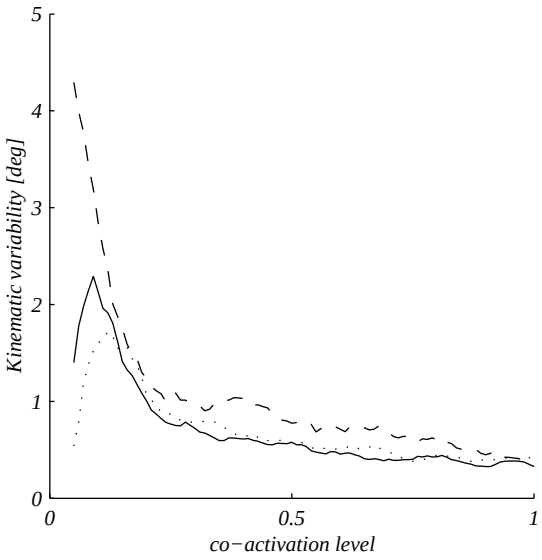

Figure 2.10: *Excitation (E_{pool}) variability and inertia manipulations in the ITM. Excitation variability was enhanced by introducing signal dependent noise (CV=0.2) in E_{pool} (dashed line, $CV = 0.2$). The dotted line presents results for a model without noise on E_{pool} and an inertia 10 times that in the standard model. The solid line represents the standard model.*

kinematic variability than the ITM. The force variability of the two models was not markedly different, suggesting that impedance is the key factor. Nevertheless, from the co-activation vs. impedance curves (left panel figure 2.9) no clear distinction can be made. When we look at the relative impedance (right panel figure 2.9) we see that the DTM is much stiffer than the ITM, especially at low co-activation levels. This accounts for the differences in the kinematic variability between the ITM and the DTM. In reality the mechanical interaction between MUs will be somewhere in between the two models. How the modulation of muscular co-activation affects kinematic variability depends, according to our model, particularly on the central and peripheral noise levels in the neural system and the mechanical interactions of individual MUs within a muscle and the mechanical interactions between muscles.

General discussion and conclusions

Our first concern in the present study was to build a model of muscular contraction, and thus force generation, that produces realistic force variability. Prior attempts to simulate force variability were all based on motor unit pool models in combination with twitch forces (Van Galen and De Jong, 1995; Jones et al., 2002; Taylor et al., 2003). These models revealed that the architecture of the MU pool plays a key role in force variability. We came to the same conclusion: The discrete nature of force generation and the MU pool architecture are essential ingredients to generate force variability. However, contrary to previous efforts, we included a contraction model. In this approach, the force is not only a function of the stimulation but also of muscle length and contraction velocity. With regard to force variability, this addition does not significantly affect the results, but the extended model allowed us to study the effects of force fluctuations on kinematic variability.

The relation between variability and motor control has recently been extensively studied in the field of computational motor control (Harris and Wolpert, 1998; Hamilton and Wolpert, 2002; Todorov and Jordan, 2002). Continuous stochastic optimal control strategies resulted in model behaviour that resembled experimental findings. Although these models provide clues about what the neural system is controlling, our results reveal some important shortcomings. First, the discrete nature of information processing influences the variability characteristics of the forces. Second, as was demonstrated here, these models lack antagonistic muscle function. Antagonistic muscles might act as a mechanical filter in that they may suppress, through co-activation, the effects of force variability on kinematic variability.

Combining a MU-pool model with a model of muscular contraction dynamics is a means to incorporate impedance into the model. The importance of adding contraction dynamics to the motor unit pool model is manifest in the relation between force variability and kinematic variability. Net moment changes due to force fluctuations of the individual muscles are attenuated and eventually suppressed by the intrinsic stabilising properties (impedance) of the antagonistic muscles. In reality, reflex components also contribute to joint dynamics in postural tasks. Reflexes contribute to the movement itself in the lower extremities in gait(e.g. Mazzaro et al., 2005). For the upper extremity such contributions are unlikely because external perturbing contact forces are absent. In the upper extremity, reflexes are likely required to overcome drift from the desired trajectory or position, which in a limited number of simulations

occurred. Further research into the function of (noisy) spindle- and Golgi-tendon feedback loops during, externally, unperturbed movements is needed. For now we want to stress that MU activation is the final common path of both central and peripheral inputs and as such determines force and moment fluctuations.

In the literature it has been suggested that kinematic variability decreases monotonically with co-activation (Van Galen and De Jong, 1995). Especially in the low co-activation range, our model is sensitive to the choice of parameters in model simulations of this hypothesis. However, our simulations started at zero levels of activation. This is unrealistic given the presence of gravity. As a result humans seldom act in the lowest co-activation range of our model. Moreover, when noise was added to the central commands a monotonic relation emerged, implying that in practise a monotonic relation between cocontraction and kinematic variability for the lower cocontraction range can be expected. Only very recently our assumption of constant CV over the range of inter spike intervals has been refuted (Moritz et al., 2005). The CV was found to decrease exponentially over the force range. Implementation of this fact in the model will probably also direct the model to monotonically decreasing kinematic variability with co-activation. At high co-activation levels, the kinematic variability of our model stabilises. In reality, synchronisation might occur at high co-activation levels, possibly leading to an increase in force variability, which becomes apparent as tremor (i.e. kinematic variability in a specific frequency band (e.g. McAuley et al., 1997)).

The ITM and DTM are two extreme cases of interdependency of the MUs, and thus of muscle impedance. In reality, the interdependency of the MUs will fall in between the ITM and DTM. Differences in kinematic variability between the ITM and DTM are only prominent at low levels of stimulation. This is, however, the working range for most tasks in daily live. But, as we stated before, model behaviour is also influenced by several other (neural) factors in this region and a deliberate classification of their importance cannot be made at the moment.

This study underscores that the strategy of the neural system to control the effects of force variability on kinematic variability strongly depends on neural noise levels and sources, muscular architecture and skeletal properties. As such, it represents a first step in understanding how energetic and accuracy constraints might interfere within the motor control system.

3

Impedance is modulated to meet accuracy demands during goal-directed arm movements

Selen L.P.J., Beek P.J. & Van Dieën J.H. (2006). Impedance is modulated to meet accuracy demands during goal-directed arm movements. *Experimental Brain Research*, 172(1), 129–138.

The original paper can be found on:
http://www.springerlink.com/content/p4010377845j0886

Abstract

The neuromuscular system is inherently noisy and joint impedance may serve to filter this noise. In the present experiment, we investigated whether individuals modulate joint impedance to meet spatial accuracy demands. Twelve subjects were instructed to make rapid, time constrained, elbow extensions to three differently sized targets. Some trials (20 out of 140 for each target, randomly assigned) were perturbed mechanically at 75% of movement amplitude. Inertia, damping and stiffness were estimated from the torque and angle deviation signal using a forward simulation and optimization routine. Increases in endpoint accuracy were not always reflected in a decrease in trajectory variability. Only in the final quarter of the trajectory the variability decreased as target width decreased. Stiffness estimates increased significantly with accuracy constraints. Damping estimates only increased for perturbations that were initially directed against the movement direction. We concluded that joint impedance modulation is one of the strategies used by the neuromuscular system to generate accurate movements, at least during the final part of the movement.

Introduction

Signal-dependent neuromotor noise is supposed to underlie variability in biological movement (Schmidt et al., 1979; Harris and Wolpert, 1998; Jones et al., 2002; Todorov and Jordan, 2002). Because of the noise in neuromuscular transmission and the orderly recruitment of motor units according to the size principle (chapter 2, Jones et al., 2002), muscular forces show an approximately linear relationship between their mean and standard deviation (SD) (Schmidt et al., 1979; Christou et al., 2002; Todorov and Jordan, 2002). Obviously, such noise will limit the accuracy of goal-directed movements. Historically, research on goal-directed movements has focused on the relation between movement speed and endpoint accuracy. Since the pioneering studies of Woodworth (1899) and Fitts (1954), various studies have corroborated the general finding that movement speed and endpoint accuracy are inversely related (see Plamondon and Alimi, 1997, for a review) and this relation has been attributed to signal-dependent neuromotor noise (Schmidt et al., 1979; Harris and Wolpert, 1998; Elliott et al., 2001). Nevertheless, the same movement, i.e. same amplitude and same movement time, can be achieved with different levels of endpoint accuracy (Laursen et al., 1998; Gribble et al., 2003; Osu et al., 2004). This raises the question which mechanisms, besides speed, are employed by the motor system to meet spatial accuracy demands.

Van Galen and De Jong (1995) proposed that modulation of joint impedance might be used to control spatial accuracy. To date, joint impedance has been studied mainly in relation to external perturbations (e.g. Burdet et al., 2001; Franklin et al., 2003). The general finding is that increasing joint impedance, both through cocontraction and reflex modulation, stabilises the limb to external force fields. Neuromuscular noise, however, is an internal source of perturbation. In this case, the muscles, paradoxically, would both form the source of motor variability and provide the means for suppressing its kinematic consequences. Modelling studies have shown that in spite of this paradox, co-activation of muscles can reduce the effects of force variability on kinematics (chapter 2, Van Galen and De Jong, 1995). It is, however, insufficiently clear whether humans actually use this control strategy.

Indirect measures of increased impedance, like pen pressure and increased EMG amplitudes, have been reported in response to increased accuracy demands (e.g. Van Gemmert and Van Galen, 1997; Laursen et al., 1998; Van Galen and Van Huygevoort, 2000; Gribble et al., 2003; Osu et al., 2004; Visser et al., 2004;

Sandfeld and Jensen, 2005; Van Roon et al., 2005). Although muscular co-activation and stiffness are related (Osu et al., 2002), direct estimates of stiffness and damping are required to quantify the magnitude of impedance modulation and to account for the dissociation of EMG and impedance with fatigue (Zhang and Rymer, 2001).

Thus far, to our knowledge, the relation between kinematic variability and impedance was only examined in two studies, in both cases as a corollary of the main research question. Shiller et al. (2002) reported that the kinematic variability in vowel production co-varied with jaw stiffness. However, the stiffness was largely determined by the jaw geometry in this study, which suggests that the reported co-variation was merely a by-product of the geometry rather than an active motor control strategy. Furthermore, accuracy was not manipulated and thus it is unknown whether the impedance level was modulated to match accuracy demands. The experiment of Burdet et al. (2001) provided more convincing evidence for the usefulness of stiffness regulation with accuracy demands. They invited subjects to make point-to-point movements in a negative elastic force field perpendicular to the movement direction. In order to hit the target, subjects increased the stiffness of the arm selectively in the direction of the force field. Strikingly, trajectory variability was lower after removal of the force field than prior to exposure to the force field, indicating that stiffness modulation can indeed help to diminish kinematic variability. Although there are some indications that impedance might be modulated in response to accuracy demands, direct mechanical evidence is lacking. The present study aims at filling this lacuna. Endpoint accuracy demands were manipulated in time-constrained elbow movements. Estimates of elbow impedance were obtained by applying torque perturbations to the arm during movement. We hypothesised that subjects modulate joint impedance to meet accuracy demands.

Methods

Subjects

Twelve subjects (4 males and 8 females) between 20 and 28 years of age participated in the experiment. All subjects had normal or corrected to normal vision and no (history of) neuromuscular disorders. The experiment was approved by the local Ethics Committee and all subjects signed informed consent forms prior to the experiment. The experiment took less than four hours and subjects were allowed to rest frequently to avoid fatigue.

Apparatus

Subjects were seated on a chair in front of a semicircular array of light emitting diodes (LEDs). Their preferred forearm, including the hand palm and wrist, was cast (Noba-Cast, Noba Verbandmittel Danz GmbH) onto a lightweight T-wedged bar. The bar was mounted onto the vertical motor shaft of a torque controlled motor (S-motor, elu93028, Fokker Control Systems), with the medial epicondyle aligned with the motor axis of rotation and the palm of the hand facing downward.

The chair height was adjusted such that the upper arm and forearm were in the horizontal plane. The upper arm was in line with the shoulders. The LED-array, consisting of 447 LEDs, was placed 1.5 m in front of the wrist of the cast arm. The arm pointed to the centre of the LED-array at an elbow angle of 90°. A small laser pointer was attached to the lightweight bar and indicated the pointing direction on the LED-array. Four LEDs were illuminated, defining the boundaries of the start and target areas (see figure 3.1).

The torque controlled motor operated in closed loop at 5 kHz. In the unperturbed trials the set point of the controller was 0 Nm, allowing smooth and frictionless movements by the subject. The angular position of the motor shaft was measured by a potentiometer (22HSPP-10, Sakae) and the remaining torque was measured by a strain gauge. Both position and torque were stored at 1kHz.

In the perturbed trials, the set point of the motor torque changed when passing the 75% point of the movement amplitude. This point was chosen because in an earlier study (Osu et al., 2004) both kinematic variability and muscular activity were influenced by accuracy demands only in the final part of the movement, suggesting that joint impedance was controlled only, or at least predominantly, in the final part of the movement. The applied torque pulse had a duration of 140ms. The torque pulse changed sign after 70ms in order to prevent the optimization routine from getting trapped by the co-linearity of angle, angular velocity and angular acceleration. Torque amplitude was set to 5Nm. The total motor-subject dynamics prohibited the system from exactly generating this value (see figure 3.2), but torque profiles were reproducible within and between experimental conditions.

Experimental task

Subjects were asked to perform rapid pointing movements, 0.26 rad in 300ms, by elbow extension from the start area to the target area. Three blocks, each with a

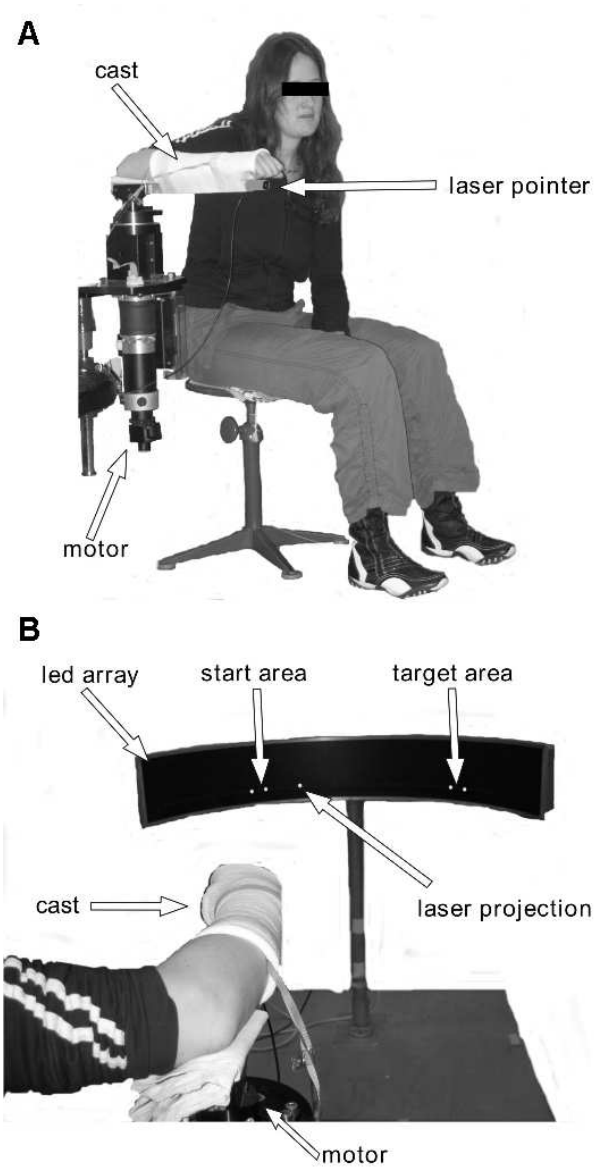

Figure 3.1: *Experimental setup for the goal-directed movements with different target areas. A) Side-front view of a subject with the forearm cast onto a lightweight bar attached to the motor. B) The led array with the start area, target area and the laser projection. The screen that provided the subject feedback about target based movement time (tarMT) and 'hit' or 'no-hit' after each trial is not depicted.*

differently sized target, of 165 trials were executed. Blocks with small, medium and large target areas, corresponding to 0.015, 0.030 and 0.045 rad elbow angle, were presented in random order. In all conditions the distance between the target centres was 0.26 rad. Each block started with 25 practise trials. From the subsequent 140 trials, 20 randomly selected trials were perturbed. Two types of perturbation were applied: 1) initial perturbation in flexion direction while extending the elbow (pFLEX) and 2) initial perturbation in extension direction while extending the elbow (pEXT). Figure 3.2 shows an example of both types of perturbation and their kinematic consequences. Although the perturbations were applied toward the end of movement, leaving insufficient time ($<$ 170ms) to voluntarily react to the perturbation before movement completion, subjects were instructed not to intervene with the perturbations and to focus on the next trial to come.

A trial started by illuminating the boundaries of the start and target boundaries upon which the subject positioned the pointer in the start area. After 500ms, a short beep indicated that the subject was allowed to start the movement. After 3000ms, the boundaries of the start and target areas were extinguished. Subsequently, the movement time was calculated and presented to the subject on a computer screen. Movement time (MT) was defined as the time between leaving the largest start area and entering the largest target area in order to keep the amplitude over which MT was calculated constant. In addition to the calculated MT, the range of desired movement times (270-330ms) was presented. The inclusion of a MT criterion was intended to suppress the natural strategy to move slower when confronted with higher accuracy constraints. Furthermore, a 'hit' or 'no-hit' signal was presented to the participant in the form of a green or red button on the same screen as the MT. A 'hit' required the subject to stay within the target area for at least 500ms after entering it. For every temporally as well as spatially correct trial the participant earned €0.05. In order to keep the subject motivated, the total accumulated credit was also presented on the screen.

Prior to the actual experiment, the same perturbations, 7 times within a time-span of 15 seconds, were applied to the stationary arm in neutral position, i.e. 90° elbow flexion in two conditions. In the 'relaxed ' condition, subjects were instructed not to tense their muscles and not to respond to the perturbations. From these perturbations independent estimates of combined arm and manipulandum inertia were obtained. In the 'stiff ' condition, subjects were instructed to maximally co-activate their muscles and to minimise the angular displacements as a result of the perturbations. The cal-

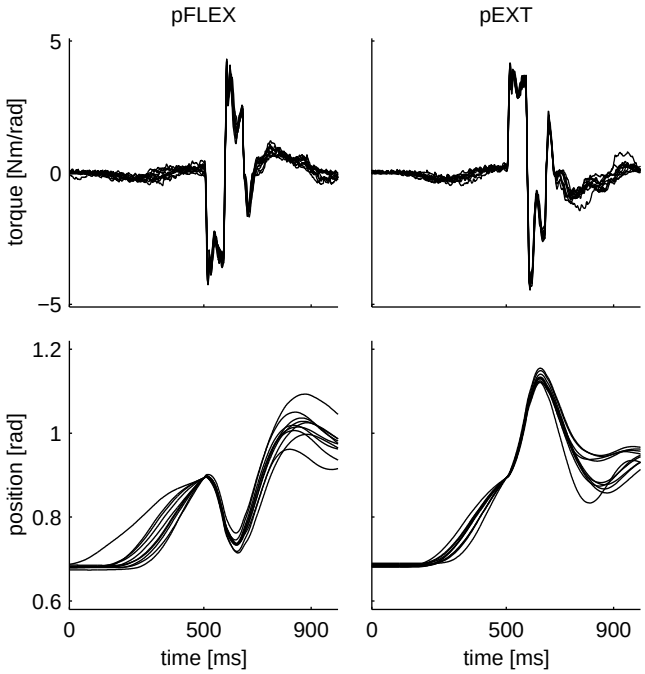

Figure 3.2: *Examples of the torque and position profiles for the two perturbation types in one subject. pFLEX torque initially opposes movement for 70ms and subsequently assists the movement for 70ms. pEXT torque initially assists movement for 70ms and subsequently opposes movement for 70ms. Torque amplitude was set to 5Nm, but total motor-subject dynamics prohibited exact generation of this profile.*

culated values for stiffness and damping were used to quantify relative stiffness and damping during movement.

Effectiveness of accuracy manipulation and MT feedback

The effectiveness of the accuracy manipulation and the MT feedback was investigated in both the entire dataset and in the subset of trials in which the imposed temporal and the spatial constraints were matched (see above). In the present study, we looked for strategies other than speed to meet accuracy demands. Therefore MT should not systematically change with target size. Temporal changes were investigated for two measures of movement time. The first measure was the one presented to the subject, it was defined as the time between leaving and entering the largest target area (from now on called 'target based MT': tarMT). The second measure was the time between movement start and movement end (from now on called 'kinematic based

MT': kinMT). Movement start was defined as the instant at which the angular velocity first exceeded 0.05 rad/s. Movement end was defined as the first instant at which the pointer was within the largest target area and the angular velocity was below 0.05 rad/s. Furthermore, the maximum velocity and the time to peak velocity after movement onset were computed in order to check for changes in the velocity profiles.

Spatial accuracy in relation to target size was investigated by calculating the standard deviation of the position at the end of the movement. Furthermore, we counted all trials, for each target area, in which the spatial and temporal constraints for the smallest target area were matched. If the accuracy manipulation had been effective, the number of trials thus counted should decrease with larger targets.

Trajectory variability was assessed by calculating the between trial SD as a function of time. Before calculating the evolution of the SD with time, position data were time normalised, between movement onset and movement end, by cubic spline interpolation.

Estimation of elbow impedance

The dynamics of a joint in response to an external mechanical perturbation can be approximated by a *K-B-I* model (*K*=stiffness, *B*=damping and *I*=inertia):

$$M_{ext} = K \cdot \varphi_{rel} + B \cdot \dot{\varphi}_{rel} + I \cdot \ddot{\varphi}_{rel} \tag{3.1}$$

The external moment (M_{ext}) leads to a position (φ_{rel}), velocity ($\dot{\varphi}_{rel}$) and acceleration ($\ddot{\varphi}_{rel}$) change relative to the intended unperturbed trajectory. The intended propagation of the perturbed trajectory can only be estimated by extrapolation of the trajectory prior to perturbation (Burdet et al., 2000; Popescu et al., 2003). Extrapolation is based on selection of unperturbed trajectories that are similar, in a least squares sense, to the perturbed trajectory prior to perturbation. In order to guarantee convergence of the perturbed and unperturbed trajectory toward the instant of perturbation, the distance was weighted exponentially prior to averaging. The similarity (S) between two trajectories was expressed as:

$$S = \sum_{t=t_0-500}^{t=t_0} e^{t-t_0+500/w} \cdot (\varphi_u(t) - \varphi_p(t))^2 \tag{3.2}$$

The weighting exponential was scaled by a factor w with a value of 100ms, resulting in a 150-fold weighting of the distance between the trajectories at perturbation relative to the weighting 500ms prior to perturbation. The variables $\varphi_u(t)$ and $\varphi_p(t)$ are the

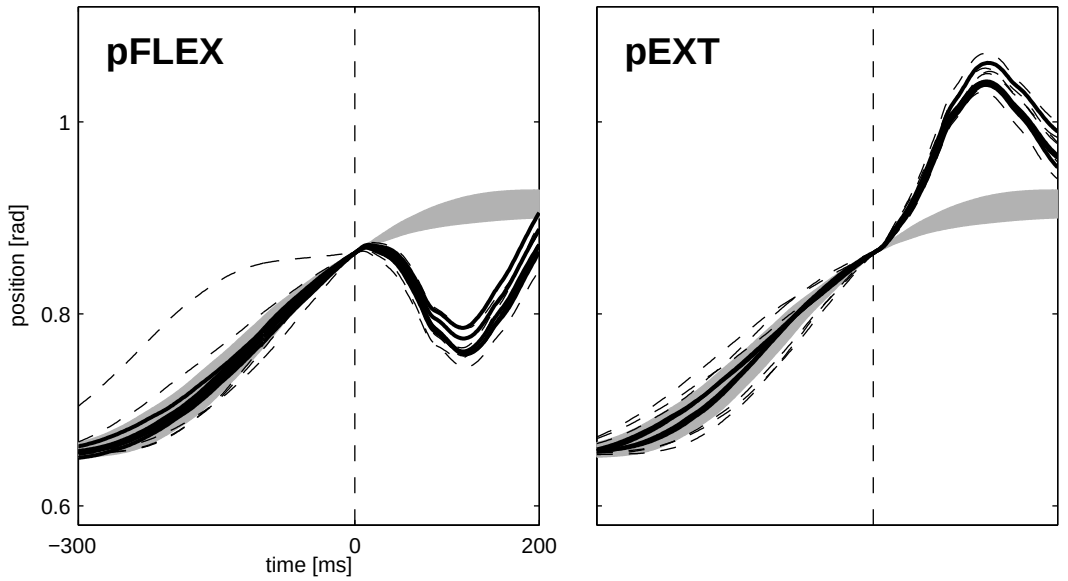

Figure 3.3: *The 95% confidence interval for the correct unperturbed trials (grey area) with superimposed the 10 perturbed trials for pEXT and pFLEX for one subject. Continuous lines represent the trials that fell within the 95% confidence interval and dashed lines those outside this interval. All trials were aligned at the perturbation angle, which is indicated by the dashed vertical line.*

unperturbed and the perturbed position, respectively. Time is expressed in milliseconds in the above equation, with t_0 representing the time that the perturbation angle is traversed.

If for each perturbed trajectory the most similar unperturbed trajectory is chosen for comparison, the number of trials to derive impedance estimates from is equal to the number of perturbed trials. Bearing in mind the imposed spatial and temporal constraints were not met in a significant number of unperturbed trials, it was expected that a similar percentage of the perturbed trials would also not have met the constraints (see figure 3.3). The best possible estimator for the correctness of a perturbed trial is the number of correct unperturbed trials that is similar (S greater than some predefined value S_{min}) to the perturbed one up to the point of perturbation. However, analysis of the unperturbed trials revealed that high similarity before a certain point in time does not necessarily result in high similarity after that point in time. Therefore the angular differences between the 10% most similar perturbed and unperturbed trajectories were selected for further analysis (thereby including the same perturbed trial multiple times, but each time with another unperturbed match). The average angular

difference between the selected trajectories (φ_{rel}) was taken as input to the parameter optimization procedure.

In order to estimate stiffness, damping and inertia for all experimental conditions, seven optimisations were performed per subject. In the first optimisation, the inertia was determined separately, from the perturbations of the relaxed arm. Given the model parameter I and the time series of M_{ext}, the angular response was simulated over 70ms using Heun's method:

$$\varphi_{sim}(T) = \int_{t=0}^{t=70ms} \left(\int_{t=0}^{70ms} \frac{M_{ext}(t)}{I} dt \right) dt \tag{3.3}$$

The inertia was optimised by minimising the objective function:

$$E_{inertia}(\varphi_{rel}, \varphi_{sim}) = [\varphi_{rel} - \varphi_{sim}] \cdot [\varphi_{rel} - \varphi_{sim}]^T + [min(\varphi_{rel} - \varphi_{sim}, 0)] \cdot [min(\varphi_{rel} - \varphi_{sim}, 0)]^T \tag{3.4}$$

The second term in equation 3.4 was introduced to force the optimisation to favour solutions that yielded an angular deviation slightly larger than the experimental data. Test optimisations revealed that inertia was overestimated without inclusion of this term, resulting in negative damping values to accommodate for the large inertia in the remaining simulations.

Given the inertia, *K* and *B* were determined for the three target areas and the two perturbation types separately over the first 170ms after the onset of the perturbation. As stated before, within this time window, subjects are unable to voluntarily react to the perturbation due to neuromuscular delays. The objective function to be minimised by optimising *K* and *B* was:

$$E(\varphi_{rel}, \varphi_{sim}) = [\varphi_{rel} - \varphi_{sim}] \cdot [\varphi_{rel} - \varphi_{sim}]^T \tag{3.5}$$

Using

$$\ddot{\varphi}_{sim}(t) = \frac{-B \cdot \dot{\varphi}_{sim}(t) - K \cdot \varphi_{sim}(t) + M_{ext}(t)}{I} \tag{3.6}$$

to calculate φ_{sim} by numerical integration.

To optimise estimates for *I*, *B*, and *K* a simulated annealing algorithm (Goffe et al., 1994) was implemented. After optimisation the variance accounted for (VAF) was calculated as an index of the validity of the parameter estimates:

$$\text{VAF} = 1 - \frac{[\varphi_{rel} - \varphi_{sim}] \cdot [\varphi_{rel} - \varphi_{sim}]^T}{[\varphi_{rel} \cdot [\varphi_{rel}]^T} \tag{3.7}$$

A value of 1 indicates that no differences exist between the measured and the simulated position deviation.

Using a similar approach, estimates of maximum stiffness and damping were calculated from the perturbations in the 'stiff ' condition.

Statistics

Both in the text and in the figures, the data are presented as means and standard deviations. To examine the effects of target size on movement time and accuracy a repeated measures ANOVA was carried out. Changes in the distribution of MT with target size were investigated using repeated measures MANOVA with the 15^{th}, 50^{th} and 85^{th} percentile of MT as dependent measures. The velocity profiles were checked for changes in skewness using a repeated measures MANOVA with peak velocity and time to peak velocity as dependent measures.

Impedance changes with target size were first examined in a two-way repeated measures MANOVA (Target Size $\times$ Perturbation Type) with *K* and *B* as measures. The same procedure was applied for the perturbation types separately. Both the one- and two-way MANOVAs were followed by repeated measures ANOVAs for *K* and *B* separately. Honest significant difference (HSD) Tukey's tests were used to further analyse significant effects in all cases. An alpha level of 0.05 was chosen for all tests.

Results

Temporal and spatial constraints

The average target based movement times (tarMT) for the small, medium and large target area were 300 (SD 31), 291 (SD 17) and 290 (SD 15) ms, respectively, and were not significantly affected by the size of the target area ($F_{(2,22)} = 1.285, p = 0.297$). Also the kinematics based movement times (kinMT) were not significantly different

Table 3.1: *Movement times for the small, medium and large target of the selected trials. The 15^{th}, 50^{th} and 85^{th} percentile ($p15$, $p50$ and $p85$) are presented for both the kinematics based target time (kinMT) and the target based movement time (tarMT). The only significant effect with target size was found for the 85^{th} percentile of kinMT.*

	kinMT [ms]			tarMT [ms]		
	$p15$	$p50$	$p85$	$p15$	$p50$	$p85$
Small	434 (45)	499 (62)	589 (60)	273 (8)	296 (10)	323 (8)
Medium	430 (23)	485 (33)	563 (38)	270 (4)	292 (6)	320 (8)
Large	431 (31)	481 (36)	549 (43)	269 (3)	291 (6)	319 (5)

($F_{(2,22)} = 0.536, p = 0.593$), with values of 513 (SD 49), 508 (SD 27) and 504 (SD 31) ms from the smallest to the largest target area. The variability of tarMT, expressed as the 15^{th} and 85^{th} percentile, differed from the predefined range of 270-330ms. The 15^{th} percentile was smaller than 270ms (233 (SD 21) ms, $t_{(35)} = -10.551, p < 0.000$) and the 85^{th} percentile was larger than 330 ms (360 (SD 39) ms, $t_{(35)} = 4.534, p < 0.000$). However, there was no effect of target size on the distribution of tarMT ($F_{(6,42)} = 0.487, p = 0.814$) nor of kinMT ($F_{(6,42)} = 1,645, p = 0.159$) with the 15^{th}, 50^{th} and 85^{th} percentile as measures.

Only those trials that met the tarMT criterion of 270-330ms were included for further analysis. For this subset the distribution of tarMT ($F_{(6,42)}, p = 0.241$) and kinMT ($F_{(6,42)}, p = 0.203$) was also not significantly different between the three target areas. From these trials, only those that remained within the target area for at least 500ms were selected. After this elimination procedure only 38 (SD 10), 48 (SD 5) and 53 (SD 5) % of the 120 unperturbed trials remained, reflecting the decreasing difficulty with increasing target area ($F_{(2,22)} = 21.573, p < 0.000$, see figure 3.6, panel D). However, for this subset kinMT differed significantly between target areas ($F_{(6,42)} = 2.248, p = 0.031$), which was attributable to a decreasing kinMT with increasing target area of the 85^{th} percentile of kinMT ($F_{(1.425,15.672)} = 6.126, p = 0.017$, see table 3.1). No significant changes were found in the skewness of the velocity profiles as a function of target size ($F_{(42,4)} = 1.173, p = 0.336$), with peak velocity and time to peak velocity as measures. The average maximum velocity and time to peak velocity over all subjects and targets were 1.01 (SD 0.05) rad/s and 178 (SD 19) ms, respectively.

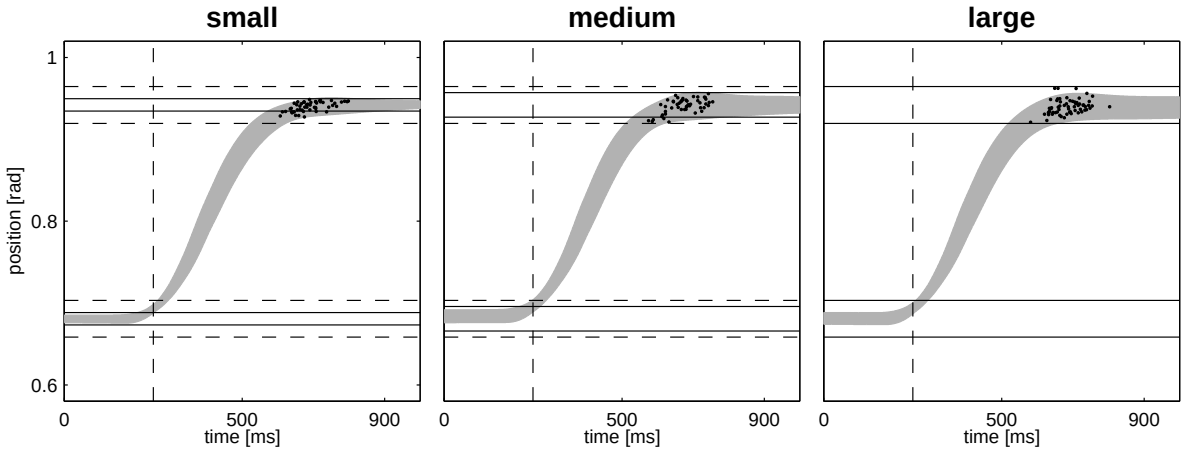

Figure 3.4: *Kinematic profiles of the correct trials of one subject. Results for the small, medium and large target area are shown from left to right. The grey area indicates the 95% confidence interval of the trials. Continuous lines depict the presented target areas and the dashed lines the largest target area. Those boundaries were used to calculate tarMT. Dots depict the time and position of movement end for the individual trials. All trials were aligned at movement onset, which is indicated by the vertical dashed line.*

Figure 3.4 shows the 95% confidence interval of the kinematic profiles of the selected trials for the different target areas for a single subject. The spatial dispersion of the endpoints, as indicated by the black dots, increased from the smallest to the largest target area. The same was true for all subjects ($F_{(2,22)} = 36.037, p < 0.000$, see figure 3.6A). Also for the entire dataset, with no constraints on MT, a similar but weaker effect was found ($F_{(2,22)} = 6.086, p = 0.008$, see figure 3.6B). To further confirm that the accuracy demands manipulation was effective, all trials that met the tarMT criterion were analyzed as if they had been performed on the smallest target. Trials were approved when they entered the smallest target area and remained there for at least 500ms. The number of correct trials decreased with increasing target area ($F_{(2,22)} = 6.46, p = 0.006$, see figure 3.6C), indicating that subjects made use of the larger areas and purposely suppressed endpoint variability for the smallest target area.

Having established that accuracy increased with smaller target areas, the question remains whether this accuracy was only achieved near the endpoint or that overall trajectory variability decreased. As can be appreciated from figure 3.5, for some subjects the variability was lower for the entire trajectory (figure 3.5A), whereas other

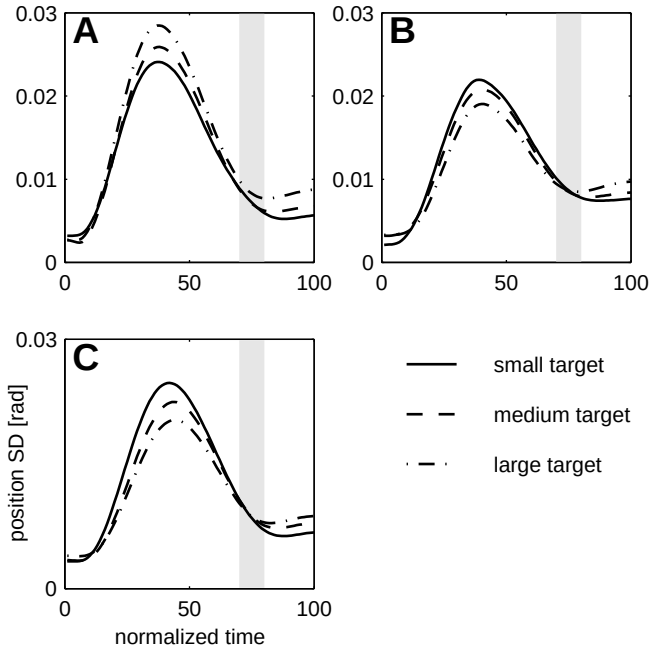

Figure 3.5: *Position variability as a function of normalised time and target size. A: Single subject showing smaller variability over the whole trajectory to the smaller target area. B: Single subject showing higher variability in the first $\frac{3}{4}$ of the trajectory to the smaller target area, only meeting the task constraints in the last $\frac{1}{4}$ of the trajectory. C: Averaged time courses across all subjects. Grey area indicates the perturbation area, coinciding with the crossing of the traces.*

subjects reduced variability near the target (figure 3.5B). For all subjects, the trajectory variability assumed the order of the target areas after 75% of the trajectory had been traversed (figure 3.5C).

Impedance modulation

Prior to the target size experiment inertia of the relaxed arm and manipulandum together and stiffness and damping estimates during maximal cocontraction were obtained. The inertia ranged from 0.0435 to 0.0828 Nms^2/rad between subjects. Stiffness and damping during maximal cocontraction ranged from 24.4 to 99.5 Nm/rad and 0.18 to 1.39 Nms/rad, respectively.

Figure 3.3 shows the 95% confidence interval for unperturbed correct trials of one subject for the medium target area with the perturbed trials superimposed. Notice

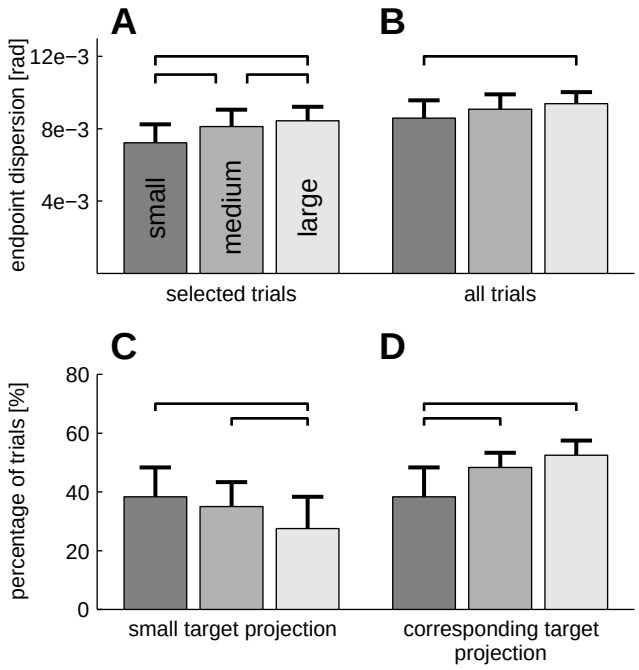

Figure 3.6: *Means and SD for the small, medium and large target area, for endpoint dispersion (A and B) and the number of correct trials (C and D). Endpoint dispersion was expressed as the standard deviation of the movement endpoints, for the selected trials (A) and for all trials (B). On the lower row the means and SD of the percentage of trials that met the tarMT and 'hit'-criterion for the smallest target area (C) and the percentage of correct trials that met the tarMT and 'hit'-criterion for the corresponding target area (D) are presented. Horizontal lines indicate significant differences between target areas ($p < 0.05$). For A: $S < M$, $p = 0.006$; $S < L$, $p = 0.001$; $M < L$, $p < 0.000$; B: $S < L$, $p = 0.015$; C: $S > L$, $p = 0.041$; $M > L$, $p = 0.013$; D: $S < M$, $p = 0.015$; $S < L$, $p < 0.000$.*

that only four and five out of ten perturbed trials, for pEXT and pFLEX, respectively, fell within the 95% confidence interval. This was a general finding for all subjects and in accordance with the small number of unperturbed trials in which both temporal and spatial constraints were met. The similarity was calculated between all perturbed trials, whether in- or outside the 95% confidence interval, and all correct unperturbed trials. The average difference between the 10% most similar trajectories was taken for further analysis. The maximum deviation from the unperturbed trajectory decreased significantly with smaller target areas ($F_{(2,22)} = 8.931, p < 0.001$), and interacted with perturbation direction ($F_{(2,22)} = 9.494, p = 0.001$). Post-hoc ANOVAs revealed that

Table 3.2: *Statistical tests of the effects of target size (TAR) and perturbation direction (DIR, type: pFLEX and pEXT) on stiffness (K) and damping (B). * indicates significant result ($p < 0.05$)*

TAR	$F_{(4,44)} = 3.430$	$p = 0.008^*$	K	$F_{(2,22)} = 6.1689$	$p = 0.011^*$
			B	$F_{(2,22)} = 0.009$	$p = 0.651$
DIR	$F_{(2,10)} = 1.383$	$p = 0.295$	K	$F_{(1,11)} = 2.958$	$p = 0.113$
			B	$F_{(1,11)} = 0.963$	$p = 0.348$
TAR × DIR	$F_{(4,44)} = 4.857$	$p = 0.003^*$	K	$F_{(2,22)} = 0.103$	$p = 0.849$
			B	$F_{(2,22)} = 7.862$	$p = 0.005^*$
TAR (pFLEX)	$F_{(4,44)} = 6.422$	$p = 0.001^*$	K	$F_{(2,22)} = 4.197$	$p = 0.029^*$
			B	$F_{(2,22)} = 4.676$	$p = 0.020^*$
TAR (pEXT)	$F_{(4,44)} = 2.412$	$p = 0.063$	K	$F_{(2,22)} = 5.428$	$p = 0.012^*$
			B	$F_{(2,22)} = 2.146$	$p = 0.141$

this interaction was attributable to pFLEX ($F_{(2,22)} = 23.350, p < 0.000$), whereas the deviation for pEXT did not change systematically ($F_{(2,22)} = 2.009, p = 0.158$). As will become apparent in the following, a lack of changes in the deviation for pEXT does not necessarily mean that there are no changes in the impedance, because differences in the timing of the peak deviation and in the external torque are still possible.

The dynamics of the elbow joint was well described by the *K-B-I* model with VAFs ranging from 0.9913 to 0.9990. Figure 3.7 shows the mean and SD for all subjects of the stiffness and damping estimates for the three target areas and the two perturbation types. The repeated measures MANOVA revealed only significant effects for target size and its interaction with perturbation type. The effect for target area was attributable to the stiffness, whereas the interaction effect was attributable to the damping. Post-hoc tests for the perturbation types separately revealed that stiffness decreased with increasing target area for both perturbation types, whereas the damping only decreased with increasing target area for pFLEX. Table 3.2 provides an overview of all test results.

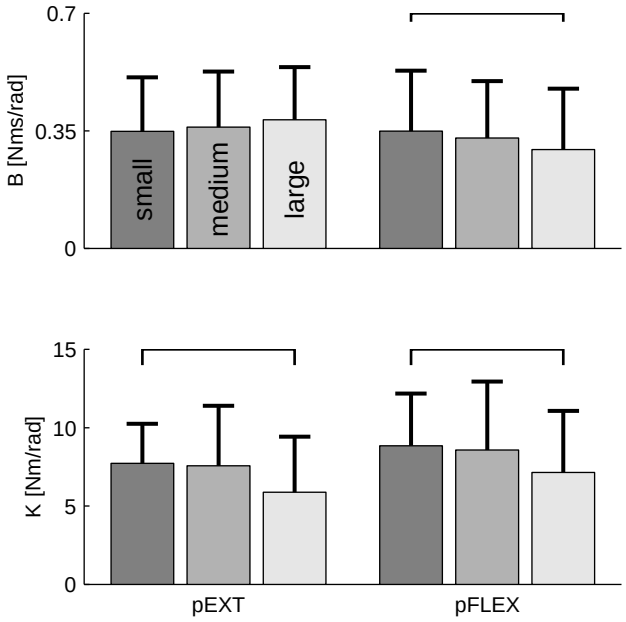

Figure 3.7: *Mean and SD of damping (B) and stiffness (K) for all subjects for the two perturbation types as a function of target area. Horizontal lines indicate significant differences between target areas ($p < 0.05$). For: (B; pFLEX) $S > L$, $p = 0.014$; (K;pEXT) $S > L$, $p = 0.040$; (K,pFLEX) $S > L$, $p = 0.011$.*

Discussion

Impedance modulation with accuracy constraints

We examined the modulation of mechanical impedance, quantified by *K* and *B*, as a function of accuracy demands in goal-directed movements. Mechanical impedance was determined when 75% of the movement amplitude was traversed. It was found that mechanical impedance, probably both of intrinsic and reflexive nature, increased with higher accuracy demands. This is in agreement with earlier studies that reported increased muscular co-activation with increasing accuracy demands, both during single (Osu et al., 2004) and multi-joint (Laursen et al., 1998; Gribble et al., 2003; Visser et al., 2004; Sandfeld and Jensen, 2005; Van Roon et al., 2005) movement. Although the estimation of impedance (especially stiffness) changes from EMG might be feasible (Osu et al., 2002), direct estimation of mechanical impedance by means of perturbations is preferable, especially when the relation between EMG and stiffness becomes

unreliable, for example because of fatigue (Zhang and Rymer, 2001).

It remains an unresolved issue why the positional variability took the order of the accuracy demands only in the final quarter of movement. Similar to our study, Osu et al. (2004) reported that the positional variability was structured only after 80% of movement amplitude had been traversed. In the same study, increases in the muscular activity of the individual muscles in response to increased accuracy demands were only found in the final stage of the movement. This might indicate that positional variability is only controlled, by impedance modulation, during this stage. These results are consistent with the suggestion of Todorov and Jordan (2002) that optimal feedback control under signal-dependent neuromotor noise would imply postponing all goal-directed corrections to the last possible moment. Although in their model stiffness is solely of a 'reflexive ' nature and does not incorporate muscle impedance, the basic idea fits with our experimental findings.

Parameter values for inertia, damping and stiffness

The inertia values of the forearm, including lightweight cast and apparatus inertia, are in the same range as those reported in the literature (Bennett et al., 1992; Bennett, 1993; Popescu et al., 2003). Also the stiffness values are generally comparable to those reported in the literature. For goal-directed movements at constant speed, elbow stiffness values between 5 and 12 Nm/rad have been reported (Kalveram et al., 2005). For goal-directed movement at different speeds, Bennett (1993) reported elbow stiffness values ranging from 3 to 15 Nm/rad depending on net torque changes with speed. Although in our study net torque did not vary, our stiffness estimates were in the same range, probably as a result of muscular co-activation with accuracy demand (Osu et al., 2004) resulting in more coupled cross-bridges and higher muscle stiffness. During cyclic movement, elbow stiffness values ranged from 2 to 15 Nm/rad over the trajectory (Bennett et al., 1992). Only the elbow stiffness values reported by Popescu et al. (2003) during goal-directed movement were five times larger than in the present study. We suspect that this difference was caused by the relatively short (biphasic, 30 ms pulse) and large (20 Nm) perturbations in Popescu's study, resulting in a strong contribution of short-range stiffness to the total muscle stiffness.

Damping values during movement have been reported less frequently in the literature. During cyclic movement the damping of the elbow joint was reported to range from 0 to 0.7 Nms/rad within a cycle (Bennett et al., 1992), whereas the damping

during goal-directed movement ranged from 0.4 to 1.2 Nms/rad between subjects (Popescu et al., 2003; Kalveram et al., 2005). Our estimates fell within the same range.

Taking a closer look at the impedance, we observe that, with increasing accuracy demands, the increases in K were more prominent than the increases in B. When we calculate the damping and stiffness relative to their maximum values, the median relative stiffness is around 10% with peaks towards 40% whereas the relative damping covers the whole range from 5 to 90%, suggesting that the damping is controlled to a lesser extent than stiffness. In isometric conditions, stiffness and damping are strongly coupled and increase linearly with activation level (e.g. Hajian and Howe, 1997; Zhang and Rymer, 1997). However, during goal-directed movement the coupling between stiffness and damping weakens in the stabilization phase (Milner and Cloutier, 1998) and during cyclic movement the damping varies much more within and between cycles than the stiffness (Bennett et al., 1992). Also during goal-directed movement, stiffness and damping do not follow the same pattern (Bennett, 1994). Although it is not clear why the coupling between stiffness and damping disappears during movement, one might speculate that the strong non-linearity of the force-velocity relation and the contribution of reflexes are involved.

The methods applied in the present study cannot distinguish between the contributions of intrinsic muscle properties and spinal reflexes to the overall joint impedance. To do so, continuous (pseudo-)random perturbations are necessary. Since the motor control system is adaptive, these perturbations would become part of the motor task and thus interfere with the impedance control in order to suppress the effects of neuromotor noise on kinematics. However, studies on position control have shown, using continuous perturbations in combination with sophisticated system identification techniques, that both intrinsic properties and reflexes contribute simultaneously to joint impedance (Kearney et al., 1997; Zhang and Rymer, 1997; Van der Helm et al., 2002). In all likelihood, this was also the case in our experiment. However, the reflexive contribution was probably only elicited by the perturbation. During unperturbed movement stability was probably guaranteed by intrinsic properties only.

Other control strategies to meet accuracy demands

Changes in impedance (figure 3.7) were less clear-cut than changes in spatial accuracy (figure 3.6A). This difference may be explained in part by methodological factors. For

example, the spatial accuracy was calculated only for the spatially and temporally correct trials, whereas it remains uncertain whether the perturbed trials would have been correct. Furthermore, the medium target may already have required maximum performance, but with more hits than when aiming at the small target.

Besides methodological factors this difference may also reflect additional control strategies. It has been proposed that changes in movement variability can be decomposed in three components (Müller and Sternad, 2004): 1. reduction of stochastic noise; 2. exploitation of task tolerance; 3. co-variation between central variables. In the present experiment task, tolerance was manipulated both by the presentation of differently sized targets and the constraints on MT. As a result the impedance increased, which is essentially a means to reduce the effects of stochastic noise on motor performance. From figure 3.6 one can appreciate that subjects made use of the tolerance, i.e. target size, offered by the task. Not only impedance was modulated in the present study, traces of speed modulation were still apparent. Within subjects, tarMT fluctuated from -20% to +20% of the desired MT, indicating that the relative contribution of the two strategies, impedance- and speed modulation, was not constant. Furthermore, there was a general tendency to move slower with smaller targets, but this came only to the fore in the 85^{th} percentile of the correct trials.

It can only be speculated that the co-variation of central variables was modulated in the present task. The only degrees of freedom available to co-vary are the muscular activations, which we did not assess. However, during learning of multi-joint Frisbee throwing co-variance between central variables changed with practice and the accompanying accuracy (Yang and Scholz, 2005). Following the uncontrolled manifold concept (UCM concept, Scholz and Schöner, 1999), total joint configuration variance was divided in the amount of kinematic variance in the subspace of joint configurations that did not interfere with performance (goal-equivalent variance, GEV) and the amount of variance in its orthogonal subspace in which variability had consequences on task performance (non goal-equivalent variance, NGEV). Although overall variability decreased with practise, GEV decreased to a larger extent than NGEV. Using the same concept, (Kang et al., 2004) showed that during learning of an unusual multi-finger force production task, overall performance increased by selectively (re-)distributing the force variability over the individual fingers. It is unclear whether humans employ the co-variation between central variables when confronted with different accuracy demands, but it is most likely that in natural tasks impedance modulation, speed modulation and variability distribution are employed in concordance,

tailored to the spatio-temporal constraints of the task and in consideration of the energetic costs.

Conclusion

We conclude that subjects modulate joint impedance, probably by making use of both intrinsic muscle properties and spinal reflexes, to meet accuracy demands during goal-directed movements, at least toward the end of movement. During less constrained, more natural tasks, impedance modulation is probably less apparent because other, less energy consuming, strategies are employed in combination with impedance modulation.

4

Impedance modulation and feedback corrections in tracking targets of variable size and frequency

Selen L.P.J., Van Dieën J.H. & Beek P.J. (2006). Impedance modulation and feedback corrections in tracking targets of variable size and frequency. *Journal of Neurophysiology*, 96(5), 2750–2759 (used with permission).

The original paper can be found on:
http://jn.physiology.org/cgi/content/full/96/5/2750

Abstract

Humans are able to adjust the accuracy of their movements to the demands posed by the task at hand. The variability in task execution due to the inherent noisiness of the neuromuscular system can be tuned to task demands by both feed forward (e.g. impedance modulation) and feedback mechanisms. In the present experiment, we investigated both mechanisms, using mechanical perturbations to estimate stiffness and damping as indices of impedance modulation and submovement scaling as an index of feedback driven corrections. Eight subjects tracked three differently sized targets (0.0135, 0.0270 and 0.0405 rad) moving at three different frequencies (0.20, 0.25 and 0.33 Hz). Movement variability decreased with both decreasing target size and movement frequency, whereas stiffness and damping increased with decreasing target size, independent of movement frequency. These results are consistent with the concept of neuromotor noise as proposed by Van Galen and Schomaker (1992, Hum Mov Sci, 11 (1-2):11–21) but challenge stochastic theories of motor control that do not account for impedance modulation and only partially for feedback control. Submovements during unperturbed cycles were quantified in terms of their gain, i.e. the slope between their duration and amplitude in the speed profile. Submovement gain decreased with decreasing movement frequency and increasing target size. The results were interpreted to imply that submovement gain is related to observed tracking errors and that those tracking errors are expressed in units of target size. We conclude that impedance and submovement gain modulation contribute additively to tracking accuracy.

Introduction

Many tasks in daily life, such as hand writing, drawing and computer work, require accurate movements. Although movement accuracy is limited by noise in the human motor system, the redundancy of this system offers control strategies to accommodate the accuracy constraints imposed by the task. For example, during key-boarding the size of the keys defines the required spatial accuracy, whereas the structure and control of the neuro-musculo-skeletal system provides as well as constrains solutions to achieve the required accuracy.

A constraint of the neuromuscular system that has received much interest in recent theories of motor control is the signal-dependency of neuromuscular noise (Harris and Wolpert, 1998; Todorov and Jordan, 2002). The proposed solution to attain a required accuracy level is to construct an optimal control signal, including feedback in the model of Todorov and Jordan (2002), in the sense that endpoint variability over successive trials is minimised. Although this approach reproduces many movement features, it fails to offer a means to control kinematic variability when confronted with different accuracy demands under strict velocity and/or duration constraints (Schaal and Schweighofer, 2005). Furthermore, this approach yields smooth movements that do not possess the characteristic irregularities observed in goal-directed aiming (e.g. Milner and Ijaz, 1990; Fishbach et al., 2005; Dounskaia et al., 2005) and tracking movements (e.g. Miall et al., 1993; Roitman et al., 2004; Pasalar et al., 2005).

What mechanism(s) might be able to reduce kinematic variability due to neuromuscular noise? Van Galen and Schomaker (1992) and Van Galen and De Jong (1995) hypothesised that mechanical impedance attenuates the effects of neuromuscular noise on movement kinematics. Although impedance has been shown to stabilise the musculo-skeletal system in response to external perturbations (e.g. Burdet et al., 2001; Franklin et al., 2003), its modulation to reduce the effects of internal destabilising perturbations appears paradoxical. On the one hand muscular activity forms the source of force variability, whereas on the other hand it provides a means of suppressing its kinematic effects (chapter 3, Schaal and Schweighofer, 2005). In any case, experimental studies of both single-joint (Osu et al., 2004) and multi-joint goal directed movements (Van Gemmert and Van Galen, 1997; Laursen et al., 1998; Van Galen and Van Huygevoort, 2000; Gribble et al., 2003; Visser et al., 2004; Sandfeld and Jensen, 2005; Van Roon et al., 2005) have shown that muscular co-activation increases with increasing accuracy demands. The hypothesis of impedance modulation was further

supported by modelling studies (chapter 2, Van Galen and De Jong, 1995) predicting a decrease of movement variability with increasing co-activation, despite increasing neuromuscular noise. The experimental evidence for impedance modulation was presented only recently (see chapter 3). We showed that the mechanical impedance of the elbow is modulated as a function of accuracy demands in time-constrained goal-directed movements. Although we observed an increase in impedance, especially in stiffness, with increased accuracy demands, subjects also tended to increase movement time both by decreasing peak velocity and by making submovements. Apparently, the tendency to prolong movement duration in response to increased accuracy demands, as reflected in Fitts' law (Fitts, 1954), is hard to suppress. This resulted in large variability in the realisation of the movements, which partially obscured the modulation of impedance in response to increases in accuracy demands.

Do submovements contribute to movement accuracy? Although the presence of submovements has been attributed to the intermittency of neural control, in goal-directed movements their scaling is supposed to represent corrective actions to accommodate the prevailing accuracy constraints (Milner and Ijaz, 1990; Dounskaia et al., 2005). The optimised submovement model of Meyer et al. (1988) offers an influential explanation of speed-accuracy relations in goal-directed aiming. The model proposes that rapid aiming movements may involve submovements whose durations are optimised in order to cope with a noisy neuromotor system, resulting in more corrective submovements and longer movement times for stricter accuracy constraints. More recently, a similar model, including both visual and proprioceptive feedback, was proposed that allowed for overlapping, prediction based, submovements (Burdet and Milner, 1998). For target tracking, it is unknown whether submovements contribute to accuracy and if and how their characteristics change with target size. Extending the results from goal-directed movements, we expect more frequent and more subtle submovements with smaller targets. In tracking, however, the velocity is pre-defined and poses constraints on the submovements. Those constraints have been found to result in submovements with invariant duration and increasing amplitude with increasing movement velocities (Miall et al., 1986; Roitman et al., 2004; Pasalar et al., 2005).

The objective of the present study was not only to further investigate impedance modulation in response to accuracy constraints, but also to examine whether and how submovements are regulated to accommodate accuracy constraints during single-joint target tracking. This task was chosen because the prescription of target motion

provides a means to constrain movement velocity and thus might help to avoid the aforementioned masking of impedance modulation caused by timing variability. Furthermore, target tracking allows for movement within the target area and thus investigation of the contribution of submovements to accuracy demands. We therefore conducted an experiment in which subjects were invited to track a target presented on a LED array. The experiment consisted of 9 conditions (3 target sizes $\times$ 3 tracking frequencies). Impedance, expressed as stiffness (K) and damping (B), was estimated by applying controlled mechanical perturbations to the elbow joint during tracking. Characteristics of submovements were investigated in the unperturbed trials.

Methods

Subjects

Eight subjects (3 men and 5 women) between 20 and 28 years of age participated in the experiment. All subjects had normal or corrected to normal vision and reported no history of neuromuscular disorders. The local Ethics Committee approved the experiment before its conductance and all subjects signed informed consent forms prior to their participation. The experiment lasted approximately two hours including preparation time. During the experiment subjects were allowed to rest as often and as long as they wished to avoid fatigue. The data of one subject were removed from the impedance analysis, but not from the accuracy and submovement analyses. For this subject, perturbations were distributed randomly over the movement cycle because of a programming error.

Apparatus

Figure 4.1 depicts the experimental setup. Subjects were seated on a chair in front of a semicircular array of light emitting diodes (LEDs). Their dominant forearm (the arm they used for writing), including hand palm and wrist, was cast (NobaCast, Noba Verbandmittel Danz GmbH) onto a lightweight T-wedged bar. The bar was mounted on the vertical shaft of a torque controlled motor (S-motor, elu93028, Fokker Control Systems), with the medial epicondyle aligned with the motor's axis of rotation and the palm of the hand facing downward. The height of the chair was adjusted such that the upper arm and forearm were in the horizontal plane. The LED array, consisting of

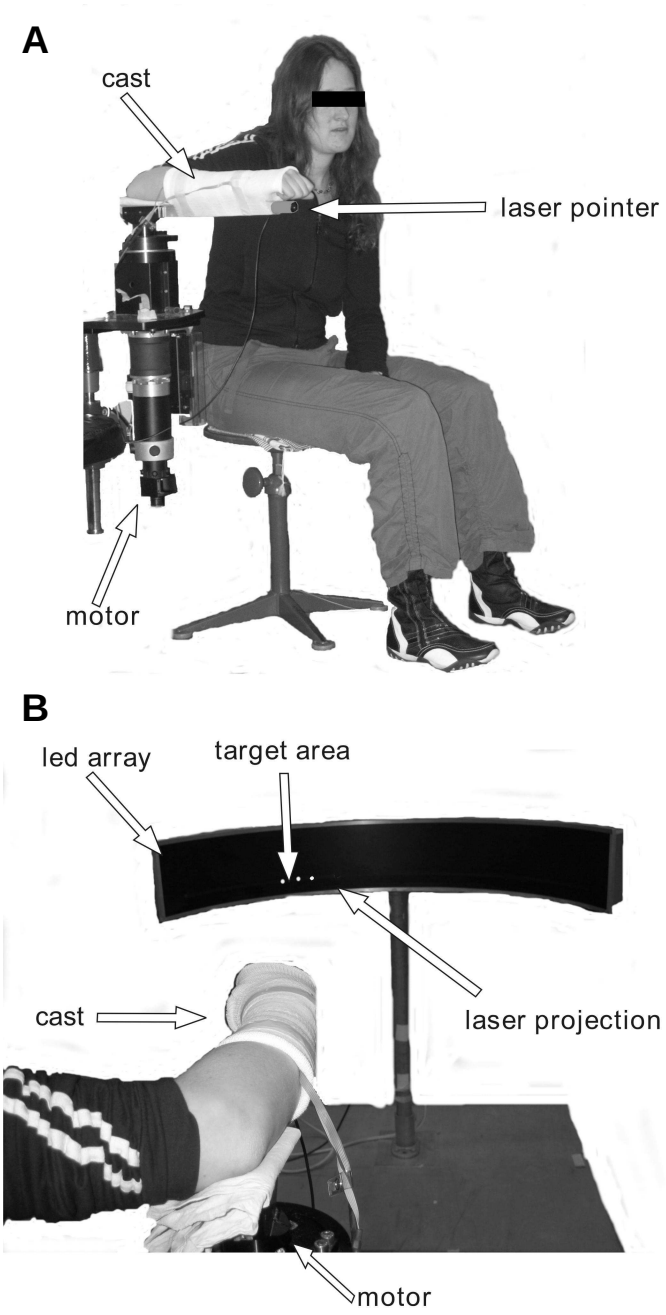

Figure 4.1: *Experimental setup of the target tracking experiment. Upper panel depicts a front-side view of a subject with the subject's forearm cast onto a lightweight bar attached to the motor. Lower panel shows the led array with the target to be tracked and the laser projection.*

447 LEDs, was placed 1.5 m in front of the wrist of the cast arm. The forearm pointed at the centre of the LED array when the elbow was flexed by 90 degrees. A small laser pointer was attached to the lightweight bar indicating the pointing direction on the LED array. Two LEDs were illuminated, defining the boundaries of the to-be-tracked target. The torque-controlled motor operated in closed loop fashion at 5 kHz. In the unperturbed cycles the set point of the controller was 0 Nm, resulting in a smooth and frictionless movement environment. The angular position of the motor shaft was measured by a potentiometer (22HSPP-10, Sakae) and the remaining torque was measured by a strain gauge. Both position and torque data were stored at 1 kHz.

Experimental task

Subjects were instructed to track a target whose boundaries were indicated by two LEDs. The target oscillated sinusoidally with amplitude (peak-peak) of 0.2 rad. Three differently sized targets (0.0135 rad, 0.0270 rad and 0.0405 rad) were tracked at three movement frequencies (0.33 Hz, 0.25 Hz and 0.2 Hz), resulting in nine experimental conditions. Each condition lasted two minutes and was performed four times in succession. Target sizes and movement frequencies were presented in random order. To estimate the impedance of the arm, six biphasic torque pulse perturbations were applied by the motor during each two-minute trial. Four perturbation types were used (see figure 4.3) and each was applied six times. The 24 perturbations in question were randomly distributed over the four two-minute trials. Trials were divided into sections of 20 seconds each, during which one perturbation was applied randomly in time with the restriction that perturbations had to be at least 5 seconds apart. As can be seen from figure 4.3, all perturbations occurred in the zero crossing of the sine wave, i.e. at an elbow angle of 90 degrees. Perturbations were biphasic and had a total duration of 140 ms. Because we were interested in the physical state of the elbow before the perturbation, perturbations had a short duration (140 ms), leaving the participant insufficient time to voluntarily react to the perturbation, whereas the analysis was performed over a short time interval (170 ms), such that the inclusion of voluntary responses in the analysis was minimised. Furthermore, subjects were instructed to move naturally without trying to anticipate the perturbations, and not to intervene voluntarily in response to the perturbations. Before the central part of the experiment, the same perturbations were applied to the relaxed arm to estimate the combined inertia of forearm and manipulandum.

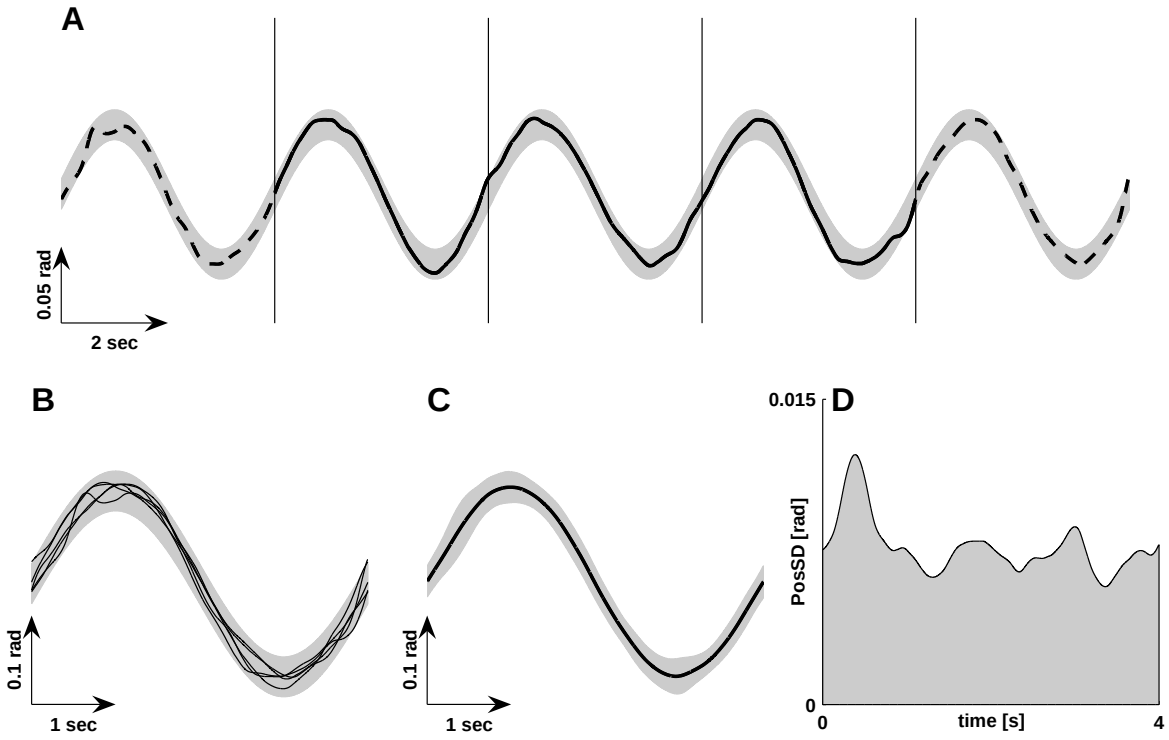

Figure 4.2: *Tracking variability. A. Section of an experimental time series of the elbow angle (black line) and the target area (grey area). Vertical lines indicate the boundaries of the cycles. B. Superposition of the cycles (black lines) and the target area (grey area). C. Mean angle (black line) and the 95% confidence interval (grey area) over cycles. D. Positional SD over the movement cycles. Motor output variability was expressed as AvePosSD and calculated by taking the mean of the time series in panel D.*

Analyses

Motor output variability

The four angular position time series of each condition were rearranged into a matrix of cycles (see figure 4.2). The variability of the unperturbed cycles was assessed by calculating the standard deviation (SD) as a function of time:

$$\text{PosSD} = \sqrt{\frac{1}{n}\sum_{j=1}^{j=n}[\varphi_j(t) - \overline{\varphi}(t)]^2} \tag{4.1}$$

where *n* is the number of unperturbed cycles included in the analysis and *t* represents time within a cycle. The number of available unperturbed cycles differed for the three movement frequencies (*n*=[96; 66; 48] for *f*=[0.33; 0.25; 0.2] Hz, respectively). To avoid spurious decrease in PosSD due to the larger number of unperturbed cycles for the higher movement frequency, 48 unperturbed cycles were randomly drawn from the 0.25Hz and 0.33Hz conditions. Subsequently, the time-averaged value of PosSD was calculated (AvePosSD). The percentage of samples that fell outside the target boundaries was determined to assess the degree to which subjects fulfilled the accuracy demands.

Estimation of elbow impedance

To estimate the dynamics of the elbow joint in response to the mechanical perturbation, a second order linear model with stiffness *K*, damping *B* and inertia *I* (denoted as *K-B-I* model) was fitted to the kinematic responses. The kinematic changes due to the perturbation were quantified by subtracting the average movement cycle angular position ($\overline{\varphi}$) from the angular positions in the perturbed cycles (φ_{pert}), corrected for their distance at perturbation onset:

$$\Delta\varphi_{pert} = [\varphi_{pert}(t) - \varphi_{pert}(t_0)] - [\overline{\varphi}(t) - \overline{\varphi}(t_0)] \tag{4.2}$$

The external moment generated in the perturbed cycles was measured directly by means of a strain gauge. During the unperturbed cycles also a small external moment was sensed by the strain gauge. The average external moment across unperturbed cycles ($\overline{M}(t)$) was subtracted from the measured external perturbation moment ($M_{pert}(t)$) and corrected such that its value was zero at perturbation onset:

$$\Delta M_{pert} = [M_{pert}(t) - M_{pert}(t_0)] - [\overline{M}(t) - \overline{M}(t_0)] \tag{4.3}$$

The parameters of the *K-B-I* model were estimated using a combined optimisation and simulation routine (see chapter 3). In the forward simulation step the kinematics (φ_{sim}) were simulated by imposing the measured external perturbation moment (ΔM_{pert}) to the *K-B-I* model. The inertia was determined from the perturbations to the relaxed arm, independently of the experimental manipulations. In the subsequent nine optimisations, estimates of *K* and *B* were obtained for the different experimental conditions. After the optimisation the variance accounted for (VAF) was calculated:

$$\text{VAF} = 1 - \frac{[\varphi_{pert} - \varphi_{sim}] \cdot [\varphi_{pert} - \varphi_{sim}]^T}{[\varphi_{pert}] \cdot [\varphi_{pert}]^T} \tag{4.4}$$

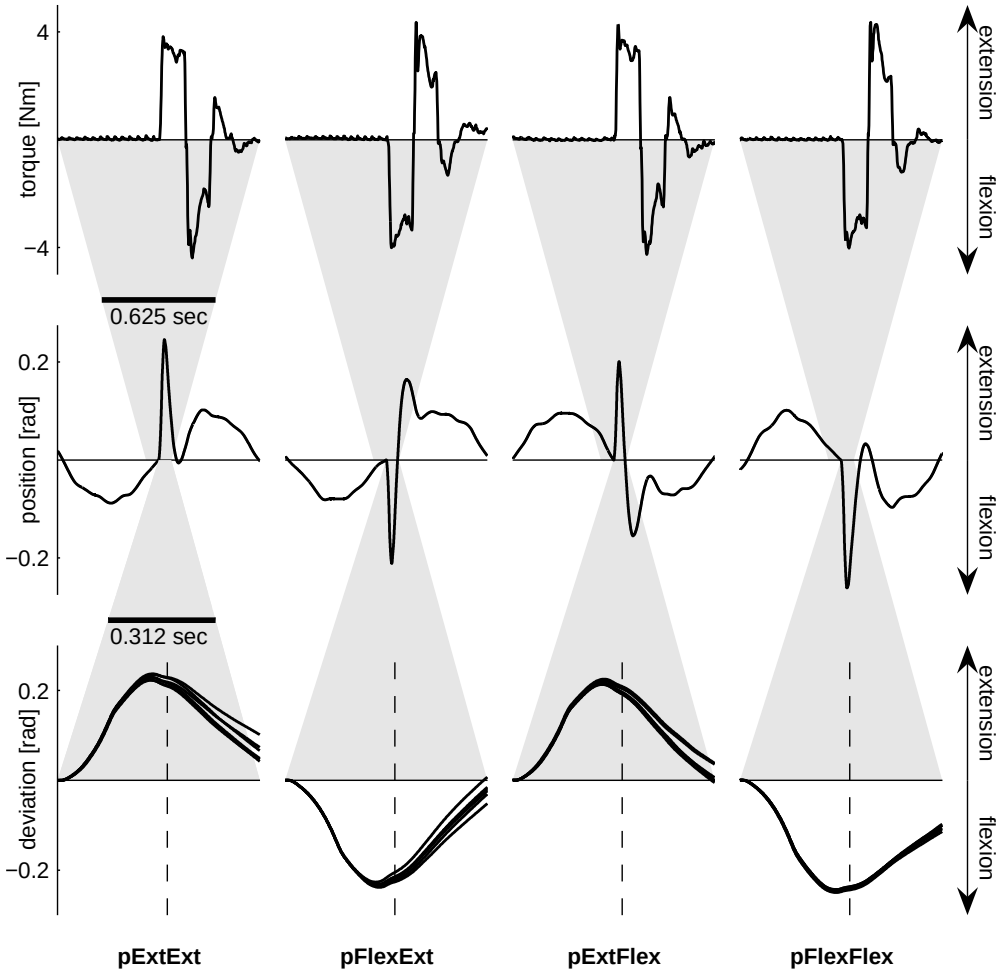

Figure 4.3: *Examples of the effects of the four perturbation types. In the two leftmost panels the subject was extending his elbow, while the perturbation started in extension (pExtExt) and flexion (pFlexExt) direction, respectively. In the two rightmost panels the subject was flexing his elbow, while the perturbations started in extension (pExtFlex) and flexion (pFlexFlex) direction, respectively. Middle row depicts full cycles (5 seconds) of the elbow angle including a perturbation. Upper row shows part of the motor torque (-312.5 to 312.5ms of perturbation onset). The lower row depicts the kinematic effects of the six perturbations after subtraction of the target sine. The vertical line indicates the end of the impedance estimation time window (i.e. 0-170ms).The grey areas indicate the difference in time scales between panels.*

Characterisation of submovements

Tracking movements are characterised by submovements that appear as oscillations in the velocity profile. Submovement characteristics were investigated in both the frequency and time domain. The main frequency of the submovements was identified as the second peak in the power spectrum (the first peak being the target movement frequency). To this aim, power spectra were calculated using Welch's averaged periodogram method. Each time series was divided into 50% overlapping sections of 2^{14} datapoints with a Hamming window, resulting in an average spectrum with a frequency resolution of 0.06 Hz.

Sophisticated submovement extraction algorithms have been proposed for the time domain (e.g. Rohrer and Hogan, 2006), but most of them are only applicable to goal-directed movements with a small number of submovements. To examine the properties of the oscillatory behaviour during tracking, we adopted the speed pulse (SP) analysis from Roitman et al. (2004) and Pasalar et al. (2005). Time series of angular position were low-pass filtered using a 5th order Butterworth filter with a cut-off frequency of 6 Hz. This relatively low frequency was chosen to avoid spurious detec-

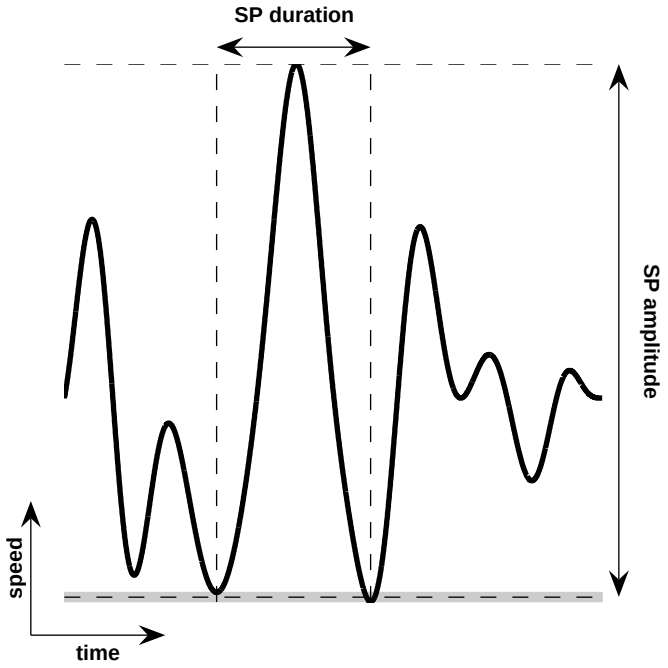

Figure 4.4: *Section of the speed profile, showing the speed pulses. The amplitude (SP amplitude) and duration (SP duration) of a single speed pulse are indicated.*

tion of submovements. Higher frequencies, such as the 12 Hz used by Roitman et al. (2004), shifted the mean and median SP duration to lower values that did not correspond to the main frequency as deduced from the power spectra. Because we were interested in the movement in the target area independent of the movement of the target area itself, the motion of the target was subtracted[1]:

$$\varphi_{rel}(t) = \varphi(t) - A\sin(2\pi t/T) \tag{4.5}$$

Subsequently, the numerical derivative was calculated to obtain angular velocity time profiles. The duration of a single SP (SP duration) was defined as the time between two successive local minima in the velocity profile. The amplitude of a SP (SP amplitude) was defined as the difference between a local maximum in the velocity profile and the average value of the two nearest minima (see figure 4.4). The linear regression between SP duration and SP amplitude provided an intercept and a slope. The latter was interpreted as error correction gain and will be referred to as SP gain in the remainder of this article.

Statistics

Both in the text and in the figures the data will be presented as means and SD. Effects of target size and movement frequency on AvePosSD, SP duration, SP amplitude and SP gain were analysed using two-way repeated measures ANOVAs (3 Target sizes $\times$ 3 Movement frequencies). The effects of the experimental manipulations on the impedance estimates were examined by performing three-way (4 Perturbation types $\times$ 3 Target sizes $\times$ 3 Movement frequencies) (M)ANOVAs on K and B separately and together. If the ANOVA revealed significant changes ($p < 0.05$) post-hoc tests with Bonferroni correction were performed to identify differences. The effect size was quantified by partial η^2 (η_p^2). All statistical tests were performed using SPSS 11.5.

[1]Note that, for both the impedance and SP analysis, the use of $A\sin(2\pi t/T)$ of $\overline{\varphi}(t)$ yields the same results.

Results

Accuracy manipulation

Figure 4.2 presents a typical example of movement variability for one subject in a single experimental condition. Movement variability was expressed as AvePosSD, which is the mean over time of the signal in panel D. Figure 4.5 shows that movement variability decreased with smaller targets ($F_{(2,14)}$ = 72.836, $p < 0.000$, η_p^2 = 0.91) and lower movement frequencies ($F_{(2,14)}$ = 44.434, $p < 0.000$, η_p^2 = 0.86), indicating that the experimental manipulation indeed induced an accuracy increment. However, a substantial number of samples fell outside the target boundaries and this number increased with smaller targets ($F_{(2,14)}$ = 204.762, $p < 0.000$, η_p^2 = 0.97) and higher movement frequencies ($F_{(2,14)}$ = 37.120, $p < 0.000$, η_p^2 = 0.84). Especially for the small target the percentage of samples outside the target boundaries was large. This

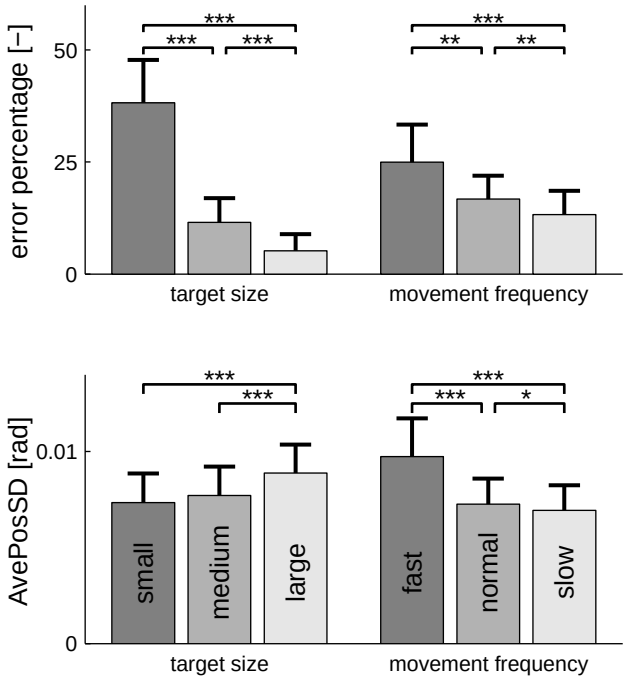

Figure 4.5: *Mean and SD over eight subjects of the cycle ensemble kinematic variability (SD(t)) averaged over time (AvePosSD) and the percentage of samples outside the target boundaries (error percentage) for the three target sizes (0.0135, 0.0270 and 0.0405 rad) and for the three movement frequencies (0.33, 0.25 and 0.2 Hz).* $^{*}p < 0.05$*;* $^{**}p < 0.01$*;* $^{***}p < 0.001$*.*

is reflected in the observation that AvePosSD did not differ significantly between the small and medium target.

Impedance modulation

The dynamics of the elbow joint was quantified by fitting a *K-B-I* model to the experimental data. The inertia was determined independently of the experimental manipulations and ranged from 0.0454 Nms^2/rad to 0.0729 Nms^2/rad across subjects. The estimates of I were robust as indicated by the high VAFs (> 0.99). Given the inertia, estimates of stiffness and damping were calculated for all experimental conditions. Again the VAFs were high (mean: 0.9935; range: 0.9527-0.9995), indicating that the *K-B-I* model accurately described the dynamics of the elbow. Bootstrapping the experimental data (Efron and Tibshiran, 1993) revealed a coefficient of variation ((SD/mean)$\times$ 100 $\%$) of the estimates of K and B of less than 10$\%$. Figure 4.6 indicates that both K and B decreased with increasing target size for all four perturbation types. Repeated measures MANOVA revealed significant effects of both target size and perturbation type on K and B. Movement frequency did not influence K and B. Because stiffness and damping are not necessarily a measure of the same process, repeated measures ANOVAs were also performed for K and B separately. The results of both analyses were similar. Table 4.1 presents the results of all statistical tests including all two-way interactions and η_p^2 as a measure of effect size.

Submovement gain modulation

Submovement characteristics were investigated by calculating the duration and amplitude of speed pulses (see Roitman et al., 2004; Pasalar et al., 2005). SP gain was defined as the slope of the regression between SP duration and SP amplitude. SP gain accounted for more than 70% (SD 0.07) of the observed variance in the data points. Figure 4.7 presents scatter plots of all combinations of SP duration and SP amplitude for the nine experimental conditions for a typical subject. The linear regression line is superimposed. Repeated measures ANOVAs (see table 4.2 and figure 4.8) revealed that SP gain declined with decreasing movement frequency and increasing target size. The average duration of a SP was independent of movement frequency and target size. SP amplitude decreased with decreasing movement frequency and increasing target size and accounted for the increase in SP gain. Figure 4.9 presents the average power spectral densities for all experimental conditions. The sharp peak corresponds to the

Table 4.1: *Statistical effects of target size (TAR), movement frequency (FREQ) and perturbation type (PERT) on stiffness (K) and damping (B). Both a MANOVA (K and B as measures) and ANOVAs on K and B separately were performed. F-values for the MANOVA were approximated from Wilks'Lambda. * Indicates that the result was significant ($p < 0.05$). Partial η^2 (η_p^2) is presented as a measure of effect size for the ANOVAs.*

	MANOVA (K and B)	
TAR	$F_{(4,22)} = 5.454$	$p = 0.003^*$
FREQ	$F_{(4,22)} = 0.375$	$p = 0.824$
PERT	$F_{(6,34)} = 21.752$	$p < 0.000^*$
TAR $\times$ PERT	$F_{(12,70)} = 1.848$	$p = 0.057$
TAR $\times$ FREQ	$F_{(8,46)} = 0.901$	$p = 0.523$
FREQ $\times$ PERT	$F_{(12,70)} = 0.419$	$p = 0.951$

	ANOVA (K)		
TAR	$F_{(2,12)} = 12.986$	$p = 0.001^*$	$\eta_p^2 = 0.684$
FREQ	$F_{(2,12)} = 0.449$	$p = 0.648$	$\eta_p^2 = 0.070$
PERT	$F_{(3,18)} = 40.616$	$p < 0.000^*$	$\eta_p^2 = 0.871$
TAR $\times$ PERT	$F_{(6,36)} = 1.624$	$p = 0.169$	$\eta_p^2 = 0.213$
TAR $\times$ PREQ	$F_{(4,24)} = 1.192$	$p = 0.340$	$\eta_p^2 = 0.166$
FREQ $\times$ PERT	$F_{(6,36)} = 0.243$	$p = 0.959$	$\eta_p^2 = 0.039$

	ANOVA (B)		
TAR	$F_{(2,12)} = 6.449$	$p = 0.013^*$	$\eta_p^2 = 0.518$
FREQ	$F_{(2,12)} = 0.541$	$p = 0.595$	$\eta_p^2 = 0.083$
PERT	$F_{(3,18)} = 11.291$	$p < 0.000^*$	$\eta_p^2 = 0.653$
TAR $\times$ PERT	$F_{(6,36)} = 1.454$	$p = 0.222$	$\eta_p^2 = 0.195$
TAR $\times$ FREQ	$F_{(4,24)} = 0.405$	$p = 0.803$	$\eta_p^2 = 0.063$
FREQ $\times$ PERT	$F_{(6,36)} = 0.391$	$p = 0.880$	$\eta_p^2 = 0.061$

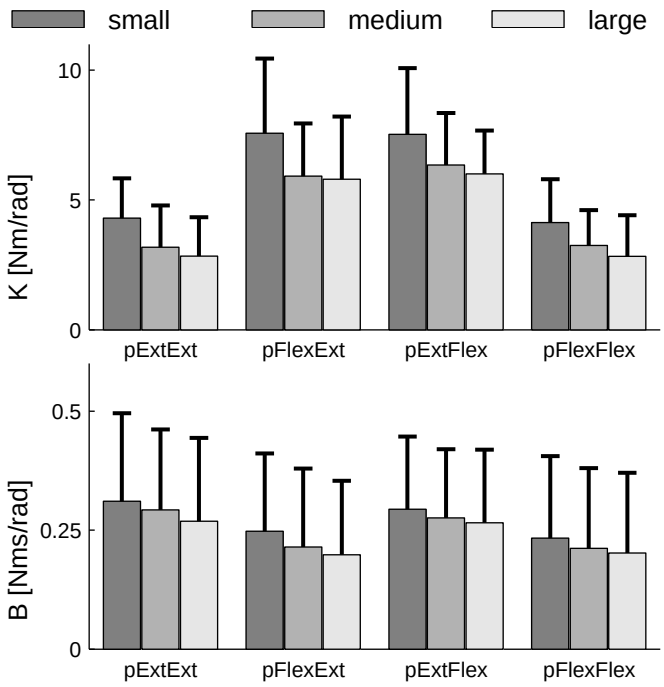

Figure 4.6: *Mean and SD of stiffness (K) and damping (B) over 7 subjects for three target sizes (0.0135, 0.0270 and 0.0405 rad) and four perturbation types. Data were averaged over movement frequencies.*

movement frequency, whereas the broad peak corresponds to the frequencies of the speed pulses. The SP peak (F_{main}) did not shift with target size ($F_{(2,14)} = 2.692$, $p = 0.101$, $\eta_p^2 = 0.31$) or movement frequency ($F_{(2,14)} = 0.911$, $p = 0.424$, $\eta_p^2 = 0.13$).

Discussion

The first purpose of the present study was to examine the effects of both target size and movement frequency on the mechanical impedance of the elbow during single-joint target tracking. It was found that the mechanical impedance of the elbow, quantified by *K* and *B*, increased with smaller targets but was unaffected by target frequency. The second purpose was to investigate adaptations in submovements with variations in target size and movement frequency. SP gain increased with increasing task difficulty, i.e. with smaller targets and at higher movement frequencies. In the following sections, the results for impedance modulation and SP gain modulation will be discussed in turn.

Table 4.2: *Statistical effects of target size (TAR) and movement frequency (FREQ) on SP gain, SP duraton and SP amplitude. * Indicates that the result was significant ($p < 0.05$). Partial η^2 (η_p^2) is presented as a measure of effect size.*

	SP gain		
TAR	$F_{(2,14)} = 28.953$	$p < 0.000^*$	$\eta_p^2 = 0.805$
FREQ	$F_{(2,14)} = 29.632$	$p < 0.000^*$	$\eta_p^2 = 0.809$
TAR × FREQ	$F_{(4,28)} = 4.178$	$p = 0.059$	$\eta_p^2 = 0.374$

	SP duration		
TAR	$F_{(2,14)} = 1.143$	$p = 0.347$	$\eta_p^2 = 0.140$
FREQ	$F_{(2,14)} = 0.697$	$p = 0.515$	$\eta_p^2 = 0.091$
TAR × FREQ	$F_{(4,28)} = 1.546$	$p = 0.216$	$\eta_p^2 = 0.181$

	SP amplitude		
TAR	$F_{(2,14)} = 27.630$	$p < 0.000^*$	$\eta_p^2 = 0.798$
FREQ	$F_{(2,14)} = 21.809$	$p = 0.001^*$	$\eta_p^2 = 0.757$
TAR × FREQ	$F_{(4,28)} = 3.732$	$p = 0.082$	$\eta_p^2 = 0.347$

Mechanical impedance

Modulation with target size and movement frequency

The fact that *K* and *B* increased with smaller targets is consistent with the hypothesis, introduced by Van Galen and colleagues (Van Galen and Schomaker, 1992; Van Galen and De Jong, 1995), that increased mechanical impedance acts as a filter of intrinsically noisy neuromuscular signals. Although this hypothesis found support in EMG studies (Laursen et al., 1998; Gribble et al., 2003; Seidler-Dobrin et al., 1998; Osu et al., 2004; Visser et al., 2004; Sandfeld and Jensen, 2005; Van Roon et al., 2005), supporting mechanical evidence has been few and far between. In a previous study, we demonstrated that the mechanical impedance increases with increasing accuracy demands when approaching the target in goal-directed aiming (chapter 3). In the present study, this finding was generalised to a situation in which accuracy demand and movement velocity were prescribed continuously by the sinusoidal movement of the target.

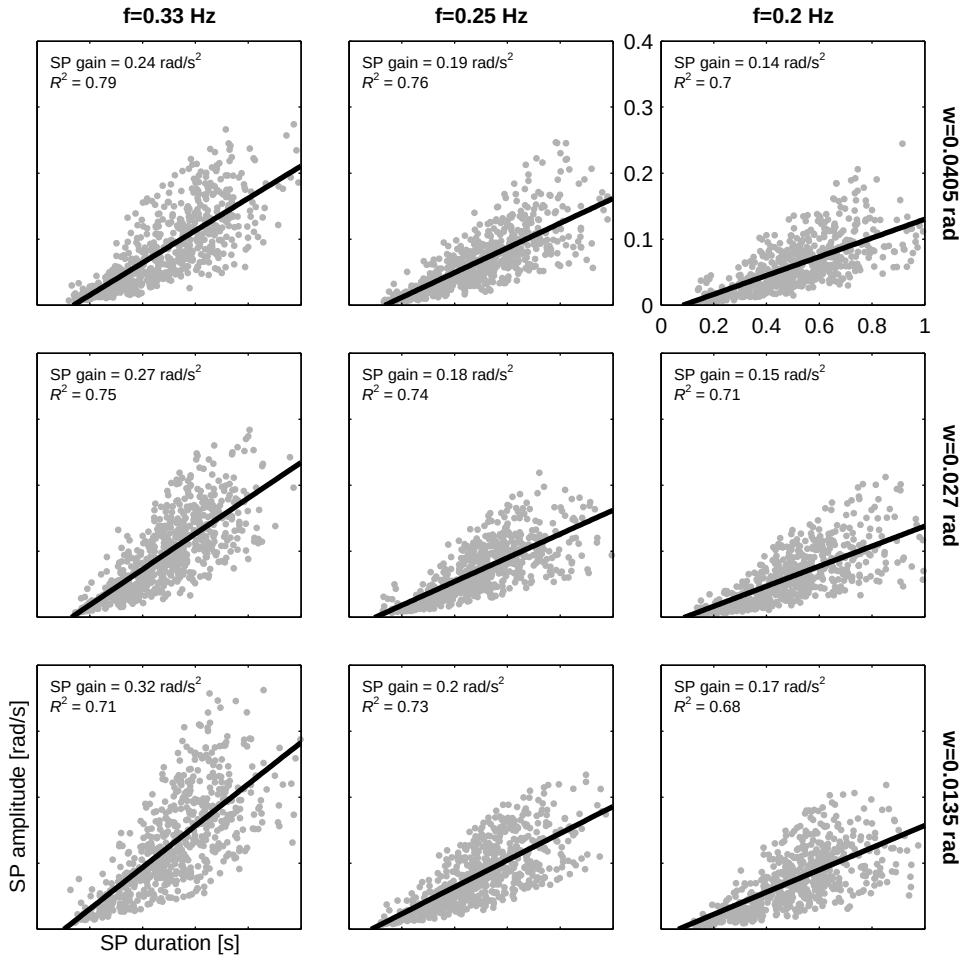

Figure 4.7: *Speed-pulse (SP) gain for a single subject for three movement frequencies (columns) and three target sizes (rows). SP gain is the regression slope of SP duration versus SP amplitude.*

Besides an effect of target size, we expected the impedance to increase with increasing frequency (i.e. peak velocity). Our reasoning in this regard was as follows. Higher movement frequencies require larger propelling forces, which coincide with greater neuromuscular noise (Schmidt et al., 1979; Jones et al., 2002), necessitating increased impedance to attain the required accuracy. Moreover, even without impedance modulation, movement frequency by itself increases impedance as a result of muscle mechanics. As a case in point, Milner (1993) measured the angular displacement produced by a torque pulse (5 Nm and 50 ms) and reported a decreasing displacement when movement velocity increased from 2 rad/s to 4 rad/s. He argued that higher movement velocities are accompanied by higher propelling forces, requir-

ing more attached parallel cross-bridges, coinciding with higher muscle stiffness and consequently higher joint stiffness. Unexpectedly, we found that, across the frequencies tested, the impedance of the elbow remained constant. Apparently, the preceding arguments did not hold at the low movement frequencies employed. Peak velocity of the target ranged from 0.1 rad/s to 0.2 rad/s, resulting in discontinuous control of movement velocity. As a consequence, the propelling forces for the resulting submovements were relatively low and did not contribute significantly to joint stiffness and force variability.

A further consideration is that lower movement frequencies allow for more visually guided feedback corrections per movement cycle and therefore would require less feed forward impedance control given the prevailing accuracy constraints. We observed that SP duration remained constant with movement frequency, resulting in approximately 33% and 66% more corrective movements per movement cycle for the 0.25 Hz and 0.2 Hz movements compared to the 0.33 Hz movement. Because increased impedance is energetically costly, it was expected that subjects would decrease mechanical impedance whenever possible. However, the achieved accuracy levels were lower than the levels demanded by the target size (see figure. 4.5). Apparently all available sources for variability reduction were deployed and none was lowered with decreasing movement frequency.

Joint stiffening has been associated with learning novel tasks (Bernstein, 1967). When confronted with a new task, degrees of freedom are frozen by stiffening joints and over the course of learning the stiffness decreases, gradually releasing degrees of freedom. However, this concept pertains to learning the dynamics of a novel multijoint movement (e.g. Franklin et al., 2003). The single-joint task investigated here precludes freezing degrees of freedom. Furthermore, the dynamics of the task did not change between the different target sizes.

Parameter values

The average stiffness values reported in the present study are in the same range as those found for the elbow in goal-directed aiming (chapter 3, Bennett, 1993; Kalveram et al., 2005). Bennett et al. (1992) estimated the time-varying stiffness of the elbow joint during paced reciprocal aiming in the horizontal plane. At peak velocity, the instant of perturbation initiation in the present study, their stiffness estimates (3Nm/rad) were lower than the average stiffness in the present study (5-6Nm/rad). Most likely this is because of continuous control of impedance in response to accuracy

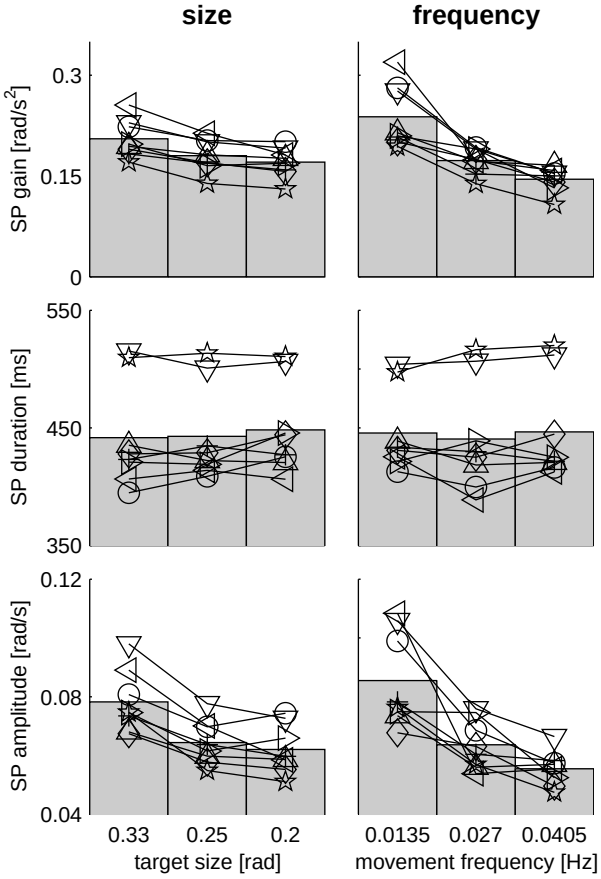

Figure 4.8: *Group mean values for SP gain, SP duration and SP amplitude for target size and movement frequency. Individual means for the subjects are superimposed. Repeated measures ANOVAs (see text) indicated significant effects for SP amplitude and SP gain.*

constraints in the present study, whereas in the study of Bennett et al. (1992) stiffness was probably only controlled when approaching the targets (chapter 3, Osu et al., 2004).

As expected, stiffness modulation with increasing target size was much stronger in the present target tracking study than observed for goal-directed movements (chapter 3). Tracking movements were more consistent and probably involved continuous impedance control in order to attain the required accuracy. Although the overall pattern of impedance modulation with accuracy and frequency demands was robust (fig-

ure 4.6), the stiffness values differed significantly across the four perturbation types. The highest stiffness values were found when the onset direction of the perturbation opposed the movement direction. In all likelihood, this perturbation type dependency was caused by the interaction of motor and elbow joint dynamics in combination with the non-linearity of the system (Kearney and Hunter, 1990; Kay et al., 1991; Kirsch et al., 1994).

Quantification of the mechanical impedance of the musculo-skeletal system has a long history (see Kearney and Hunter, 1990). The mechanical impedance of a system is best described by its transfer function, which can only be estimated using continuous perturbations. However, such perturbations interact with the natural behaviour of the motor control system (Kirsch et al., 1994). Transient perturbations, as used in the present study, provide information about the state of the system just prior to the perturbation. Making a priori assumptions about the system under study is inevitable when quantifying impedance. In the present study, the musculo-skeletal system was approximated with a second-order model. The elbow joint system is of much higher order and one might therefore question the exactness of the obtained stiffness and damping estimates. However, we were interested in the modulation of stiffness and damping and not in their exact values.

The time window over which changes in stiffness and damping were observed suggests that both intrinsic muscle properties and reflex components contributed to impedance modulation. Even voluntary reactive activity may have occurred at the very end of the estimation window. However, we believe that the instruction not to intervene to the subjects effectively suppressed voluntary responses. This is supported by the high consistency of the kinematic traces. Only after the estimation window of 170ms the traces started to disperse (see figure 4.3).

Submovement characteristics

The second purpose of the present study was to examine how submovement characteristics, such as SP duration, SP amplitude and SP gain, relate to task constraints (i.e. movement frequency and target size). For movement frequency variations, we had explicit hypotheses derived from the literature, but for the target size manipulation our investigation was more explorative.

For increasing movement frequency, we observed an increase of both SP amplitude and SP gain and no effect for SP duration, consistent with previous results for sinu-

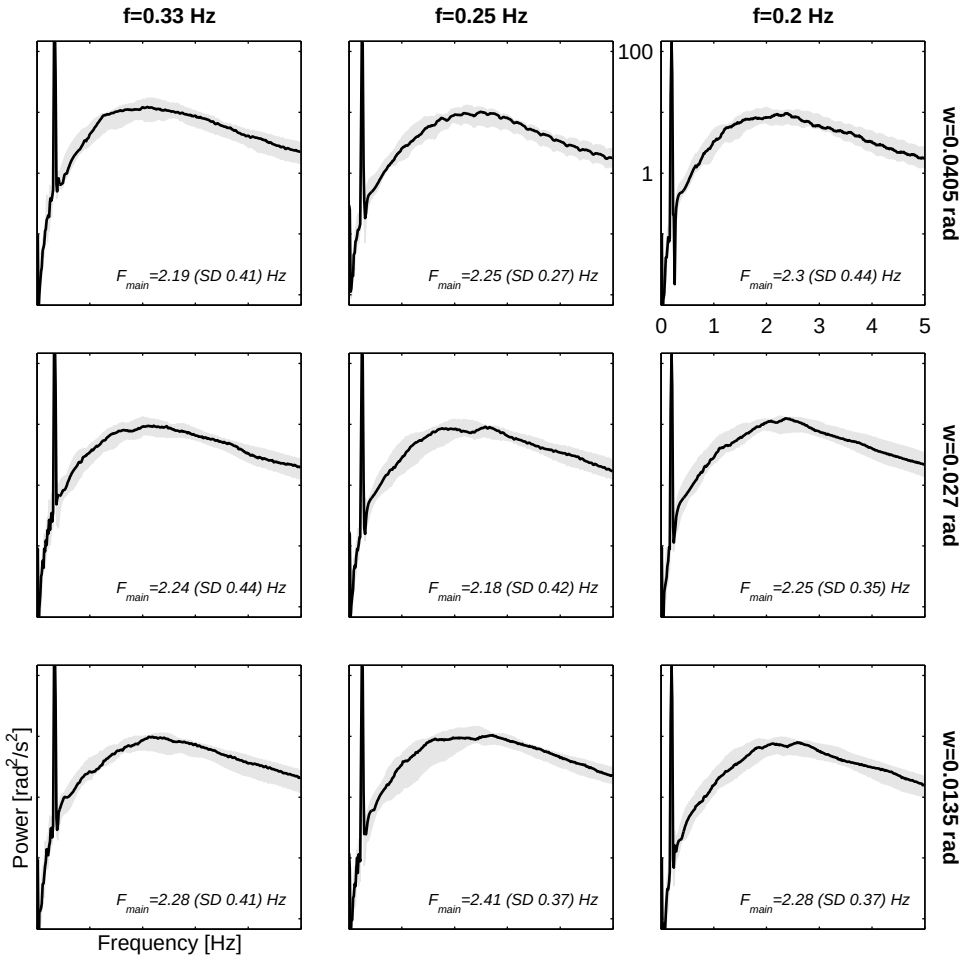

Figure 4.9: *Power spectra averaged over all subjects (black line) for three movement frequencies (columns) and three target sizes (rows). Grey area indicates the 95% confidence interval. The sharp peaks correspond to the movement frequencies and the broad peaks are caused by the speed pulses. F_{main} is the main frequency of the speed pulses.*

soidal tracking in monkeys (Miall et al., 1986) and constant velocity circular drawing of monkeys (Roitman et al., 2004) and humans (Pasalar et al., 2005). We share the interpretation of Pasalar et al. (2005) that increases in SP gain are a consequence of the greater tracking errors generated at faster speeds. During a fixed time interval, faster targets travel further, necessitating larger corrections resulting in larger SP amplitude and SP gain. The constancy of SP duration either suggests that more frequent corrections are impossible or inconvenient.

Changes in submovement characteristics in relation to target size have not been

investigated before. For decreasing target size, we observed increases in SP amplitude and SP gain, whereas SP duration was unaffected by target size. These results indicate that submovements are organised differently in tracking movements compared to goal-directed movements. As we highlighted in the introduction, goal-directed movements, unlike tracking movements, allow for more subtle, i.e. more frequent and smaller, submovements when aiming for smaller targets.

Pasalar et al. (2005) examined the effects of external force field magnitude on the regulation of submovements in circular drawing. SP gain and SP amplitude increased with increasing force field magnitude, whereas SP duration decreased. Pasalar et al. (2005) argued that SP gain was tuned in response to tracking errors by showing that tracking error increased with faster speeds as well as with higher force field magnitudes. The same argument might hold for the varying target sizes in the present experiment. If we assume that tracking errors are defined in units of target size, the same absolute error will generate a larger correction, reflected in SP gain, for the smaller target.

Are impedance modulation and changes in the organisation of submovements as a function of variations in task conditions related? Or, put more specifically, could the observed changes in the submovements be caused by changes in the natural frequency of the forearm due to stiffness changes? The data suggest that this was not the case. Given the inertia and stiffness estimates obtained, the natural frequency of the forearm would be about 1.5 Hz (SD 0.4 Hz), which is lower than the identified frequency of the submovements. Furthermore, the natural frequency varied as a function of the experimental conditions, whereas submovement duration seemed constant across conditions. Both observations indicate that impedance modulation and SP gain changes represent independent and additive accuracy control mechanisms. The frequency content of the speed profiles of about 2 Hz, as deduced from the frequency and time series analyses, suggests that the speed pulses are driven by visual feedback .

Generalisation to multi-joint movement

Single-joint movements occur rarely in daily life. It is therefore important to investigate whether the findings of the present study on single-joint movements can be generalised to more natural, multi-joint movements. There exists only indirect evidence for impedance modulation in response to accuracy constraints in multi-joint move-

ments. Muscular co-activation increases in response to higher accuracy constraints in pointing movements (Laursen et al., 1998; Gribble et al., 2003). Studies on multi-joint movement do show that humans are able to adapt endpoint stiffness to the instability of the task and that this increased stiffness reduces trajectory variability (e.g. Burdet et al., 2001). The question is whether multi-joint impedance also changes in response to accuracy demands. An indication to this effect can be gleaned from the work by Perreault (2005), showing that subjects orient their endpoint stiffness (largely dependent on body configuration) in line with the accuracy constraint.

The effects of movement speed on the organisation of submovements was previously investigated in multi-joint movement (Roitman et al., 2004; Pasalar et al., 2005). The results were similar to our results in the single-joint case. To our knowledge, however, the effects of accuracy constraints on the organisation of submovements have not been investigated before.

Conclusion

The present study underscores the importance of impedance modulation in controlling movement accuracy. It supports the claim of Van Galen and Schomaker (1992) and Van Galen and De Jong (1995) and the experimental findings of Burdet et al. (2001) and chapter 3, that greater impedance enhances movement accuracy. Furthermore, the present study provides new evidence that intermittently controlled submovements are natural components of motor behaviour and that their characteristics are modulated in response to task constraints, such as accuracy demands. The data suggest that impedance modulation and SP gain modulation contribute additively, i.e. independently, to the accuracy of target tracking.

Acknowledgements

The authors thank Nicolien de Langen for collecting the data.

5

Fatigue induced changes of impedance and performance in target tracking

Selen L.P.J., Beek P.J. & Van Dieën J.H. (2006). Fatigue induced changes of impedance and performance in target tracking. *Experimental Brain Research*, under review.

Abstract

Kinematic variability is caused, in part, by force fluctuations. It has been shown that the effects of force fluctuations on kinematics can be suppressed by increasing joint impedance. Given that force variability increases with muscular fatigue, we hypothesised that joint impedance would increase with fatigue to retain a prescribed accuracy level. To test this hypothesis, subjects tracked a target by elbow flexion and extension both with fatigued and unfatigued elbow flexor and extensor muscles. Joint impedance was estimated from controlled perturbations to the elbow. Contrary to the hypothesis, elbow impedance decreased, whereas performance, expressed as time-on-target, was unaffected by fatigue. Further analyses of the data revealed that subjects changed their control strategy with increasing fatigue. Although their overall kinematic variability increased, task performance was retained by staying closer to the centre of the target when fatigued. In conclusion, the present study reveals a limitation of impedance modulation in the control of movement variability.

Introduction

Prolonged exercise induces muscle fatigue. Muscle fatigue is generally defined as an activity induced loss of the ability to produce force with a muscle or muscle group (Gandevia, 2001) because of central and peripheral processes. The central nervous system (CNS) can compensate for a loss in the force generating capacity of the individual motor units (peripheral fatigue) by increasing the central drive to the motoneuronpool, resulting in higher firing frequencies of already active motor units and additional recruitment of larger motor units. Muscle fatigue eventually results in task failure (Hunter et al., 2002, 2004).

In the present study we were interested in how fatigue influences the variability of motor performance prior to task failure. Motor output variability is, at least in part, caused by variability in muscular force output. Besides the effort required to generate a constant force output under fatigue, also the variability of the force output increases with fatigue (e.g. Lippold, 1981; Hunter et al., 2004; Lorist et al., 2002; Huang et al., 2006). Most tasks constrain the range of permissible positional variations and therefore the CNS has to control the effects of force variability on the overt kinematics.

The neuromotor noise theory (NNT; Van Galen and De Jong, 1995) states that in order to obtain a desired level of positional accuracy of the end-effector (e.g. hand, finger, computer-mouse), the effects of force variability are filtered out by increasing joint stiffness through muscular co-activation. Most empirical support for the use of impedance to filter out neuromuscular noise is based on indirect evidence, such as increased pen tip pressure in writing (e.g. Van den Heuvel et al., 1998) and on EMG increases with increasing precision demands (e.g. Gribble et al., 2003; Osu et al., 2004). In recent studies, we provided direct evidence that individuals increase joint stiffness in order to attain the prevailing accuracy demands (chapters 3 and 4). This modulation of joint stiffness is particularly evident in target tracking.

As an extension of NNT, Van Dieën et al. (2003) argued that increases of neural and motor noise with fatigue might necessitate increased co-activation to attain the desired accuracy. Increased co-activation on the other hand would further accelerate fatigue development, resulting in a vicious circle of fatigue development and muscular co-activation under strict task constraints. Indications of increased co-activation with fatigue have been found (Gagnon et al., 1992; Psek and Cafarelli, 1993), but given that the EMG-force relationship is affected by fatigue, this provides only tentative support.

Apart from an increase in force variability with fatigue, also the muscle impedance changes with fatigue. With fatigue, muscle stiffness decreases for a constant isometric force, whereas the damping increases (Zhang and Rymer, 2001). This would exacerbate the vicious circle identified by Van Dieën et al. (2003) because a disproportionate increase in activation would be needed to generate satisfactory stiffness.

In previous studies, we showed that not only elbow impedance changed with accuracy demand, but subjects also tended to adapt their movement speed within the margins imposed by the task. For time-constrained goal directed movements, this resulted in a small but significant decrease of movement velocity with smaller targets (chapter 3). During target tracking, in which movement velocity is more severely constrained, subjects changed the organisation of corrective movements (chapter 4).

In the present study we aimed to further extend our understanding of the control of joint impedance in relation to motor output variability. Following our previous manipulations of accuracy demand, we now manipulated the neuromuscular noise by inducing muscular fatigue. We hypothesised that joint impedance would increase in order to compensate for the fatigue induced neuromuscular noise and concomitant kinematic variability.

Methods

Subjects

Ten healthy subjects (5 men and 5 women) between 20 and 25 years of age participated in the experiment. All subjects had normal or corrected to normal vision and reported no history of neuromuscular disorders. All subjects were right handed, in the sense that this was the hand they normally used for writing. The Local Ethics Committee approved the experiment and all subjects signed informed consent forms prior to their participation.

Overview of the experiment

The subjects performed two tasks. In the first task they tracked a sinusoidally moving target (figure 5.1A) by making elbow flexion and extension movements in the horizontal plane. The second task was intended to induce muscular fatigue (figure 5.1B) and consisted of resisting a time varying motor torque. Figure 5.1C depicts an overview

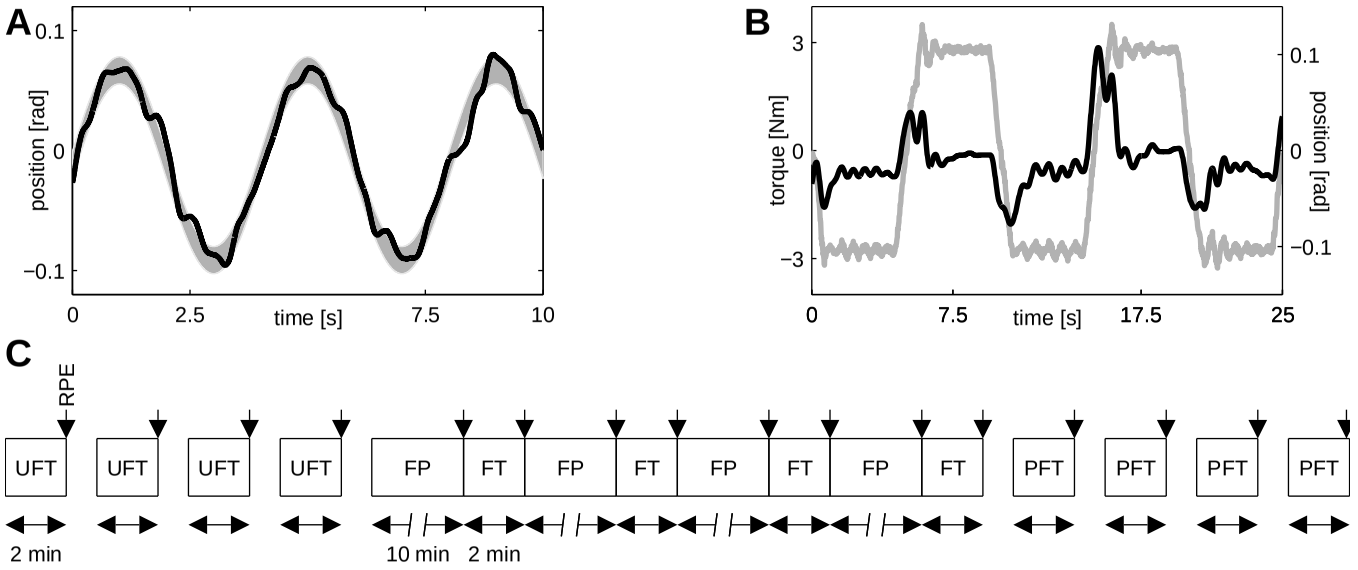

Figure 5.1: *Schematic description of the experiment. A. Section of a tracking trial. The grey area indicates the target area and the black line the projection of the pointer position. B. Section of the fatigue protocol. Time varying torque is indicated in grey and the elbow angle in black. C. Time line of the experiment. UFT and PFT trials were followed by one minute rest. The FP was followed immediately by FT. UFT: unfatigued tracking, FP: fatigue protocol, FT: fatigued tracking, PFT: post-fatigue tracking, RPE: rating of perceived exertion.*

of the order in which both tasks were performed. First, four two-minute unfatigued tracking trials were performed (UFT). Second, the fatigue protocol (FP) alternated with, now fatigued, tracking (FT). To control for learning effects, the tracking task was repeated for 5 out of 10 subjects after a recovery period of 5 minutes (PFT, post fatigue tracking). After every tracking period and after every fatigue protocol, subjects were asked to rate their perceived exertion (RPE) in the arm on a 10-point Borg scale (Borg, 1982).

Prior to the actual experiment, estimates of maximum voluntary torque, limb inertia and maximum voluntary stiffness were obtained. In the following sections, the experimental setup and procedure will be explained in more detail.

Experimental setup

Subjects were seated on a chair in front of a semicircular array of light emitting diodes (LEDs). The forearm used for writing was tightly cast onto the vertical shaft of a torque controlled motor (S-motor, elu93028, Fokker Control Systems), with the medial epicondyle aligned with the axis of rotation and the palm of the hand facing downward. Both torque and position data were stored at 1 kHz.

Experimental procedure

Maximum voluntary torque assessment

The torque level of the fatigue protocol was based on an estimate of the maximum voluntary torque (MVT) of the elbow. A force transducer was attached 30 cm distal to the elbow joint, orthogonal to the cast forearm. Three MVT attempts in both flexion and extension direction were performed, alternated with 1 minute rest. The maximum value, out of six, was selected as the MVT.

Inertia and maximum voluntary stiffness estimation

After the forearm had been attached to the torque motor, subjects were instructed to relax as much as possible. Sixteen biphasic torque perturbations (8 flexion and 8 extension) were applied randomly to the forearm. The perturbations had a duration of 70ms and an amplitude of 5Nm. Positions and torques were used to estimate inertia of forearm and manipulandum.

The same sequence of perturbations was applied to the forearm to estimate maximum values of stiffness and damping. Subjects were instructed to maximally coactivate their forearm muscles and to minimise the angular displacements caused by the perturbations.

Unfatigued tracking (UFT)

During UFT, FT and PFT, subjects tracked a target that had a width of 0.027 rad (which is approximately 1^o) and oscillated at 0.25Hz with an amplitude of 0.2 rad (see figure 5.1A). Subjects were instructed to keep the projection of the laser pointer within the target area. In some cycles, the motor applied a biphasic torque to the forearm. Subjects were instructed not to intervene voluntarily with those torque perturbations. From these perturbations, estimates of elbow stiffness and damping were calculated.

Two perturbation types were used and each was applied 12 times for every experimental condition. Perturbations were applied during flexion (pFLEX) and during extension (pEXT) and started with a torque opposite to the movement direction. The 24 perturbations in question were distributed randomly over the four two-minute trials with the restriction that they had to be at least 5 seconds apart. All perturbations occurred in the zero crossing of the target sine wave, i.e. at maximum velocity. Perturbations were biphasic, had an amplitude of 5Nm and a total duration of 70ms.

Fatigue protocol (FP)

Fatigue was induced by counteracting a torque generated by the motor (see figure 5.1B). This *positional* task is believed to generate fatigue much faster than an isometric force production task (Hunter et al., 2004). The time varying motor torque was constant for 4 seconds and changed sign in 1 second. Peak values of the torque were 5% MVT. Subjects opposed this torque pattern for 10 minutes, immediately followed by FT.

Fatigued tracking (FT)

The fatigued tracking task was exactly the same as in UFT. Subjects tracked the target immediately after the fatigue protocol for two minutes, during which six randomly distributed perturbations were applied. The combination of FP and FT was repeated four times.

Post-fatigue tracking (PFT)

For 5 out of 10 subjects, the UFT protocol was repeated after the FT protocol. These data were analysed to test for learning effects and retention in both performance and impedance.

Analyses

Tracking performance

The instruction to the subjects was to keep the pointer between the target boundaries. Fulfilment of this performance constraint was quantified as the percentage of time that the pointer was on target (%TT). In order to reveal changes in control, also the percentage of samples that lagged (%LAG) the centre of the target was calculated. Kinematic variability was assessed by calculating the mean distance to the centre of the target (MDT), the RMS (root mean square) value of the distance to the centre of the target (RMSDT) and the standard deviation of the distance to the centre of the target (SDDT). The latter two were calculated as a function of cycle time and subsequently averaged over the cycle.

Impedance estimation

The dynamics of the elbow joint were estimated by fitting a second order linear model with stiffness K, damping B and inertia I to the kinematic deviations in response to the torque perturbations. The inertia was estimated in a separate step and kept constant over conditions (UFT, FT and PFT) and movement directions (pFLEX and pEXT). The time window for the optimisation was 150ms, avoiding contributions of voluntary responses, but including spinal reflexes to the impedance estimates. After the optimisation procedure the variance accounted for (VAF) was calculated. For a detailed description of the optimisation procedure (see chapters 3 and 4).

Characterisation of submovements

Tracking movements are composed of small submovements. These submovements are best visible in the velocity domain and then called speed pulses (SP) (see chapter 4 and Roitman et al., 2004). To quantify SPs, angular data were filtered with a 5th order Butterworth filter with a cut-off frequency of 6 Hz and subsequently numerically differentiated. The duration of a single SP (SP duration) was defined as the

time between two successive local minima in the velocity profile. The amplitude of an SP (SP amplitude) was defined as the difference between a local maximum in the velocity profile and the average value of the two nearest minima. The slope of the linear regression between SP duration and SP amplitude was interpreted as an error correction gain (SP gain). SP gain has been shown to increase with increasing movement velocity (chapter 4 and Roitman et al., 2004) and increasing accuracy demand (chapter 4).

Statistics

Both in the text and figures data will be presented as mean and SD. In the figures, the four separate trials per condition will be presented. However, to remove learning effects, statistics will be presented for the last two trials only. Unless mentioned otherwise, there was no difference from the statistics as determined for all four trials. Statistics for stiffness and damping will be presented for all four trials together.

The focus will be on the difference between UFT and FT. The effects of fatigue were examined by performing two-way (two or four trials $\times$ two conditions) repeated measures ANOVAs on all 10 subjects. Additional two-way (two trials $\times$ three conditions) repeated measures ANOVAs were performed on the subgroup of five subjects that also performed PFT.

Results

Fatigue

All subjects completed the four repetitions of the 10 minute fatigue protocol. Figure 5.2 presents the summary of their RPE scores. Subjects reported increased exertion due to the FP, which slightly decreased during FT but remained above baseline level of unfatigued tracking. During PFT RPE scores had returned to UFT levels.

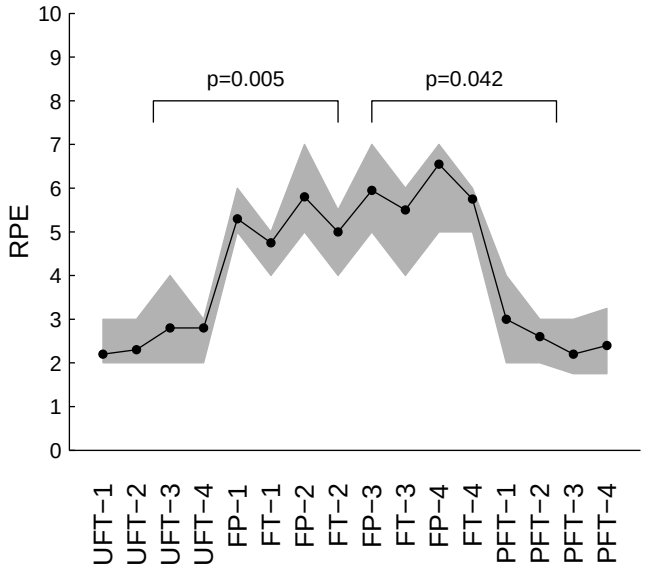

Figure 5.2: *Mean ratings of perceived exertion (RPE) over the entire experimental protocol. The grey area indicates the interquartile range . Ratings were obtained immediately after unfatigued tracking (UFT), the fatigue protocol (FP), fatigued tracking (FT) and post-fatigue tracking (PFT). RPE scores after FT were used for statistical comparisons between conditions.*

Tracking performance

Measures of tracking performance are depicted in figure 5.3, itemised for the 4 two-minute trials per condition. The statistics related to UFT and FT as calculated for the final 2 trials per condition are presented in table 5.1. At first sight, the results appear to indicate an increase of %TT over time. However, no significant effect of trial number was found for any performance measure, either with all four trials or with only the last two trials included.

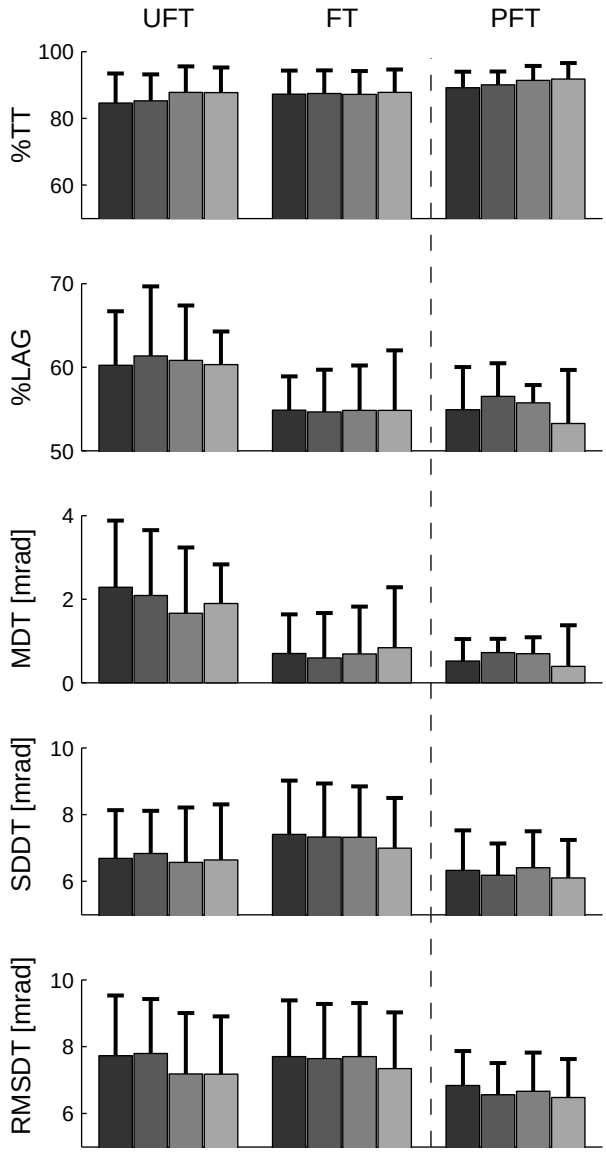

Figure 5.3: *Mean and SD over subjects of tracking performance measures, itemised for the four repeated trials and the three experimental conditions. Note that for UFT and FT the results are based on 10 subjects and for PFT on 5 subjects. This is indicated by the vertical dashed line. See main text for explanation of the performance variables.*

%TT is the performance measure that corresponds with the instruction to the subjects to stay on target. Despite the fatigue protocol, no changes in tracking performance were observed. However, fatigue resulted in larger kinematic fluctuations (SDDT). Without changes in control this would have resulted in lower %TT. The decrease in MDT and %LAG with fatigue indicates that subjects changed their control strategy to stay closer to the centre of the target.

Separate repeated measures ANOVAs were executed for the 5 subjects that per-

Table 5.1: *Statistical effects of the physical state of the subjects (STATE) and trial number (TRIAL) on performance measures. STATEs are unfatigued (UFT) and fatigued (FT). TRIALs are the four two-minute tracking periods.* * *Indicates that the result was significant ($p < 0.05$). Partial η^2 (η_p^2) is presented as a measure of effect size.*

	%TT		
STATE	$F_{(1,9)} = 0.062$	$p = 0.809$	$\eta_p^2 = 0.007$
TRIAL	$F_{(1,9)} = 0.000$	$p = 0.289$	$\eta_p^2 = 0.124$
STATE × TRIAL	$F_{(1,9)} = 0.000$	$p = 0.434$	$\eta_p^2 = 0.069$

	%LAG		
STATE	$F_{(1,9)} = 14.878$	$p = 0.004^*$	$\eta_p^2 = 0.623$
TRIAL	$F_{(1,9)} = 0.000$	$p = 0.810$	$\eta_p^2 = 0.007$
STATE × TRIAL	$F_{(1,9)} = 0.000$	$p = 0.819$	$\eta_p^2 = 0.006$

	MDT		
STATE	$F_{(1,9)} = 9.596$	$p = 0.013^*$	$\eta_p^2 = 0.516$
TRIAL	$F_{(1,9)} = 0.401$	$p = 0.541$	$\eta_p^2 = 0.043$
STATE × TRIAL	$F_{(1,9)} = 0.019$	$p = 0.892$	$\eta_p^2 = 0.002$

	SDDT		
STATE	$F_{(1,9)} = 0.5764$	$p = 0.040^*$	$\eta_p^2 = 0.390$
TRIAL	$F_{(1,9)} = 2.519$	$p = 0.447$	$\eta_p^2 = 0.219$
STATE × TRIAL	$F_{(1,9)} = 4.669$	$p = 0.614$	$\eta_p^2 = 0.064$

	RMSDT		
STATE	$F_{(1,9)} = 0.428$	$p = 0.530$	$\eta_p^2 = 0.045$
TRIAL	$F_{(1,9)} = 3.344$	$p = 0.072$	$\eta_p^2 = 0.271$
STATE × TRIAL	$F_{(1,9)} = 1.112$	$p = 0.351$	$\eta_p^2 = 0.110$

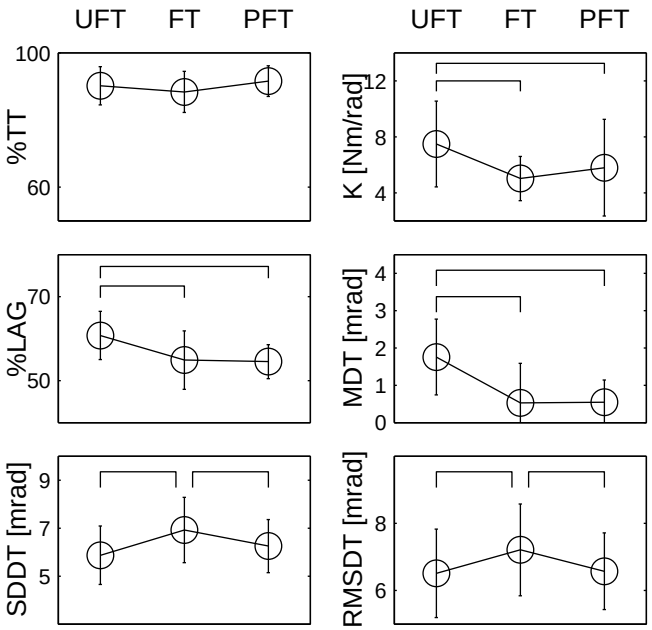

Figure 5.4: *Mean and SD of tracking parameters for the 5 subjects that performed the additional PFT task. Repeated measures ANOVAs were executed for the mean of the performance variables in the last two trials of each condition. Stiffness values were averaged over movement directions. Overlines indicate p values smaller than 0.15.*

formed PFT in addition to UFT and FT. Figure 5.4 shows the mean data over those 5 subjects for all performance variables and the stiffness. All p values smaller than 0.15 are presented. Again, no differences in %TT were revealed between the three conditions. Both %LAG and MDT seemed to stay at their FT values, whereas SDDT and RMSDT returned to their baseline, UFT, values during PFT.

Additional analyses revealed that performance variables became much less variable with fatigue. The left panel of figure 5.5 shows the average value of performance measures split into 8 one minute sections for a single subject. The right panel shows the mean and SD over all subjects of the standard deviation over the 8 minute sections. It is evident that performance was much steadier in the fatigued condition.

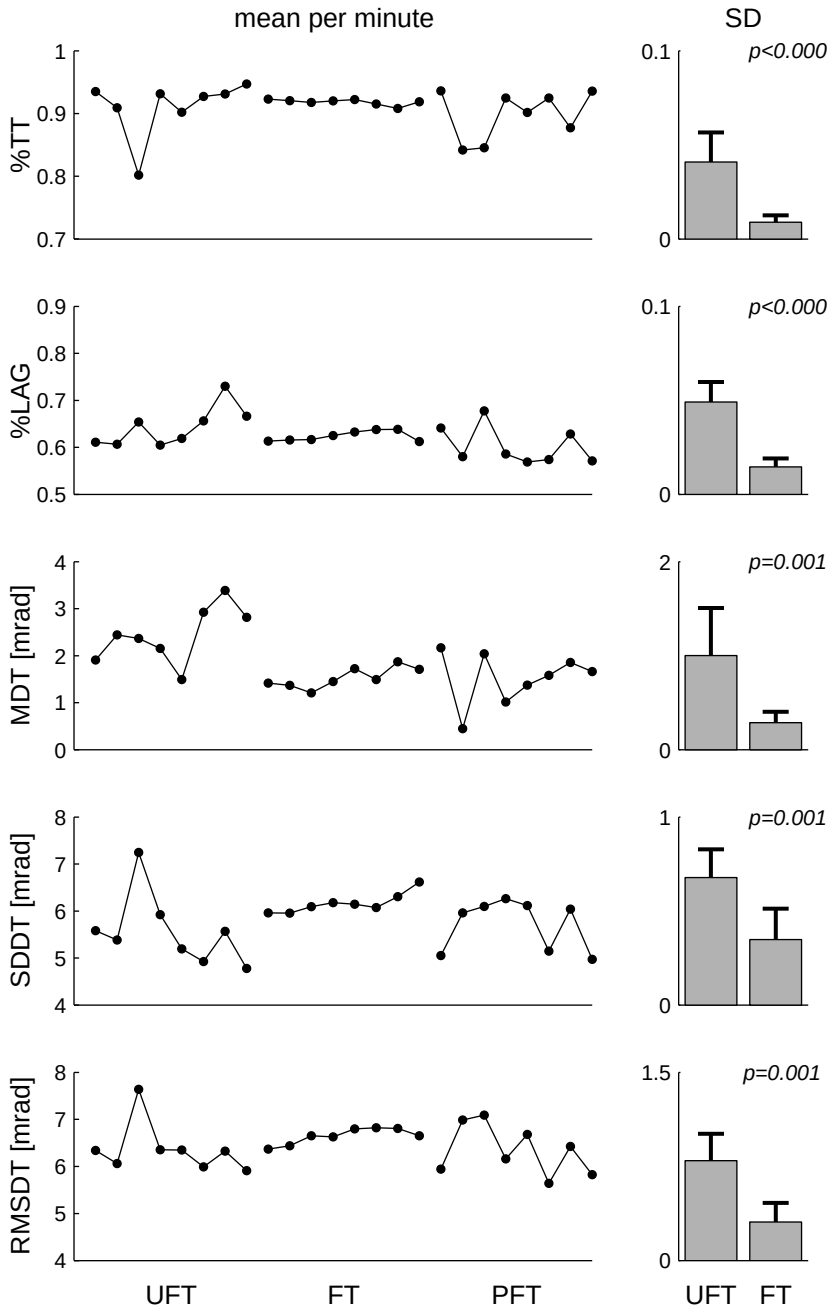

Figure 5.5: *Control variability. Left column shows the mean performance measures from minute to minute unfatigued (UFT), fatigued (FT) and post fatigue tracking (PFT) for a typical subject. Right column shows the mean and SD of the standard deviation collapsed for all subjects over the 8 minutes to show that the depicted effect generalised across subjects. Statistical significance is also indicated. See main text for a description of the performance variables.*

Table 5.2: *Statistical effects of the physical state of the subjects (STATE) and movement direction (DIR) on impedance measures. STATEs are unfatigued (UFT) and fatigued (FT). DIRections are elbow flexion and extension.* * *Indicates that the result was significant* ($p < 0.05$)*. Partial* η^2 (η_p^2) *is presented as a measure of effect size.*

	stiffness (*K*)		
STATE	$F_{(1,9)} = 24.238$	$p = 0.001^*$	$\eta_p^2 = 0.729$
DIR	$F_{(1,9)} = 30.474$	$p < 0.000^*$	$\eta_p^2 = 0.772$
STATE × DIR	$F_{(1,9)} = 11.562$	$p = 0.008^*$	$\eta_p^2 = 0.562$

	damping (*B*)		
STATE	$F_{(1,9)} = 0.634$	$p = 0.449$	$\eta_p^2 = 0.073$
DIR	$F_{(1,9)} = 3.274$	$p = 0.108$	$\eta_p^2 = 0.290$
STATE × DIR	$F_{(1,9)} = 0.408$	$p = 0.541$	$\eta_p^2 = 0.049$

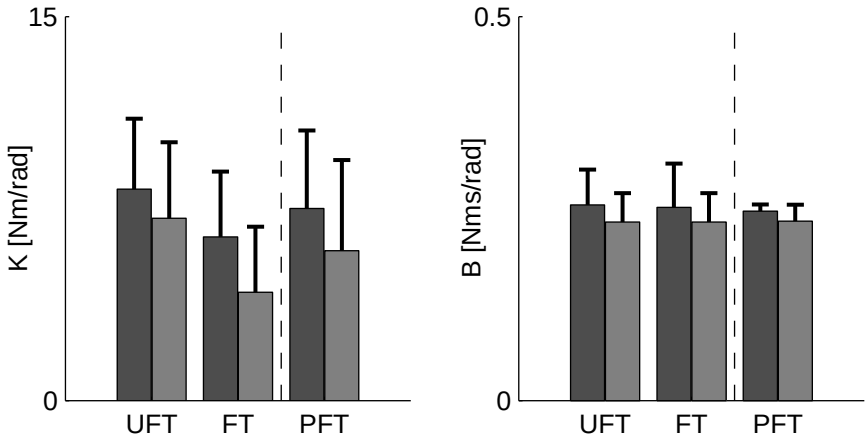

Figure 5.6: *Mean and SD of stiffness (K, left) and damping (B, right) for the experimental conditions. Dark and light bars indicate estimates during elbow extension and elbow flexion, respectively.*

Impedance

The impedance of the elbow joint was estimated by fitting a *K-B-I* model to the experimental data. The inertia was estimated independently of *K* and *B* and ranged from 0.047 Nms^2/rad to 0.0833 Nms^2/rad. Maximum voluntary stiffness was 61 (SD 17) Nm/rad and maximum voluntary damping was 0.81 (SD 0.22) Nms/rad. Figure 5.6 presents impedance estimates, expressed as stiffness and damping and table 5.2 presents the corresponding statistics. The fatigue protocol resulted in lower stiffness values. During PFT the stiffness recovered slowly, but not significantly (figure 5.4). Damping estimates did not change in response to fatigue. Both stiffness and damping were lower for elbow extension. In all cases the VAF was higher than 0.9.

Apart from fatigue, the stiffness estimate was also affected by perturbation direction. The stiffness was higher during extension than during flexion.

Speed pulses

Speed pulses were extracted from the speed profiles of the unperturbed movement cycles. Their characteristics (SP amplitude, SP duration and SP gain) are depicted in figure 5.7 for the individual trials and conditions. After a strong learning effect in the first two trials of UFT ($F_{(1,9)} = 10.018, p = 0.000, \eta_p^2 = 0.590$ for SP gain), no differences in the organisation of speed pulses were observed between the unfatigued and fatigued condition for the remaining trials (see table 5.3).

Table 5.3: *Statistical effects of the physical state of the subjects (STATE) on speedpulse characteristics. STATEs are unfatigued (UFT) and fatigued (FT). Partial η^2 (η_p^2) is presented as a measure of effect size.*

SP amplitude	$F_{(1,9)} = 0.004$	$p = 0.949$	$\eta_p^2 = 0.000$
SP duration	$F_{(1,9)} = 0.128$	$p = 0.729$	$\eta_p^2 = 0.014$
SP gain	$F_{(1,9)} = 0.427$	$p = 0.530$	$\eta_p^2 = 0.045$

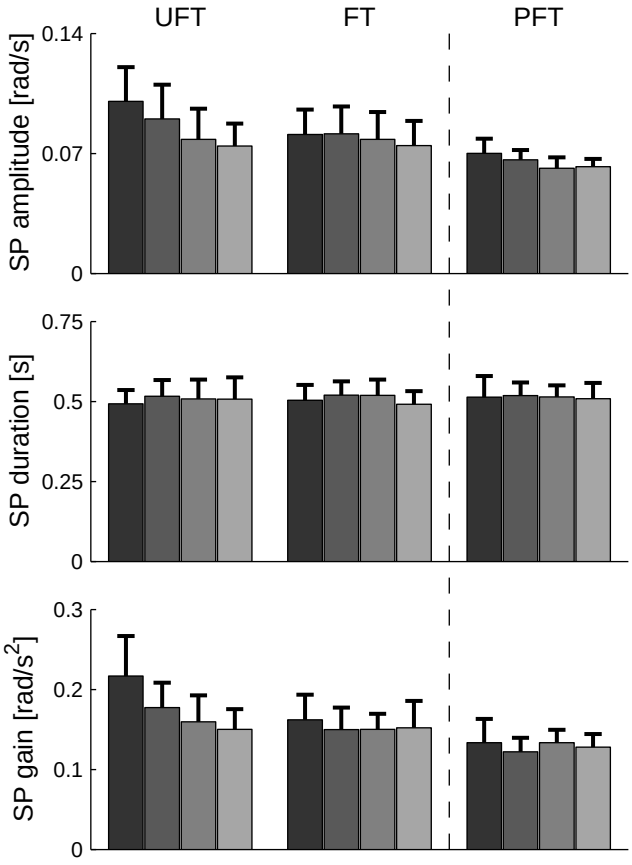

Figure 5.7: *Mean and SD over subjects of speed pulse characteristics, itemised for the four repeated trials and the three experimental conditions. Note that for UFT and FT the results are based on 10 subjects and for PFT on 5 subjects. This is indicated by the vertical dashed line. See main text for explanation of the speedpulse variables.*

Discussion

In the present study we tested the hypothesis that fatigue induced increase of force variability would result in increased elbow impedance in order to retain the accuracy required by the task. Based on %TT, no effects of fatigue on task performance were revealed. Contrary to our hypothesis, however, this was not accompanied by an increase in elbow impedance (i.e. stiffness), suggesting that the vicious circle between fatigue development and muscular co-activation as proposed by Van Dieën et al. (2003) does not exist or is circumvented. This is supported by the finding that muscular activity does not increase in response to fatigue in multi-joint target tracking (Huysmans et al., 2006).

In the following sections we will first discuss why joint impedance did not increase and how other mechanisms might have contributed to preserving task performance in the face of fatigue-induced increased neuromuscular noise. Subsequently, we will explain the results in view of reduced solution spaces and explorative behaviour. Finally, we will draw some general conclusions about the implications of the present findings for the concept of impedance modulation as a generic means to cope with neuromuscular noise.

Before discussing the present results, we have to ascertain that the fatigue protocol was effective. Fatigue was only assessed indirectly by ratings of perceived exertion as previous studies showed that RPE is a good indicator of muscle fatigue (e.g. Hummel et al., 2005; Kankaanpää et al., 1997; Huysmans et al., 2006). As expected, RPE increased in response to the fatigue protocol. Besides this expected increase in RPE, the decrease of joint impedance and the increase of SDDT also indicate that the fatigue protocol was effective. The increase in SDDT further indicates increased neuromuscular noise due to fatigue, as reported previously for isometric force (Lippold, 1981; Lorist et al., 2002; Hunter et al., 2004; Huang et al., 2006).

Although there was a significant increase in RPE, concomitant with an increase in neuromuscular noise, no decrease in performance was observed. Based on earlier studies in which joint impedance was found to increase with increasing accuracy demand (chapters 3 and 4), we expected joint impedance to increase in the present experiment as well. This expectation was based on the consideration that increasing the accuracy demand and increasing the noise are equivalent in that they both require adaptations from the neural control system to increase the signal-to-noise ratio. Nevertheless, joint stiffness decreased by 30% (SD 19%).

Could it have been the case that a further increase of impedance was impossible under the prevailing task conditions? We suspect not. Prior to fatigue, stiffness levels were relatively low (about 10 % of their maximum). Due to fatigue the maximum stiffness decreases to about 60% (Zhang and Rymer, 2001). This leaves enough margin to increase joint impedance, although excessive muscular co-activation would be necessary, and renders it unlikely that subjects were unable to increase impedance.

What then prevented the neural control system from increasing joint impedance? Was it some kind of cost consideration or was an impedance strategy no longer adequate to serve the task goal when fatigued? Cost considerations might have played a role. First, just to reach the stiffness level of UFT, co-activation has to increase at least 100% during FT (Zhang and Rymer, 2001). This is much more than the increase in stiffness of up to 30% we found in previous studies involving a three-fold increase in accuracy demand (chapters 3 and 4). Second, the control system may have learned to circumvent the vicious circle associated with impedance modulation (Van Dieën et al., 2003). On the other hand, it is conceivable that impedance modulation is no longer an adequate strategy when fatigued. The delicate balance between increases in neuromuscular noise and impedance (see chapter 2) with cocontraction may have shifted towards an increase in kinematic variability with increasing impedance. Based on the present data it is impossible to differentiate between the aforementioned possibilities, but it follows from the observed decrease in joint impedance that the neural control system must have relied on some other strategy to compensate for the detrimental effects of increased neuromuscular noise due to fatigue.

What could this strategy be? In principle, the neural control system may have resorted to both feedback and feed forward control strategies to preserve movement accuracy. Part of the feedback control strategies can be revealed by the analysis of submovements. In a previous study, we observed systematic changes in the control of submovements when tracking targets of different frequency and different width (chapter 4). Both higher target frequencies and smaller targets resulted in an increase of SP gain as a result of an increase in SP amplitude. Similarly, Pasalar et al. (2005) reported that SP gain increases for larger external perturbing force fields in circular drawing. All those increases may be interpreted as a result of a feedback controlled (relative) error correction mechanism. In particular for the external perturbing force field manipulations, parallels may be drawn to fatigue-induced increase in neuromuscular noise as both manipulations imply an increase of the perturbing forces. However, we observed no changes in SP gain, SP amplitude or SP duration with fatigue.

Only an initial decrease of SP gain and SP amplitude was observed in the first few unfatigued trials, which was most likely due to adaptation to the prevailing task conditions. Apparently, control of submovements did not change in response to fatigue. Instead, it is apparent from the present data that, when sufficiently fatigued, the neural control system adopted a feed forward strategy of staying closer to the centre of the target, as evidenced by decreased %LAG and decreased MDT. The predictability of the sine motion of the target allowed for this feedforward strategy, although in both the unfatigued and fatigued states, subjects lagged behind the target most of the time. Adopting this feedforward strategy is understandable because it allows the task constraints to be retained in spite of the increase in variability (SDDT and RMSDT).

Besides a strategy change due to fatigue, we observed that the execution of that strategy became stereotyped when fatigued. The variability of all performance measures decreased as fatigue increased over time. How should we interpret this observation? In all likelihood, the experimental manipulation reduced the solution space in two ways, namely by increasing neuromuscular noise and by changing the biophysical properties of the neuromuscular system. We submit that during UFT the neural control system was exploring the solution space, whereas during FT it was not because this would hamper performance. Further support for this hypothesis comes from the observation that variability increased and stereotypy decreased again during PFT (see figure 5.5), indicating that the solution space was again being explored. Interestingly, comparable observations of stereotypical, i.e. less variable, control strategies were made in patients with tardive dyskinesia (Newell et al., 1993) and with patellofemoral pain (Hamill et al., 1999) while standing and running, respectively. It is conceivable that also those stereotypical motor behaviours were associated with a reduction of the solution space, in this case as a result of an underlying pathology.

The PFT data also suggest that subjects adhered to the strategy they adopted during fatigue and stayed close to the centre of the target (%LAG, MDT), despite the recurrence of explorative behavior. This might either be taken to imply that subjects simply adhered to the newly discovered control strategy, or that the neuromuscular system was not fully recovered from fatigue, preventing them from a switch to their UFT strategy.

If subjects discovered a new control strategy of staying close to the centre of the target, then why did they not discover it prior to fatigue? An impedance strategy is energetically demanding (Franklin et al., 2004) and one might expect the neural control system to select an energy saving strategy from the outset. On the other hand,

an impedance strategy is generic and has low control cost. Possibly, subjects would have discovered the strategy of staying close to the target in the long run. However, fatigue appeared to have forced them into this new strategy. Similar instances of not discovering alternative strategies have been reported for goal directed movements in a divergent force field (Osu et al., 2003). When subjects move to a target in a divergent force field that pushes them away from a straight line, they increase endpoint stiffness to overcome the instability. An equally effective strategy would be to move through the force field, by making curved paths, thus learning the dynamics of the field. However, subjects only discover this strategy when explicitly instructed to do so. Alternatively, subjects might have switched back to their UFT strategy in the long term. Although SDDT and RMSDT returned to their baseline values during PFT, joint stiffness did not return to baseline and therefore could not contribute to the control of movement variability.

Conclusions

Impedance modulation is not the strategy of choice to preserve movement accuracy in the face of muscle fatigue, suggesting that the vicious circle of continuously increasing impedance with fatigue (Van Dieën et al., 2003) does not exist or is circumvented. Instead, subjects make use of the predictability of the target motion and stay closer to the centre of the target in the fatigued state than in the unfatigued state, resulting in unaffected task performance despite increased kinematic variability.

Acknowledgements

The authors thank Hanneke van Dongen for collecting the data and for comments on the manuscript.

6
Epilogue

Introduction

In the preceding chapters, propositions derived from Neuromotor Noise Theory (NNT) as proposed and developed by Van Galen and colleagues (e.g. 1992, 1995, 2000, 2002) were evaluated. The central tenet of NNT is that the modulation of joint stiffness is a relevant degree of freedom in controlling movement variability by filtering out neuromuscular noise. Both neuromuscular noise and joint impedance control act through the muscles, creating the paradoxical situation that, on the one hand, the muscles are the source of force variability while on the other hand they are supposed to help suppress its effects on kinematics. In chapter 2, this paradox was examined by constructing a neuro-musculo-skeletal model. The model showed that, in principle, muscular co-activation can suppress the effects of neuromuscular noise, in spite of the signal dependent nature of this noise.

In chapter 1, two lacunae in previous tests of the propositions of NNT were identified. To reiterate, the first lacuna was the absence of studies explicitly estimating the mechanical impedance of the neuro-musculo-skeletal system in relation to neuromuscular noise and task constraints. Instead, indirect measures, such as pen pressure and EMG (e.g. Van Gemmert and Van Galen, 1997; Van Galen and Van Huygevoort, 2000; Visser et al., 2004), were used as estimates of joint impedance. The second lacuna was the small number of studies explicitly addressing the effects of accuracy constraints on impedance modulation (Laursen et al., 1998; Van Galen and Van Huygevoort, 2000). In chapter 3, we provided direct evidence that the mechanical impedance of the elbow increases in response to increases in accuracy demands during goal-directed aiming. In accordance with this finding, Gribble et al. (2003) and Osu et al. (2004) reported increased muscular co-activation with increased accuracy demand in similar tasks. In chapter 4, this result was substantiated further by showing that elbow joint impedance also increases in response to increased accuracy demands during target tracking movements.

In chapter 5, the neuromuscular noise level was manipulated. Following the numerous studies reporting increased cocontraction in response to cognitive stressors (Van Gemmert and Van Galen, 1997, 1998; Van Galen et al., 2002; Van den Heuvel et al., 1998; Bloemsaat et al., 2005; Meulenbroek et al., 2005), which are supposed to increase neuromuscular noise, Van Dieën et al. (2003) hypothesised that increased neuromuscular noise due to fatigue would also result in increased joint impedance. The tracking study presented in chapter 5 falsified this claim. Joint impedance de-

creased and subjects adopted a strategy of staying closer to the centre of the target in the fatigued condition. Also for goal-directed movements (chapter 3) and for target tracking (chapter 4), alternative strategies were observed in addition to impedance modulation.

In this epilogue, I will discuss the main contributions of the present thesis regarding our understanding of the role of joint impedance in the control of accurate movement in combination with additional strategies. Before doing so, I will briefly evaluate the limitations of the adopted methodological approach.

Methodological considerations

This section is divided in a section dealing with the neuromuscular modelling approach pursued in chapter 2 and a section dealing with the experimental approach pursued in chapters 3, 4 and 5. Finally, some remarks will be made on the differences between force control and kinematic control.

Neuromuscular modelling

The numerical model in chapter 2 was inspired by a pioneering study of Van Galen and De Jong (1995), who were the first to numerically investigate the noise filtering properties of joint impedance in attenuating the effects of neuromuscular noise. In the present thesis, this work was extended by including more realistic models of both the motor neuron pool and the muscular contraction mechanism. The most important extension was the inclusion of muscular dynamics, resulting in a system in which impedance and force fluctuations acted through the same system(s), the muscle(s). Although our model is much more realistic from a physiological point of view than the one studied by Van Galen and De Jong (1995), it may still lack relevant details.

First, although Hill-type muscle models are widely used, their suitability for simulating natural movement (Perreault et al., 2003) and estimating muscle intrinsic stiffness (Stroeve, 1999) has been questioned. However, these conclusions were drawn from Hill models that do not incorporate length dependent calcium sensitivity (LDCS), which has been shown to result in a twofold increase of low-frequency stiffness (Kistemaker et al., 2005). Furthermore, given that the stiffness values in our model are on the lower side of the spectrum, stiffer models will suppress the effects of neuromuscular noise on kinematics only better and thus only strengthen our conclu-

sion that muscular cocontraction can effectively suppress the effects of neuromuscular noise on kinematics.

Second, the model used in chapter 2 includes no delayed feedback loops. All stabilising effects arise from the intrinsic properties of the force-length relationship in combination with LDCS. Both the frequency spectrum of the force fluctuations (Christakos et al., 2006) and the stabilising properties of the neuromuscular system (Stroeve, 1999) will change when delayed force, length and velocity feedback are added. However, the final common path is recruitment of motor units, which is believed to be the main source of SDN. Hence feedback will also result in noisy motor signals and the paradox therefore remains. We believe that feedback is especially important in preventing the limb to drift, as we already discussed in chapter 2.

The stimulus patterns generated by the motor neurons are a simplification vis-à-vis natural spike patterns. Extending our model with spiking behaviour is possible (Van Zandwijk et al., 1998) and will, most likely, result in larger force fluctuations in the last recruited motor units because of less fused contractions. Given the delicate interplay of neuromuscular noise and the biophysical properties of the limb, the implications of this extension for the kinematic variability are uncertain.

Impedance estimation

The experimental studies in chapters 3 to 5 relied on the identification of elbow joint dynamics. To this end, a second order model, including inertia, damping and stiffness, was fitted to the kinematic response to the torque perturbation. Here, I will discuss the appropriateness of this procedure.

The dynamics of single- and multi-joint systems have been studied extensively over the last thirty years or so. However, both the research questions addressed and the identification techniques used varied widely. Motor control issues related to the modulation of joint impedance include equilibrium-point control (e.g. Feldman and Latash, 2005; Kistemaker et al., 2006), the compensation for interaction torques (e.g. Gribble and Ostry, 1999), stability to external perturbations (e.g. Cholewicki et al., 2000; Lee et al., 2006), the contribution of intrinsic and reflexive properties to the stability (e.g. Kirsch and Kearney, 1997; Van der Helm et al., 2002) and adaptation to new environmental dynamics (e.g. Franklin et al., 2003). Depending on the type of question of interest, different identification techniques are available. Long time series of (pseudo-)random perturbations with a broad bandwidth provide most information

about the system's dynamics (Kearney and Hunter, 1990) and allow separation of muscle intrinsic and reflexive contributions (Zhang and Rymer, 1997; Van der Helm et al., 2002). However, the neuro-musculo-skeletal system is adaptive, i.e. it will react to the perturbations. As a consequence, the perturbations become part of the task. In the present thesis, the response to internally generated perturbations could have been masked by reactions to continuous external perturbations. Therefore, in order to estimate stiffness and damping of the system prior to perturbation onset, biphasic perturbations were applied sparingly and unexpectedly. Although one might question the exact values of the stiffness and damping estimated, relative changes in their values were readily revealed by this method.

Force and position control

The numerical and experimental studies in this thesis focused on positional and movement control, respectively. Those tasks were deliberately chosen, because we believe they are the only motor control tasks in which impedance control can contribute to accuracy. In particular, when exerting an isometric force on a force transducer, force variability due to neuromuscular noise will not decrease as a result of co-activation because muscle dynamics are hardly involved. For example, Matthews and Muir (1980) found that when an (isometric) force was exerted on a force transducer the force spectrum was fundamentally different than when subjects exerted the same force on a spring. Studies on the control of isometric force production and the concomitant variability provide insight into the neural control mechanisms involved, but cannot be extended or generalised to the control of kinematic variability. This also becomes apparent when comparing endurance times of isometric force production on a force transducer to the production of the same force when holding a mass (Hunter et al., 2005). Time to task failure is much shorter in the latter situation. Furthermore, a clear transition can be seen in muscular control when a finger *moves toward* a force transducer and subsequently *exerts force on* the transducer (Valero-Cuevas et al., 2006).

Impedance modulation, a generic strategy?

Anyone who has ever threaded a needle will remember how difficult it is to match the relative position of one' s hands within the margin of error allowed. Many other tasks in daily life, such as writing, drawing, computer input work, and controlling the

steering wheel of a car while parking, also impose constraints on the precision with which we have to position and move our hands or hand-held tools.

The results reported in this thesis provided evidence that the modulation of the mechanical impedance of a single joint contributes to the control of movement accuracy. They also indicated, however, that impedance modulation is not a generic strategy that can be extended without reservation to multi-joint movement and daily life. Signs of other strategies were observed in chapters 3 and 4, whereas subjects actually switched to another strategy than impedance modulation in the experiment reported in chapter 5. Obviously, impedance modulation is not the only strategy and in some situations impedance modulation is not even an option. In the following, I will discuss other strategies besides impedance modulation that might be employed to control movement variability.

During the experiment on goal-directed movements reported in chapter 3, feedback of movement time and accuracy was provided after every single trial. Nonetheless, subjects had great difficulty in repetitively generating accurate movements of fixed duration. Even for the subset of trials that met both the accuracy and timing constraints (270-330ms), movements to the smallest target were significantly slower. This demonstrates how powerful the speed-accuracy trade-off (Fitts, 1954) is. From a neuromuscular noise perspective, it makes sense to opt for modulation of movement speed because the noise levels of the driving force are lower and prolonged movement time allows more corrections in the form of submovements. Moreover, the energetic demands of such a strategy are lower than of impedance control.

Submovements have been studied predominantly in the context of goal-directed movements (Meyer et al., 1988; Burdet and Milner, 1998), where submovements are supposed to reflect control processes to overcome the detrimental effects of neuromuscular noise. However, submovements are also observed in tracking movements and their characteristics change with movement velocity (Roitman et al., 2004) and external force fields (Pasalar et al., 2005). In chapter 4, we showed that, besides the modulation of joint impedance, also the characteristics of the submovements change in response to changes in target size, presumably as a consequence of changes in error correction.

The musculoskeletal system is redundant in the sense that there are more muscles available than are strictly necessary to control the degrees of freedom of the joints. This provides the neural control system the option to spread the noise over multiple muscles, thereby minimising its effects on motor performance (Hamilton et al., 2004;

Haruno and Wolpert, 2005). In addition, redundancy may be exploited by covariation of task related variables (Scholz and Schöner, 1999; Müller and Sternad, 2004). For example, during learning of multi-joint Frisbee throwing covariance between kinematic variables changed with practise in order to enhance throwing accuracy (Yang and Scholz, 2005). Also Kang et al. (2004) showed that during learning of an unusual multi-finger force production task, overall performance increased by selectively (re-)distributing the force variability over the individual fingers.

The effects of accuracy constraints on cocontraction and joint impedance appear to be much more substantial for motions in free space (Gribble et al., 2003; Osu et al., 2004, chapter 3, chapter 4) compared to tasks in which there is a pronounced mechanical interaction with the environment. Van Galen and Van Huygevoort (2000) did not find effects of target size on pen pressure in a graphical aiming task. Visser et al. (2004) reported only slightly increased flexor activity in aiming with a computer mouse, and did not find effects on extensor EMG, grip force and click force. In the same study no effects of precision demand during tracking were found. Finally, Sandfeld and Jensen (2005) found very small effects of manipulations of mouse gain on forearm EMG in an aiming task. Nonetheless, in all of these studies, performance measures were influenced by the precision demand. We hypothesise that the tactile afference from the pen and mouse provides continuous information, parallel to visual and proprioceptive information, about the current position of the hand and that this information is used for online corrections of the movement. Others have shown that tactile information about finger endpoint position decreases movement variability during pointing (Rao and Gordon, 2001), and also that postural sway is reduced by finger contact (Jeka and Lackner, 1994).

In multi-joint movement, an impedance modulation strategy would involve the control of the endpoint stiffness of the effector. This can be accomplished by modulating stiffness of the individual joints, but also their configuration, i.e. the Jacobian of the system, can have significant effects on the endpoint stiffness. Evidence for the optimal posture selection in response to accuracy constraints can be found in the work of Perreault (2005).

In summary, several, most likely additive, strategies to control movement variability might be employed by the motor control system. The single-joint nature of the tasks in combination with the strict constraints on both the timing and accuracy of the movements in the experiments in this thesis resulted in a dominant role for impedance modulation when the muscles were unfatigued. However, in daily life tasks constraints

are often not that tight. And even when they are, subjects are able to find new strategies when neuromuscular noise is increased due to fatigue and impedance no longer offers solace (chapter 5). Also in other situations, joint impedance may not counteract the effects of neuromuscular noise. Recently, Reeves et al. (2006) asked subjects to sit on a 30 cm diameter hemisphere. During balancing on this unstable seat, postural control degraded when cocontracting trunk muscles. In this case the effects of increased neuromuscular noise are not counteracted by the stabilising effects of joint impedance because there is no stationary world, or nearly stationary world due to large inertia, to stabilise against.

The question arises how a control strategy, or a combination of control strategies, emerges. As demonstrated in the present thesis, both the state of the neuromuscular system and the constraints imposed by the task influence the choice of strategy. In the next section, I will discuss future lines of research that might help to reveal the mechanisms and factors involved in the emergence of motor control strategies fitting the constraints imposed by the task.

Future research directions

Both computational and experimental studies will be required to understand the control of accurate movement, both in terms of its physiological demand and task constraints. I will review some computational and experimental directions for future research separately, although, of course, those endeavours will have to be complementary.

Computational approaches

The modelling study in chapter 2 illustrates that creating noisy neuromuscular models is a non-trivial enterprise. If we want to understand how stability and accuracy are guaranteed in the presence of neuromuscular noise, for example, when making a goal-directed movement or while standing upright, neuromuscular models of the type presented in this thesis will be indispensable. The computational effort will be high, especially when the model used is extended with feedback loops and spiking behaviour, but I believe this will be essential to reveal the processes underlying stable and accurate actions of the neuro-musculo-skeletal system. Recently, Todorov and Jordan (2002) introduced a powerful tool to understand the control of the noisy sensorimo-

tor system in the form of a stochastic optimal control model with signal dependent noise in both the control and feedback signals. However, in this model, the description of the plant, i.e. the neuro-musculo-skeletal system, is reduced to a point mass. The challenge in the coming years will be to couple stochastic optimal control theory to more realistic models of the neuro-musculo-skeletal system in order to examine how different control strategies, such as impedance modulation, contribute to model behaviour.

Extending our stationary model to goal-directed and multi-joint movements could be an intermediate step in this endeavour. Optimisation approaches like the minimum variance model (Harris and Wolpert, 1998) could be applied, with the complicating factor that for multi-joint models the problem of kinematic redundancy will have to be resolved. However, to replicate phenomena like the selective control of kinematic variability near the target area (Osu et al., 2004, chapter 3) and the covariation of task related variables (Scholz and Schöner, 1999; Müller and Sternad, 2004), closed loop controllers of the type presented by Todorov and Jordan (2002) are, most likely, necessary.

Experimental approaches

The experimental results of Osu et al. (2004) and of chapter 3 and the simulation results of Todorov and Jordan (2002) suggest that kinematic variability is selectively regulated close to the target region. Although I argued in the methodological section that closed loop system identification would mask the regulation of joint impedance related to the suppression of neuromuscular noise, this technique might still be applied to examine whether the impedance of the neuro-musculo-skeletal system is also only selectively modulated near the target region. Furthermore, the contribution of muscle intrinsic properties and reflex loops to task performance might be unravelled, also with respect to different accuracy demands.

The experiments presented in chapters 3, 4 and 5 were all constrained to single-joint movement. To understand the contribution of other mechanisms, such as covariation of task related variables and optimal posture selection, in the control of movement accuracy, experiments investigating multi-joint movement will be necessary. Using the uncontrolled manifold concept (Scholz and Schöner, 1999), one might be able to reveal changes in the covariation of task related variables in response to changes in accuracy demand. Furthermore, multi-joint identification of endpoint stiffness during

goal directed movement may reveal the contribution of joint stiffness and postural stability to overall performance. The contribution of covariation of task related variables can also be investigated in single joint movement. However, the variables of interest are now the forces or control signals of the individual muscles and their covariation.

The experiment in chapter 4 revealed systematic changes in the organisation of submovements in response to accuracy constraint changes. However, the cyclic nature of the task prevented an in-depth investigation of submovements. To understand whether the underlying control mechanism is indeed related to error corrections, circular tracking experiments are needed in which multi-joint movements are performed in pursuit of differently sized targets moving at constant velocity.

The observation in chapter 5 that subjects stay closer to the centre of the target when fatigued needs further investigation. This strategy is only effective when the target motion is predictable and therefore the experiment should be extended to multi-joint target tracking at constant velocity but with unpredictable movement direction (e.g. Huysmans et al., 2006).

Finally, during everyday movements different strategies will be combined and employed in parallel to control movement accuracy. The emergence of a combination of strategies will, among other factors, depend on the energetic and control costs, previous movements, the physical state of the neuro-musculo-skeletal system and the expectation of future costs and consequences. The solution space associated with all those constraints will be the playing field of the motor control system. The experiment presented in chapter 5 provided a window on the appearance of movement stereotypy when the solution space becomes largely constrained. Others have shown that induced muscle pain also results in control strategy changes (Ervilha et al., 2005). However, those phenomena are poorly understood: more research is needed to elucidate how the emergence of control strategies, stereotypical or not, is related to neuro-musculo-skeletal and task constraints.

Overall conclusion

Impedance modulation is just one of potentially many strategies that the control system has at its disposal to control movement variability. Depending on the prevailing task constraints and the physical state of the neuromuscular system, different combinations of strategies might be used. When, in a given situation, joint impedance can be modulated to enhance task performance, this strategy is likely to be applied.

However, excessive use is probably avoided because of its energetic demands and, in other situations, for example when fatigued or when a stationary world is absent, the extra neuromuscular noise due to increased impedance cannot be counteracted and recourse will be taken to other strategies to meet the prevailing task demands.

References

Adam, A., De Luca, C. J., and Erim, Z. (1998). Hand dominance and motor unit firing behavior. *J Neurophysiol*, 80(3):1373–82.

Bennett, D. J. (1993). Torques generated at the human elbow joint in response to constant position errors imposed during voluntary movements. *Exp Brain Res*, 95(3):488–98.

Bennett, D. J. (1994). Stretch reflex responses in the human elbow joint during a voluntary movement. *J Physiol*, 474(2):339–51.

Bennett, D. J., Hollerbach, J. M., Xu, Y., and Hunter, I. W. (1992). Time-varying stiffness of human elbow joint during cyclic voluntary movement. *Exp Brain Res*, 88(2):433–42.

Bernstein, N. (1967). *The co-ordination and regulation of movements*. Oxford: Pergamon Press.

Berthier, N. E., Rosenstein, M. T., and Barto, A. G. (2005). Approximate optimal control as a model for motor learning. *Psychol Rev*, 112(2):329–346.

Bloemsaat, J. G., Meulenbroek, R. G. J., and Galen, G. P. V. (2005). Differential effects of mental load on proximal and distal arm muscle activity. *Exp Brain Res*, 167(4):622–634.

Borg, G. A. (1982). Psychophysical bases of perceived exertion. *Med Sci Sports Exerc*, 14(5):377–381.

Burdet, E. and Milner, T. E. (1998). Quantization of human motions and learning of accurate movements. *Biol Cybern*, 78(4):307–318.

Burdet, E., Osu, R., Franklin, D. W., Milner, T. E., and Kawato, M. (2001). The central nervous system stabilizes unstable dynamics by learning optimal impedance. *Nature*, 414(6862):446–9.

Burdet, E., Osu, R., Franklin, D. W., Yoshioka, T., Milner, T. E., and Kawato, M. (2000). A method for measuring endpoint stiffness during multi-joint arm movements. *J Biomech*, 33(12):1705–9.

Cholewicki, J., Simons, A. P., and Radebold, A. (2000). Effects of external trunk loads on lumbar spine stability. *J Biomech*, 33(11):1377–1385.

Christakos, C. N., Papadimitriou, N. A., and Erimaki, S. (2006). Parallel neuronal mechanisms underlying physiological force tremor in steady muscle contractions of humans. *J Neurophysiol*, 95(1):53–66.

Christou, E. A., Grossman, M., and Carlton, L. G. (2002). Modeling variability of force during isometric contractions of the quadriceps femoris. *J Mot Behav*, 34(1):67–81.

Christou, E. A., Jakobi, J. M., Critchlow, A., Fleshner, M., and Enoka, R. M. (2004). The 1- to 2-Hz oscillations in muscle force are exacerbated by stress, especially in older adults. *J Appl Physiol*, 97(1):225–235.

Dounskaia, N., Wisleder, D., and Johnson, T. (2005). Influence of biomechanical factors on substructure of pointing movements. *Exp Brain Res*, 164(4):505–516.

Efron, B. and Tibshiran, R. J. (1993). *An introduction to the bootstrap*. London: Chapman & Hall.

Elliott, D., Helsen, W. F., and Chua, R. (2001). A century later: Woodworth's (1899) two-component model of goal-directed aiming. *Psychol Bull*, 127(3):342–57.

Ervilha, U. F., Farina, D., Arendt-Nielsen, L., and Graven-Nielsen, T. (2005). Experimental muscle pain changes motor control strategies in dynamic contractions. *Exp Brain Res*, 164(2):215–224.

Feldman, A. G. and Latash, M. L. (2005). Testing hypotheses and the advancement of science: recent attempts to falsify the equilibrium point hypothesis. *Exp Brain Res*, 161(1):91–103.

Fishbach, A., Roy, S. A., Bastianen, C., Miller, L. E., and Houk, J. C. (2005). Kinematic properties of on-line error corrections in the monkey. *Exp Brain Res*, 164(4):442–457.

Fitts, P. (1954). The information capacity of the human motor system in controlling the amplitude of movement. *J Exp Psychol*, 47(6):381–91.

Franklin, D. W., Burdet, E., Osu, R., Kawato, M., and Milner, T. E. (2003). Functional significance of stiffness in adaptation of multijoint arm movements to stable and unstable dynamics. *Exp Brain Res*, 151(2):145–157.

Franklin, D. W., So, U., Kawato, M., and Milner, T. E. (2004). Impedance control balances stability with metabolically costly muscle activation. *J Neurophysiol*, 92(5):3097–3105.

Fuglevand, A. J., Winter, D. A., and Patla, A. E. (1993). Models of recruitment and rate coding organization in motor-unit pools. *J Neurophysiol*, 70(6):2470–2488.

Gagnon, D., Asrenault, A. B., Smyth, G., and Kemp, F. (1992). Cocontraction changes in muscular fatigue at different levels of isometric contraction. *Int J Ind Ergon*, 9:343–348.

Gandevia, S. C. (2001). Spinal and supraspinal factors in human muscle fatigue. *Physiol Rev*, 81(4):1725–1789.

Goffe, W., Ferrier, G., and Rogers, J. (1994). Global optimization of statistical functions with simulated annealing. *J. Econometrics*, 60:65–99.

Gribble, P. L., Mullin, L. I., Cothros, N., and Mattar, A. (2003). Role of cocontraction in arm movement accuracy. *J Neurophysiol*, 89(5):2396–405.

Gribble, P. L. and Ostry, D. J. (1999). Compensation for interaction torques during single- and multijoint limb movement. *J Neurophysiol*, 82(5):2310–2326.

Guigon, E., Baraduc, P., and Desmurget, M. (2006). Computational motor control: feedback and accuracy. *submitted*.

Hajian, A. Z. and Howe, R. D. (1997). Identification of the mechanical impedance at the human finger tip. *J Biomech Eng*, 119(1):109–14.

Hamill, J., van Emmerik, R. E., Heiderscheit, B. C., and Li, L. (1999). A dynamical systems approach to lower extremity running injuries. *Clin Biomech (Bristol, Avon)*, 14(5):297–308.

Hamilton, A. F., Jones, K. E., and Wolpert, D. M. (2004). The scaling of motor noise with muscle strength and motor unit number in humans. *Exp Brain Res*, 157(4):417–430.

Hamilton, A. F. and Wolpert, D. M. (2002). Controlling the statistics of action: obstacle avoidance. *J Neurophysiol*, 87(5):2434–2440.

Harris, C. M. and Wolpert, D. M. (1998). Signal-dependent noise determines motor planning. *Nature*, 394(6695):780–784.

Haruno, M. and Wolpert, D. M. (2005). Optimal control of redundant muscles in step-tracking wrist movements. *J Neurophysiol*, 94(6):4244–4255.

Huang, C.-T., Hwang, I.-S., Huang, C.-C., and Young, M.-S. (2006). Exertion dependent alternations in force fluctuation and limb acceleration during sustained fatiguing contraction. *Eur J Appl Physiol*, 97(3):362–371.

Hummel, A., Läubli, T., Pozzo, M., Schenk, P., Spillmann, S., and Klipstein, A. (2005). Relationship between perceived exertion and mean power frequency of the EMG signal from the upper trapezius muscle during isometric shoulder elevation. *Eur J Appl Physiol*, 95(4):321–326.

Hunter, S. K., Critchlow, A., Shin, I.-S., and Enoka, R. M. (2004). Fatigability of the elbow flexor muscles for a sustained submaximal contraction is similar in men and women matched for strength. *J Appl Physiol*, 96(1):195–202.

Hunter, S. K. and Enoka, R. M. (2003). Changes in muscle activation can prolong the endurance time of a submaximal isometric contraction in humans. *J Appl Physiol*, 94(1):108–118.

Hunter, S. K., Rochette, L., Critchlow, A., and Enoka, R. M. (2005). Time to task failure differs with load type when old adults perform a submaximal fatiguing contraction. *Muscle Nerve*, 31(6):730–740.

Hunter, S. K., Ryan, D. L., Ortega, J. D., and Enoka, R. M. (2002). Task differences with the same load torque alter the endurance time of submaximal fatiguing contractions in humans. *J Neurophysiol*, 88(6):3087–3096.

Huysmans, M. A., Hoozemans, M. J. M., Van der Beek, A. J., De Looze, M. P., and Van Dieën, J. H. (2006). Fatigue effects on tracking performance and muscle activity. *Journal of Electromyography and Kinesiology*, in revision.

Jeka, J. J. and Lackner, J. R. (1994). Fingertip contact influences human postural control. *Exp Brain Res*, 100(3):495–502.

Jones, K. E., Hamilton, A. F., and Wolpert, D. M. (2002). Sources of signal-dependent noise during isometric force production. *J Neurophysiol*, 88(3):1533–1544.

Kalveram, K. T., Schinauer, T., Beirle, S., Richter, S., and Jansen-Osmann, P. (2005). Threading neural feedforward into a mechanical spring: how biology exploits physics in limb control. *Biol Cybern*, 92(4):229–40.

Kang, N., Shinohara, M., Zatsiorsky, V. M., and Latash, M. L. (2004). Learning multi-finger synergies: an uncontrolled manifold analysis. *Exp Brain Res*, 157(3):336–350.

Kankaanpää, M., Taimela, S., Webber, C. L., Airaksinen, O., and Hänninen, O. (1997). Lumbar paraspinal muscle fatigability in repetitive isoinertial loading: EMG spectral indices, Borg scale and endurance time. *Eur J Appl Physiol Occup Physiol*, 76(3):236–242.

Kay, B. A., Saltzman, E. L., and Kelso, J. A. (1991). Steady-state and perturbed rhythmical movements: a dynamical analysis. *J Exp Psychol Hum Percept Perform*, 17(1):183–197.

Kearney, R. E. and Hunter, I. W. (1990). System identification of human joint dynamics. *Crit Rev Biomed Eng*, 18(1):55–87.

Kearney, R. E., Stein, R. B., and Parameswaran, L. (1997). Identification of intrinsic and reflex contributions to human ankle stiffness dynamics. *IEEE Trans Biomed Eng*, 44(6):493–504.

Kirsch, R. F., Boskov, D., and Rymer, W. Z. (1994). Muscle stiffness during transient and continuous movements of cat muscle: perturbation characteristics and physiological relevance. *IEEE Trans Biomed Eng*, 41(8):758–770.

Kirsch, R. F. and Kearney, R. E. (1997). Identification of time-varying stiffness dynamics of the human ankle joint during an imposed movement. *Exp Brain Res*, 114(1):71–85.

Kistemaker, D. A., Van Soest, A. J., and Bobbert, M. F. (2005). Length-dependent [Ca2+] sensitivity adds stiffness to muscle. *J Biomech*, 38(9):1816–1821.

Kistemaker, D. A., Van Soest, A. J., and Bobbert, M. F. (2006). Is equilibrium point control feasible for fast goal-directed single-joint movements? *J Neurophysiol*, 95(5):2898–2912.

Laidlaw, D. H., Bilodeau, M., and Enoka, R. M. (2000). Steadiness is reduced and motor unit discharge is more variable in old adults. *Muscle Nerve*, 23(4):600–12.

Laursen, B., Jensen, B. R., and Sjogaard, G. (1998). Effect of speed and precision demands on human shoulder muscle electromyography during a repetitive task. *Eur J Appl Physiol Occup Physiol*, 78(6):544–8.

Lee, P. J., Rogers, E. L., and Granata, K. P. (2006). Active trunk stiffness increases with co-contraction. *J Electromyogr Kinesiol*, 16(1):51–57.

Lippold, O. (1981). The tremor in fatigue. In: R. Porter and J. Whelan (Eds.), *Human muscle fatigue* (pp. 234–248). London: Pitman medical.

Lorist, M. M., Kernell, D., Meijman, T. F., and Zijdewind, I. (2002). Motor fatigue and cognitive task performance in humans. *J Physiol*, 545(Pt 1):313–319.

Matthews, P. B. (1996). Relationship of firing intervals of human motor units to the trajectory of post-spike after-hyperpolarization and synaptic noise. *J Physiol*, 492 (Pt 2):597–628.

Matthews, P. B. and Muir, R. B. (1980). Comparison of electromyogram spectra with force spectra during human elbow tremor. *J Physiol*, 302:427–441.

Mazzaro, N., Grey, M. J., and Sinkjaer, T. (2005). Contribution of afferent feedback to the soleus muscle activity during human locomotion. *J Neurophysiol*, 93(1):167–77.

McAuley, J. H., Rothwell, J. C., and Marsden, C. D. (1997). Frequency peaks of tremor, muscle vibration and electromyographic activity at 10 Hz, 20 Hz and 40 Hz during human finger muscle contraction may reflect rhythmicities of central neural firing. *Exp Brain Res*, 114(3):525–41.

Meulenbroek, R. G. J., Galen, G. P. V., Hulstijn, M., Hulstijn, W., and Bloemsaat, G. (2005). Muscular co-contraction covaries with task load to control the flow of motion in fine motor tasks. *Biol Psychol*, 68(3):331–352.

Meyer, D. E., Abrams, R. A., Kornblum, S., Wright, C. E., and Smith, J. E. (1988). Optimality in human motor performance: ideal control of rapid aimed movements. *Psychol Rev*, 95(3):340–370.

Miall, R. C., Weir, D., Wolpert, D. W., and Stein, J. (1993). Is the cerebellum a Smith predictor? *J Mot Behav*, 25(3):203–216.

Miall, R. C., Weir, D. J., and Stein, J. F. (1986). Manual tracking of visual targets by trained monkeys. *Behav Brain Res*, 20(2):185–201.

Milner, T. E. (1993). Dependence of elbow viscoelastic behavior on speed and loading in voluntary movements. *Exp Brain Res*, 93(1):177–180.

Milner, T. E. and Cloutier, C. (1998). Damping of the wrist joint during voluntary movement. *Exp Brain Res*, 122(3):309–317.

Milner, T. E. and Ijaz, M. M. (1990). The effect of accuracy constraints on three-dimensional movement kinematics. *Neuroscience*, 35(2):365–374.

Müller, H. and Sternad, D. (2004). Decomposition of variability in the execution of goal-oriented tasks: three components of skill improvement. *J Exp Psychol Hum Percept Perform*, 30(1):212–233.

Moritz, C. T., Barry, B. K., Pascoe, M. A., and Enoka, R. M. (2005). Discharge rate variability influences the variation in force fluctuations across the working range of a hand muscle. *J Neurophysiol*, 93(5):2449–59.

Newell, K. M., Van Emmerik, R. E. A., Lee, D., and Sprague, R. L. (1993). On postural variability and stability. *Gait & posture*, 4:225–230.

Noteboom, J. T., Barnholt, K. R., and Enoka, R. M. (2001). Activation of the arousal response and impairment of performance increase with anxiety and stressor intensity. *J Appl Physiol*, 91(5):2093–2101.

Osu, R., Burdet, E., Franklin, D. W., Milner, T. E., and Kawato, M. (2003). Different mechanisms involved in adaptation to stable and unstable dynamics. *J Neurophysiol*, 90(5):3255–3269.

Osu, R., Franklin, D. W., Kato, H., Gomi, H., Domen, K., Yoshioka, T., and Kawato, M. (2002). Short- and long-term changes in joint co-contraction associated with motor learning as revealed from surface EMG. *J Neurophysiol*, 88(2):991–1004.

Osu, R. and Gomi, H. (1999). Multijoint muscle regulation mechanisms examined by measured human arm stiffness and EMG signals. *J Neurophysiol*, 81(4):1458–68.

Osu, R., Kamimura, N., Iwasaki, H., Nakano, E., Harris, C. M., Wada, Y., and Kawato, M. (2004). Optimal impedance control for task achievement in the presence of signal-dependent noise. *J Neurophysiol*, 92(2):1199–1215.

Pandy, M. G., Zajac, F. E., Sim, E., and Levine, W. S. (1990). An optimal control model for maximum-height human jumping. *J Biomech*, 23(12):1185–98.

Pasalar, S., Roitman, A. V., and Ebner, T. J. (2005). Effects of speeds and force fields on submovements during circular manual tracking in humans. *Exp Brain Res*, 163(2):214–225.

Perreault, E. J. (2005). Influence of voluntary posture selection on endpoint stiffness. In *Abstracts for International Society of Biomechanics XXth congress. Cleveland, OH, 2005. [available at http://www.isb2005.org/proceedings/abstracts/0851.pdf]*.

Perreault, E. J., Heckman, C. J., and Sandercock, T. G. (2003). Hill muscle model errors during movement are greatest within the physiologically relevant range of motor unit firing rates. *J Biomech*, 36(2):211–218.

Perreault, E. J., Kirsch, R. F., and Acosta, A. M. (1999). Multiple-input, multiple-output system identification for characterization of limb stiffness dynamics. *Biol Cybern*, 80(5):327–337.

Plamondon, R. and Alimi, A. M. (1997). Speed/accuracy trade-offs in target-directed movements. *Behav Brain Sci*, 20(2):279–303; discussion 303–49.

Popescu, F., Hidler, J. M., and Rymer, W. Z. (2003). Elbow impedance during goal-directed movements. *Exp Brain Res*, 152(1):17–28.

Psek, J. A. and Cafarelli, E. (1993). Behavior of coactive muscles during fatigue. *J Appl Physiol*, 74(1):170–175.

Rao, A. K. and Gordon, A. M. (2001). Contribution of tactile information to accuracy in pointing movements. *Exp Brain Res*, 138(4):438–445.

Reeves, N., Everding, V., Cholewicki, J., and Morrisette, D. (2006). The effects of trunk stiffness on postural control during unstable seated balance. *Exp Brain Res*.

Ridderikhoff, A., Peper, C. L., Carson, R. G., and Beek, P. J. (2004). Effector dynamics of rhythmic wrist activity and its implications for (modeling) bimanual coordination. *Hum Mov Sci*, 23(3-4):285–313.

Rohrer, B. and Hogan, N. (2006). Avoiding spurious submovement decompositions II: a scattershot algorithm. *Biol Cybern*, 94(5):409–414.

Roitman, A. V., Massaquoi, S. G., Takahashi, K., and Ebner, T. J. (2004). Kinematic analysis of manual tracking in monkeys: characterization of movement intermittencies during a circular tracking task. *J Neurophysiol*, 91(2):901–911.

Sandfeld, J. and Jensen, B. R. (2005). Effect of computer mouse gain and visual demand on mouse clicking performance and muscle activation in a young and elderly group of experienced computer users. *Appl Ergon*, 36(5):547–555.

Schaal, S. and Schweighofer, N. (2005). Computational motor control in humans and robots. *Curr Opin Neurobiol*, 15(6):675–682.

Schmidt, R. A., Zelaznik, H., Hawkins, B., Frank, J. S., and Quinn, J. T., J. (1979). Motor-output variability: a theory for the accuracy of rapid motor acts. *Psychol Rev*, 47:415–451.

Scholz, J. P. and Schöner, G. (1999). The uncontrolled manifold concept: identifying control variables for a functional task. *Exp Brain Res*, 126(3):289–306.

Scholz, J. P., Schöner, G., and Latash, M. L. (2000). Identifying the control structure of multijoint coordination during pistol shooting. *Exp Brain Res*, 135(3):382–404.

Seidler-Dobrin, R. D., He, J., and Stelmach, G. E. (1998). Coactivation to reduce variability in the elderly. *Motor Control*, 2(4):314–330.

Shannon, C. and Weaver, W. (1949). *The mathematical theory of communication*. Urbana: University of Illinois.

Sherrington, C. S. (1906). *The integrative action of the nervous system*. Yale University Press (reprint 1947).

Shiller, D. M., Laboissiere, R., and Ostry, D. J. (2002). Relationship between jaw stiffness and kinematic variability in speech. *J Neurophysiol*, 88(5):2329–40.

Slifkin, A. B. and Newell, K. M. (1999). Noise, information transmission, and force variability. *J Exp Psychol Hum Percept Perform*, 25(3):837–51.

Sosnoff, J. and Newell, K. (2006). Are age-related increases in force variability due to decrements in strength? *Exp Brain Res*.

Sporns, O. and Edelman, G. M. (1993). Solving Bernstein's problem: a proposal for the development of coordinated movement by selection. *Child Dev*, 64(4):960–981.

Stroeve, S. (1999). Impedance characteristics of a neuromusculoskeletal model of the human arm I. Posture control. *Biol Cybern*, 81(5-6):475–494.

Taylor, A. M., Christou, E. A., and Enoka, R. M. (2003). Multiple features of motor-unit activity influence force fluctuations during isometric contractions. *J Neurophysiol*, 90(2):1350–61.

Todorov, E. and Jordan, M. I. (2002). Optimal feedback control as a theory of motor coordination. *Nat Neurosci*, 5(11):1226–35.

Tracy, B. L., Maluf, K. S., Stephenson, J. L., Hunter, S. K., and Enoka, R. M. (2005). Variability of motor unit discharge and force fluctuations across a range of muscle forces in older adults. *Muscle Nerve*, 32(4):533–540.

Tseng, Y. W., Scholz, J. P., Schöner, G., and Hotchkiss, L. (2003). Effect of accuracy constraint on joint coordination during pointing movements. *Exp Brain Res*, 149(3):276–88.

Vaillancourt, D. E., Larsson, L., and Newell, K. M. (2003). Effects of aging on force variability, single motor unit discharge patterns, and the structure of 10, 20, and 40 Hz EMG activity. *Neurobiol Aging*, 24(1):25–35.

Valero-Cuevas, F. J., McNamara, R. V., Santos, V., Venkadesan, M., Song, S., and Grace-Martin, K. (2006). The nervous system transitions rapidly between incompatible control strategies by predictively exploiting the margins of error of the task. In *Journal of Biomechanics, Abstracts of the 5th World Congress of Biomechanics, Munich, Germany, S95(7142)*.

Van Beers, R. J., Haggard, P., and Wolpert, D. M. (2004). The role of execution noise in movement variability. *J Neurophysiol*, 91(2):1050–1063.

Van den Heuvel, C. E., Van Galen, G. P., Teulings, H. L., and Van Gemmert, A. W. (1998). Axial pen force increases with processing demands in handwriting. *Acta Psychol (Amst)*, 100(1-2):145–159.

Van der Burg, J. C. E., Casius L. J. R., Kingma, I., Van Dieën, J. H., and Van Soest, A. J. (2005). Factors underlying the perturbation resistance of the trunk in the first part of a lifting movement. *Biol Cybern*, 93(1):54–62.

Van der Helm, F. C. T., Schouten, A. C., Erwin De Vlugt, E., and Brouwn, G. G. (2002). Identification of intrinsic and reflexive components of human arm dynamics during postural control. *J Neurosci Methods*, 119(1):1–14.

Van Dieën, J. H., Visser, B., and Hermans, V. (2003). The contribution of task-related biomechanical constraints to the development of work-related myalgia. In H. Johansen, U. Windhorst, M. Djupsjöbacka and M. Passatore (Eds.), *Chronic work-related myalgia: Neuromuscular mechanisms behind work-related chronic muscle pain syndromes* (pp. 83–93.) Gävle: Gävle University Press.

Van Galen, G. P. and De Jong, W. (1995). Fitts' law as the outcome of a dynamic noise filtering model of motor control. *Hum Mov Sci*, 12:539–571.

Van Galen, G. P., Müller, M. L. T. M., Meulenbroek, R. G. J., and Van Gemmert, A. W. A. (2002). Forearm EMG response activity during motor performance in individuals prone to increased stress reactivity. *Am J Ind Med*, 41(5):406–419.

Van Galen, G. P. and Schomaker, L. R. B. (1992). Fitts' law as a low-pass filter effect of muscle stiffness. *Hum Mov Sci*, 11(1-2):11–21.

Van Galen, G. P. and Van Huygevoort, M. (2000). Error, stress and the role of neuromotor noise in space oriented behaviour. *Biol Psychol*, 51(2-3):151–171.

Van Gemmert, A. W. and Van Galen, G. P. (1997). Stress, neuromotor noise, and human performance: a theoretical perspective. *J Exp Psychol Hum Percept Perform*, 23(5):1299–1313.

Van Gemmert, A. W. and Van Galen, G. P. (1998). Auditory stress effects on preparation and execution of graphical aiming: a test of the neuromotor noise concept. *Acta Psychol (Amst)*, 98(1):81–101.

Van Roon, D., Steenbergen, B., and Meulenbroek, R. J. G. (2005). Trunk use and co-contraction in cerebral palsy as regulatory mechanisms for accuracy control. *Neuropsychologia*, 43(4):497–508.

Van Soest, A. J. and Bobbert, M. F. (1993). The contribution of muscle properties in the control of explosive movements. *Biol Cybern*, 69(3):195–204.

Van Zandwijk, J. P., Bobbert, M. F., Harlaar, J., and Hof, A. L. (1998). From twitch to tetanus for human muscle: experimental data and model predictions for m. triceps surae. *Biol Cybern*, 79(2):121–130.

Visser, B., De Looze, M., De Graaff, M., and Van Dieën, J. H. (2004). Effects of precision demands and mental pressure on muscle activation and hand forces in computer mouse tasks. *Ergonomics*, 47(2):202–17.

Wagner, H. and Blickhan, R. (2003). Stabilizing function of antagonistic neuromusculoskeletal systems: an analytical investigation. *Biol Cybern*, 89(1):71–9.

Welter, T. G. and Bobbert, M. F. (2002). Initial arm muscle activation in a planar ballistic arm movement with varying external force directions: a simulation study. *Motor Control*, 6(3):217–29.

Woodworth, D. (1899). The accuracy of voluntary movement. *Psychol Rev*, 3:1–119.

Yang, J.-F. and Scholz, J. P. (2005). Learning a throwing task is associated with differential changes in the use of motor abundance. *Exp Brain Res*, 163(2):137–158.

Zhang, L. Q. and Rymer, W. Z. (1997). Simultaneous and nonlinear identification of mechanical and reflex properties of human elbow joint muscles. *IEEE Trans Biomed Eng*, 44(12):1192–1209.

Zhang, L. Q. and Rymer, W. Z. (2001). Reflex and intrinsic changes induced by fatigue of human elbow extensor muscles. *J Neurophysiol*, 86(3):1086–1094.

Summary

Impedance modulation: a means to cope with neuromuscular noise

Human movement is variable, yet efficient. Movement variability is an inevitable consequence of the stochastic processes involved in the generation of motor output and may even be purposeful in the exploration of alternative movement strategies. To be effective, however, the motor control system also has to cope with possible detrimental effects of variability.

In the early nineties of the previous century, Van Galen and colleagues forwarded the idea that joint impedance acts as a filter between muscular forces and kinematics in their Neuromotor Noise Theory (NNT). The work reported in this thesis may be viewed as an evaluation of the scope and merits of this idea.

Chapter 2 presents a numerical model to examine the paradoxical claim of NNT that increasing joint impedance may result in less kinematic variability despite increased levels of neuromuscular noise in the individual muscles. A prerequisite of such a model is that it produces realistic force variability. Standard Hill-type muscle models failed to show the monotonic relationship between the mean force and its standard deviation that is observed experimentally. In contrast, a combined motor-unit pool model of parallel Hill-type motor units produced a realistic increase of force variability with increases in mean force. The latter model was simulated as an antagonistic muscle pair, controlling the position of a frictionless hinge joint. Increasing the impedance through muscular co-activation resulted in less kinematic variability, except at the lowest levels of co-activation. In this region, model behaviour was affected by the noise amplitude and the inertial properties of the model. The simulations showed that increasing joint impedance is in principle an effective strategy to meet accuracy demands.

The experiments reported in chapters 3, 4 and 5 were intended to provide empirical evidence for the use of joint impedance modulation in controlling the variability of movement. In all three experiments, controlled mechanical perturbations were applied occasionally and unexpectedly to the forearm during precision tasks. Estimates of inertia, damping and stiffness were derived from the responses to these mechanical perturbations.

In the first experiment, presented in chapter 3, subjects made rapid, time constrained elbow extensions to three differently sized targets. Smaller targets resulted in lower endpoint variability, but not necessarily in smaller variability over the entire trajectory. In accordance with the claim of NNT, joint stiffness and damping, estimated at 75% of the movement amplitude, increased with smaller targets. In addition, in spite of the time constraint, movement times significantly increased with decreasing target size, suggesting that modulation of movement speed is the more natural strategy.

The task used in chapter 3 appeared not sensitive enough to be able to investigate the effects of fatigue. Therefore, an additional experiment was conducted on the modulation of joint impedance while tracking sinusoidally moving targets of different size and frequency. This experiment is reported in chapter 4. Movement variability decreased with both decreasing target size and movement frequency, whereas stiffness and damping increased with decreasing target size and was independent of movement frequency. In addition, the organisation of submovements changed systematically with both target size and movement frequency. These changes were interpreted in terms of a feedback controlled error correction mechanism. In conclusion, impedance and submovement modulation contributed additively to tracking accuracy.

In chapter 5 the neuromuscular noise itself was manipulated, rather than movement accuracy as in chapters 3 and 4. Given that force variability increases with muscular fatigue, it was hypothesised that joint impedance would increase with fatigue to retain a prescribed accuracy level. To test this hypothesis, subjects tracked a target both with fatigued and unfatigued elbow flexor and extensor muscles. Unexpectedly, elbow impedance decreased, whereas performance, expressed as the time-on-target, remained unaffected by fatigue. Instead, subjects stayed closer to the centre of the target, allowing them to have more kinematic variability without a reduction in task performance.

All in all, the work presented in this thesis corroborates the claim that the modulation of joint impedance can reduce and, in particular cases is used to reduce the kinematic variability caused by neuromuscular noise. Conversely, it also shows that

impedance modulation is only one of several strategies that the motor control system has at its disposal. In real life situations, a combination of strategies will be used and in some instances, such as when fatigued, impedance modulation does not appear to be the primary strategy of choice.

Samenvatting

Impedantie regulatie: een strategie om neuromusculaire ruis te onderdrukken

Het menselijk bewegen is, ondanks haar variabiliteit, zeer doeltreffend. De variabiliteit is onlosmakelijk verbonden met de stochastische processen die betrokken zijn bij de totstandkoming van bewegingen en kan zelfs nuttig zijn voor het ontdekken van alternatieve bewegingsstrategieën. Om doeltreffend te zijn moet het neurale systeem echter rekening houden met de nadelige gevolgen van variabiliteit.

In de vroege jaren negentig van de vorige eeuw opperde Van Galen met enkele collega's het idee dat gewrichtsstijfheid als een filter zou kunnen werken tussen variabiliteit in spierkracht en de kinematica van de beweging. Dit idee werd verwoord in de Neuromotorische Ruistheorie. In dit proefschrift wordt de geloofwaardigheid en reikwijdte van deze theorie getoetst.

In hoofdstuk 2 wordt een simulatie model gepresenteerd om de paradox te toetsen dat verhoogde gewrichtsstijfheid zou kunnen resulteren in een afname van de bewegingsvariabiliteit, ondanks dat de variabiliteit van de individuele spierkrachten toeneemt. Een randvoorwaarde voor een dergelijk simulatie model is dat het realistische krachtvariabiliteit toont. Standaard spiermodellen, zoals voorgesteld door Hill, vertonen geen monotoon stijgende krachtvariabiliteit bij toename van de gemiddelde kracht, zoals experimenteel vastgesteld. Een model opgebouwd uit losse motor-units in combinatie met een pool van motorneuronen, vertoont echter wel het gewenste patroon van krachtvariatie. Twee van dergelijke spiermodellen werden als tegenoverliggende spieren gesimuleerd met een inertie ertussen. Ondanks dat de krachtvariabiliteit van de individuele spieren toenam bij verhoogde co-activatie, nam de kinematische variabiliteit af. Voor lage activatie van de spieren was dit echter niet waar. Het kwalitatieve gedrag van het model bleek bij lage co-activatie kritisch afhanke-

lijk van de ruisamplitude en de inertie van het model. De algemene conclusie van hoofdstuk twee is dat het verhogen van de gewrichtsstijfheid in principe een effectieve strategie kan zijn om te voldoen aan nauwkeurigheidseisen.

De experimenten in de hoofdstukken 3, 4 en 5 hadden tot doel om empirische ondersteuning te vergaren voor de aanpassing van gewrichtsstijfheid om de kinematische variabiliteit van een beweging te controleren. In alle drie de studies werden onverwacht mechanische verstoringen uitgeoefend op de elleboog tijdens precisietaken. Schattingen voor inertie, demping en stijfheid werden afgeleid uit de reacties op deze verstoringen.

In het eerste experiment, beschreven in hoofdstuk 3, maakten proefpersonen snelle elleboogstrekkingen met een voorgeschreven tijd naar doelen van drie verschillende groottes. Kleinere doelen resulteerden in minder variatie van het eindpunt, maar niet noodzakelijkerwijs in minder variatie tijdens de beweging. In overeenstemming met de Neuromotorische Ruistheorie namen de stijfheid en demping, geschat op 75% van het bewegingstraject, van de elleboog toe bij kleine doelen. Bovendien bewogen proefpersonen langzamer naar de kleinere doelen, ondanks het feit dat we de bewegingstijd experimenteel probeerden te controleren. Klaarblijkelijk is het aanpassen van de bewegingssnelheid een meer natuurlijke strategie om de eindpuntvariabiliteit te controleren.

De taak die de proefpersonen in hoofdstuk 3 uitvoerden bleek niet gevoelig genoeg om de effecten van spiervermoeidheid op de regulatie van gewrichtsstijfheid te kunnen onderzoeken. Daarom werd een vergelijkbaar experiment uitgevoerd waar de stijfheid en demping werden geschat tijdens het volgen van cyclisch bewegende doelen. Zowel de bewegingsfrequentie als de grootte van de doelen werden gevarieerd. De bewegingsvariabiliteit nam af met kleinere doelen en bij lagere bewegingsfrequenties. De stijfheid en demping namen alleen toe als de doelen kleiner werden, maar bleven constant voor de verschillende bewegingsfrequenties. Verder veranderde de organisatie van de deelbewegingen rond het centrum van het doel met zowel de doelgrootte als de bewegingsfrequentie. Deze veranderingen werden door ons geïnterpreteerd in termen van een visueel gestuurd correctie mechanisme. Zowel de impedantie als de organisatie van deelbewegingen dragen bij aan de precisie tijdens het volgen van een doel.

In hoofdstuk 5 werd de neuromusculaire ruis gemanipuleerd, dit in tegenstelling tot de bewegingsprecisie in de hoofdstukken 3 en 4. Gegeven het feit dat krachtvariabiliteit toeneemt met vermoeidheid, verwachtten we dat de gewrichtsstijfheid

eveneens toe zou nemen om te kunnen blijven voldoen aan de precisie eisen. Om deze hypothese te testen volgden proefpersonen een doel, zowel met onvermoeide en vermoeide spieren rond de elleboog. In tegenstelling tot onze verwachting, nam de impedantie van de elleboog af met vermoeidheid, terwijl de prestatie, uitgedrukt als de tijd dat proefpersonen binnen het te volgen doel bleven, niet beïnvloed werd. Het bleek dat proefpersonen dichter bij het centrum van het doel bleven waardoor ze meer variabiliteit konden toestaan zonder dat hun taakprestatie achteruit ging.

De studies in dit proefschrift ondersteunen de bewering dat de modulatie van de gewrichtsimpedantie de effecten van neuromusculaire ruis op de bewegingsuitvoering kan onderdrukken. Maar het laat ook zien dat de modulatie van de impedantie slechts één van de vele strategieën is die het bewegingssysteem tot zijn beschikking heeft. In dagelijkse situaties zal een combinatie van strategieën gebruikt worden en in sommige gevallen, zoals bij vermoeidheid, lijkt de modulatie van gewrichtsimpedantie geen duidelijke bijdrage te leveren.

Dankwoord

Twaalf jaar na het verlaten van de middelbare school ligt er een proefschrift van mijn hand. In die twaalf jaar heb ik ontdekt waar mijn interesses liggen. Enkele mensen die mijn pad hebben gekruist en stukken hebben meegelopen wil ik expliciet bedanken, echter zonder anderen te kort te willen doen.

Prof. Dr. Van Dieën, beste Jaap, mijn sluimerende interesse voor de bewegingswetenschappen werd aangewakkerd door jou. Ooit, lang geleden in 1999 kwamen we elkaar voor het eerst tegen tijdens mijn afstudeerstage voor de HTS. Hoewel ik mij op dat moment nog bekwaamde in het modelleren van tussenwervelschijven, verschoven onze discussies al vaak naar de sturing van bewegingen. Na afloop van mijn stage nam jij de laatste twijfels weg om bewegingswetenschappen te gaan studeren. Toen het einde van mijn studententijd naderde kwam je met het voorstel te promoveren. Het projectvoorstel waarop ik 'ja' zei, was een samenraapsel van ideeën van jou en Peter Beek. Ik stel me zo voor dat jullie het projectvoorstel hebben geschreven op een mooie zomerse avond onder het genot van één of meerdere flessen wijn. Dat heb ik geweten... Sinds onze eerste kennismaking zijn zeven jaren verstreken. Ik heb de samenwerking in die jaren altijd als heel prettig ervaren. Jouw brede interesse, expertise en werkhouding waren zeer inspirerend, waarvoor mijn welgemeende dank.

Prof. Dr. Beek, beste Peter. Mijn eerste contact met jou was tijdens de cursus bewegingscoördinatie. Waar de meeste studenten deze cursus als (te) abstract beschouwden, bevestigde deze cursus dat ik de juiste keuze had gemaakt om verder te studeren. Aan dit proefschrift heb jij met voornamelijk een schrijvende bijdrage geleverd. Ik hoop ooit de zinnen die zo makkelijk uit jouw pen vloeien of via het toetsenbord op je scherm verschijnen, te kunnen benaderen. Verder hield jij me scherp als het er echt om ging spannen of we een deadline gingen halen. Dank voor je inzet om dit project tot een goed einde te brengen.

Ik heb een brede interesse voor het menselijk bewegen. Enkele medewerkers van

de faculteit der bewegingswetenschappen (FBW) wil ik expliciet bedanken voor het voeden van deze interesse. Onno Meijer, hoewel ik het nooit voor elkaar heb gekregen een afgerond gesprek met je te voeren, heb ik al je cursussen met veel plezier gevolgd. Claire Michaels, jij hebt het vuurtje echt aangewakkerd om wetenschap te bedrijven. Hoewel ik voor een totaal andere hoek heb gekozen, was jij degene die me liet zien hoe leuk wetenschap kan zijn. Tot slot, Maarten Bobbert. Naast Jaap ben jij een van de mensen waar ik altijd op terug kan vallen. Hoewel niet direct betrokken bij mijn promotie project was je altijd belangstellend hoe het ging, of het nou wetenschap, schaatsen of andere dagelijkse beslommeringen betrof.

Daarnaast was er de lunchgroep. Het was heerlijk om iedereen op te trommelen als het toch even niet liep met programmatuur of apparatuur (Oh ja, ABSA bedankt dat je het einde van mijn promotie project hebt gehaald . . .). Naast het bespreken van frustraties hebben we veel lol gehad tijdens de lunches.

Niet alleen was ik vijf dagen per week op de FBW, ik was minstens zoveel dagen van de week in de weer voor de schaatssport. De vraag zal altijd blijven of ik gepromoveerd ben dankzij deze uitlaatklep of ondanks alle uren op de ijsbaan. In ieder geval heb ik een fantastische tijd gehad met alle sporters van, in het bijzonder, SKITS. Kees de Vrij, als collega trainer hebben we heel wat boeiende discussies over schaatsen en de organisatie van de sport gevoerd. Ik wil je echter met name danken voor het feit dat jij nooit uit het oog verloor dat ik ook nog ‘die andere baan’ had.

De paranimfen, Maaike Huysmans en Aukje de Vrijer. Maaike, als collega promovendus doe jij onderzoek naar de meer praktische kant van stijfheidsmodulatie. Vier jaar geleden zagen we de overlap tussen onze projecten nog niet zo. Maar naar mate we vorderden bleken er veel meer overeenkomsten tussen onze projecten te bestaan dan we dachten. Ik heb met name de discussies in het afgelopen jaar zeer gewaardeerd. Je had altijd tijd als ik weer eens een resultaat met je wilde bespreken of in perspectief wilde plaatsen met jouw bevindingen. Ik hoop dat we, ondanks dat ik nu niet meer op de FBW rondloop, onze discussies voortzetten en onze ideeën blijven delen. Aukje, ik zal nooit vergeten hoe jij als eerstejaars student mij het leven zuur maakte tijdens de werkcolleges biomechanica die ik begeleidde. Je kwam er openlijk voor uit dat je niks had voorbereid, maar naarmate de werkgroep vorderde werd de kans op lastige vragen steeds groter. Ook als schaatsster maakte je het mij, je trainer, niet makkelijk. Maar, daarnaast kwam jij tijdens mijn hele promotie project geregeld mijn kamer binnenlopen om van alles, maar vaak wetenschappelijke zaken, te bespreken. Weet je trouwens dat de promovendus de lastige vragen door mag spelen

naar de paranimfen . . . ?

Pap en mam, daar waar anderen hun wenkbrauwen fronsten als ik, weer eens, van studierichting veranderde, moedigden jullie me altijd aan mijn ontdekkingstocht voort te zetten. Ook waren jullie altijd bereid de helpende hand te bieden, van de verhuizing naar mijn eerste studentenkamertje in Enschede, via verbouwingsactiviteiten in Diemen tot de recente oversteek naar Cambridge. Dank voor al die steun en inzet.

Wendy, hoewel onze gedeelde interesse voor bewegingssturing jou een felle discussie partner, een kritische lezer, een luisterend oor en een helpende hand maakte, betekende dit soms ook dat ik je tot irriterend toe heb vermoeid met mijn werk. Jouw kritiek op mijn werk was soms genadeloos, maar wellicht maakte dat mijn schrijfsels 'reviewer-proof 'Ḣet was een boeiende tijd om samen te ontdekken in deze wondere wereld. Heel veel dank voor alle liefde en voor het feit dat je onze gezamenlijke ontdekkingsreis voort wil zetten in Cambridge.

Publications

Articles in international journals

Van Dieën, J. H., Selen, L. P. J. and Cholewicki, J. (2003). Trunk muscle activation in low-back pain patients, an analysis of the literature. *J Electromyogr Kinesiol*, 13(4):333–351.

Selen, L. P. J., Beek, P. J., and Van Dieën, J. H. (2005). Can co-activation reduce kinematic variability? A simulation study. *Biol Cybern*, 93(5):373–381.

Selen, L. P. J., Beek, P. J., and Van Dieën, J. H. (2006). Impedance is modulated to meet accuracy demands during goal-directed arm movements. *Exp Brain Res*, 172(1):129–138.

Selen, L. P. J., Van Dieën, J. H., and Beek, P. J. (2006). Impedance modulation and feedback corrections in tracking targets of variable size and frequency. *J Neurophysiol*, 96(5):2750–2759.

Selen, L. P. J., Beek, P. J., and Van Dieën, J. H. (2006). Fatigue induced changes of impedance and performance in target tracking. *Exp Brain Res*, under review.

Book chapters

Van Dieën, J. H., Selen, L. P. J., and Beek, P. J. (2007). Suppression of neuromuscular noise through impedance modulation. In: T. O. Williams (Ed.), *Biological Cybernetics Research Trends*. Hauppauge, NY: Nova Science Publishers Inc.

Articles in Dutch journals

Selen, L. P. J., Vaartjes, S. R., and Conemans, J. M. H.. (1999). Mag je erytrocytenconcentraat met de infusiepomp toedienen? *Klinische Fysica*, 4:19–22.

Conference proceedings

Selen, L. P. J., Beek, P. J., and Van Dieën, J. H. (2006). Joint impedance attenuates neuro-muscular noise during target tracking. *Proceedings of the Vth World Congress of Biomechanics*, Munich, Germany.

Selen, L. P. J., Beek, P. J., and Van Dieën, J. H. (2006). Organizational principles in target tracking: modulation of impedance and feed-back gain in response to target speed and target size changes. *Proceedings of the XVIth Annual Neural Control of Movement Society Meeting*, Key Biscayne, Florida.

Selen, L. P. J., Beek, P. J., and Van Dieën, J. H. (2006). Impedance Modulation With Precision Demands In Discrete Movements. *Proceedings of the XXth Congress of the International Society of Biomechanics*, Cleveland, Ohio.

Selen, L. P. J., Beek, P. J., and Van Dieën, J. H. (2004). Does coactivity reduce the influence of neural noise on motor performance? *Proceedings of the 14th European Society of Biomechanics Conference*, ' s Hertogenbosch, The Netherlands.

Stinstra, J. G., Selen, L. P. J., and Peters, M. J. (1999). The processing of foetal magnetocardiograms. *Recent advances in Biomagnetism*, Sendai, Japan, 971–974.